AD NUMBER

AD823214

NEW LIMITATION CHANGE

TO

Approved for public release, distribution unlimited

FROM

Distribution authorized to U.S. Gov't. agencies and their contractors; Critical Technology; JUL 1967. Other requests shall be referred to Air Force Rocket Propulsion Lab., Edwards AFB, CA.

AUTHORITY

AFRPL ltr, 27 Oct 1971

AFRPL-TR-67-277

METHODS FOR ELIMINATION OF CORROSION PRODUCTS OF NITROGEN TETROXIDE

Final Report

Chemical and Material Sciences
Research Division of Rocketdyne
A Division of North American Aviation, Inc.
Canoga Park, California

TECHNICAL REPORT AFRPL-TR-67-277

July 1967

Air Force Rocket Propulsion Laboratory
Research and Technology Division
Edwards, California
Air Force Systems Command
United States Air Force

When U.S. Government drawings, specifications, or other data are used for any purpose other than a definitely related Government procurement operation, the Government thereby incurs no responsibility nor any obligation whatsoever, and the fact that the Government may have formulated, furnished, or in any way supplied the said drawings, specifications, or other data, is not to be regarded by implication or otherwise, or in any manner licensing the holder or any other person or corporation, or conveying any rights or permission to manufacture, use, or sell any patented invention that may in any way be related thereto.

AFRPL-TR-67-277

METHODS FOR ELIMINATION OF CORROSION PRODUCTS OF NITROGEN TETROXIDE

Final Report

Chemical and Material Sciences
Research Division of Rocketdyne
A Division of North American Aviation, Inc.
Canoga Park, California

TECHNICAL REPORT AFRPL-TR-67-277

July 1967

Air Force Rocket Propulsion Laboratory
Research and Technology Division
Edwards, California
Air Force Systems Command
United States Air Force

FOREWORD

The research reported herein was sponsored by the Air Force Rocket Propulsion Laboratory, Research and Technology Division, Edwards Air Force Base, California, under Contract AF04(611)-11620. The monitoring agency was RPCL; the contract monitor was Lt. R. Fargnoli. The technical effort was conducted over the period 1 May 1966 through 30 June 1967.

The program was conducted by Chemical and Material Sciences (formerly Chemistry Research Section) of the Rocketdyne Research Division. Dr. J. Silverman was the original Program Manager, and Dr. E. F. C. Cain was the Responsible Scientist. Dr. Cain subsequently became Program Manager. The principal areas of study and the contributing personnel were as follows:

Phase I:	Compound Formation	Phase II:	Compound Identification
	Dr. A. E. Axworthy (Responsible Scientist)		Dr. J. Gerhauser Dr. A. E. Axworthy (Responsible Scientists)
	Dr. W. Nigh		Dr. J. Ray
	Dr. J. Katekaru		Dr. R. Greenough
	Dr. H. Schultz		Dr. J. Hon
			Mr. P. Ennis
Phase III:	Compound Solubility and	Phase V:	Efficiency of Elimination
Phase IV:	Compound Elimination		Dr. S. Rodriguez Dr. J. Sinor (Responsible Scientists)
	Dr. C. Fujikawa (Responsible Scientist)		
	Dr. F. C. Gunderloy, Jr.		
	Dr. J. Katekaru		
	Dr. H. Schultz		

This report has been assigned the Rocketdyne report No. R-7136.

This report has been reviewed and approved.

W. H. EBELKE, Colonel, USAF
Chief, Propellant Division

ABSTRACT

A 14-month program has been conducted to define and determine elimination techniques for the phenomenon known as "flow decay". Flow decay has been shown to arise from the deposition of an N_2O_4-soluble iron compound, $NO^+\left[Fe(NO_3)_4\right]^-$, in valve orifices. This deposition impedes the flow of propellant, and, in extreme cases, clogs the valve completely.

Five tasks (Phases) comprised this program. The results of each are given in the following paragraphs.

PHASE I: COMPOUND FORMATION

Anhydrous nitrogen tetroxide has been shown to dissolve iron, reaching a solubility limit on the order of 1 to 2 ppm of iron. The source of iron may be pure iron, 304 and 316 stainless steel, or 1018 carbon steel; the source had little effect. The value of 1 to 2 ppm of iron appears to be definitely a solubility limit, rather than being imposed by the solubility of a trace impurity, or resulting from passivation of the iron surface. Water enhanced both the rate of solution and the solubility of iron in N_2O_4, and in concentrations approaching 1 weight percent led to a second viscous liquid phase, presumably a concentrate of ferric nitrate in HNO_3.

PHASE II: COMPOUND IDENTIFICATION

The techniques of nuclear magnetic resonances, nuclear quadrupole resonance, broadline n.m.r., e.p.r. spectroscopy, and Mossbauer spectroscopy were applied to the flow decay problem. None of these techniques, in their present state of development, proved sufficiently sensitive to allow meaningful studies of the extremely dilute iron/N_2O_4 solutions that result in flow decay. However, some of these techniques did yield information regarding the structure of the solid flow-decay type materials.

PHASE III: COMPOUND SOLUBILITY

Synthetic flow-decay compound, $Fe(NO_3)_3 \cdot N_2O_4$, was prepared from the reaction of N_2O_4 and iron carbonyl, and shown to be identical with real flow-decay deposit by infrared spectrum, X-ray diffraction, and elemental analysis. Structurally, the compound may be formulated as $NO^+\left[Fe(NO_3)_4\right]^-$. The solubility of synthetic flow-decay compound in anhydrous N_2O_4 is in the range of 1 to 2 ppm of iron, with a slight positive temperature coefficient of solubility. Water at the military specification limit (0.1 weight percent) and NO (up to 1 weight percent) have no effect on solubility. Higher water concentrations increase the solubility.

PHASE IV: COMPOUND ELIMINATION

Organic coordinating compounds were screened as additives for N_2O_4, under the premise that complexing $Fe(NO_3)_3 \cdot N_2O_4$ with an organic ligand might alter its solubility and eliminate flow decay. Based on tests of $Fe(NO_3)_3 \cdot N_2O_4$ solubility, N_2O_4 compatibility, and resistance to N_2O_4 at 165 F, the following candidates were selected: acetonitrile, perfluoroacetonitrile, benzonitrile, perfluorobenzonitrile, ethyl acetate, and perfluoroacetone. INTO (NO_2F in N_2O_4) was tested, and converted the $Fe(NO_3)_3 \cdot N_2O_4$ to NO_2FeF_4. A small laboratory flow device was constructed, in which flow-decay compound could be observed depositing in a glass U-trap. Acetonitrile added to N_2O_4 dissolved this deposit.

PHASE V: EFFICIENCY OF ELIMINATION

A flow bench was constructed for the study of N_2O_4 behavior in valves and orifices under various conditions. Data accumulated in operating the bench indicate the flow decay is indeed a solubility phenomenon, with solution, nucleation, and precipitating steps leading to the buildup of flow-decay deposits. Organic additives, acetonitrile, benzonitrile, ethyl acetate, and perfluorobenzonitrile, at 0.25 weight percent

concentration, will eliminate flow decay. Perfluorobenzonitrile lost its effectiveness with time. INTO yielded only very small decreases in flow-rate, and flow decay may never be a real problem with INTO. Hydrofluoric acid in N_2O_4 (from spent INTO) also appears to eliminate flow decay.

CONTENTS

ILLUSTRATIONS

TABLES

INTRODUCTION

Often during space engine test programs, flowmeters (both turbine and drag-body types) have performed erratically. In a large number of cases, no apparent explanation for this erratic behavior could be derived. Flowmeters would operate erratically, be returned for calibration, and then be found to operate satisfactorily without any corrective measures or repairs. At times, contamination was observed which would disappear before a laboratory examination could be conducted.

In November 1964, an intensive investigation was initiated at Rocketdyne for the solution to this problem which is referred to as "the flow-decay process." The first significant breakthrough was achieved in March 1965 when a sight gage valve with a glass port over the needle was observed and photographed under flow-decay conditions. For the first time, a cause of the flow-decay problem presented itself when a solid deposit formed on the needle (Fig. 1).

A company-funded investigation of the flow-decay phenomenon was initiated in March 1965. The results of this study are reported in Ref. 1.

Chemical analysis of the flow-decay deposit established that the material is an iron nitrate compound solvated with N_2O_4 and has the empirical formula $Fe(NO_3)_3 \cdot xN_2O_4$, where x may vary from 1 to 9. The material, while stable in an N_2O_4 atmosphere, decomposes quite rapidly on exposure to air and appears to lose the solvated N_2O_4 on standing unless it is maintained in an atmosphere of N_2O_4.

Limited studies were also conducted to determine the effect of operating parameters on the formation of the deposit (Ref. 1). Flow decay was consistently induced in the facility used to calibrate flowmeters, by temperature soaking the N_2O_4 at 100 to 115 F and then dropping the temperature at the same time flow was started.

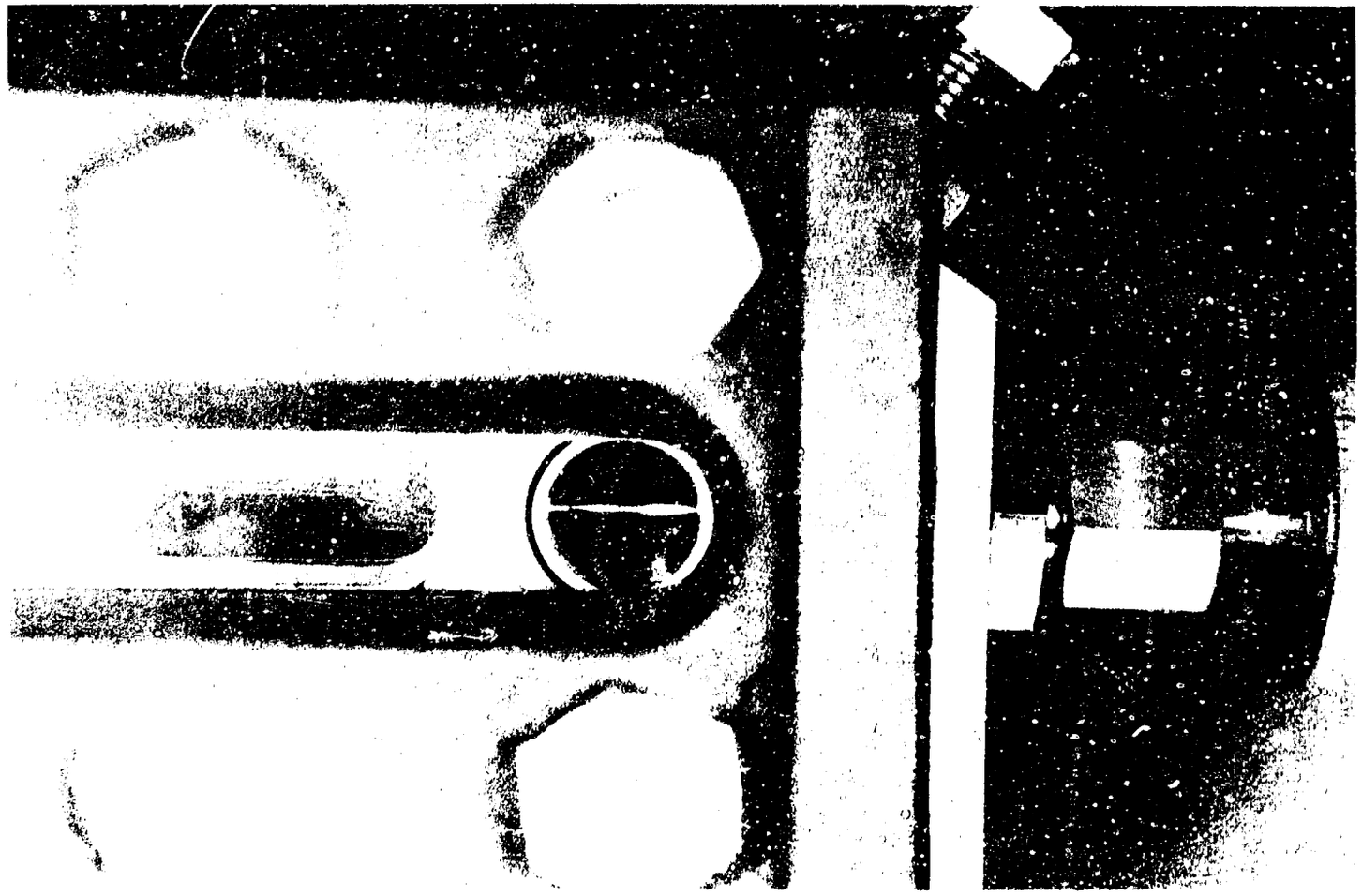

Figure 1. Flow-Decay Deposit on Needle Valve

The flow-decay material forms as the result of corrosion of iron alloys by nitrogen tetroxide. The program conducted under Contract AFO4(611)-11620 was a 14-month study to define the flow-decay phenomenon in detail, and to determine methods for its elimination. Five areas of study were defined; a description (work statement) of the objectives of each area is presented in the following paragraphs.

PHASE I: COMPOUND FORMATION

Investigation of the metal compound formation mechanism in N_2O_4 was to be conducted with alloys of iron, aluminum, and titanium, and the appropriate oxides of the three metals. The alloys were to be limited to those materials of construction in existing and prototype space systems. The influence of up to 1 weight percent nitric oxide or water added to N_2O_4 was also to be investigated. The effect of temperature variation was also to be evaluated.

PHASE II: COMPOUND IDENTIFICATION

The chemical structures and formulations of the compounds were to be determined as they exist in solid or liquid form. The compounds were also to be identified as they exist in solution with N_2O_4.

PHASE III: COMPOUND SOLUBILITY

The compounds identified were to be prepared synthetically in sufficient quantities to conduct solubility studies with N_2O_4. During the solubility studies, the temperature of the N_2O_4 was to be varied from 32 to 100 F (0 to 37.8 C). In addition, the concentrations of nitric oxide and water in the N_2O_4 were to be varied from 0 to 1 percent and from 0.1 to 1.0 percent, respectively.

PHASE IV: COMPOUND ELIMINATION

The effects of appropriate chelating agents were to be studied in an effort to render the metal compound soluble in N_2O_4 over the temperature range cited in the preceding paragraph. Other methods of elimination were to be investigated only if the chelating approach were not successful.

PHASE V: EFFICIENCY OF ELIMINATION

A bench-scale flow device was to be constructed to test the effectiveness of the elimination mechanism. The flow bench was to simulate operational conditions encountered by the N_2O_4.

PHASE I: COMPOUND FORMATION

INTRODUCTION

The objective of this task was to determine the mechanism of formation of the species involved in the flow-decay process.

The initial approach of the task was to measure the kinetics of the dissolution of iron in purified N_2O_4 by following the total iron concentration, and from this to determine the mechanism of the dissolution process. It was determined early in the program that the solubility of iron in purified or propellant-grade N_2O_4 was much less ($\sim$ 1 ppm) than had been reported previously (Ref. 1), and that N_2O_4 saturates with iron at a relatively rapid rate. The low solubility prevented measurement of the total iron concentration to better than approximately $\pm$25 percent in most experiments. These problems prevented a detailed study of the kinetics of formation of the iron-containing species in N_2O_4. However, a study was conducted of the equilibrium iron concentration under various conditions, and the results obtained yielded considerable insight into the mechanism of the dissolution process.

EXPERIMENTAL PROCEDURE

Aliquot Technique in Glass/Teflon Apparatus

The apparatus consisted of a reaction chamber and pipette-condenser unit. Both of these portions were jacketed to allow individual control of their temperatures. The entire apparatus was constructed of glass and Teflon. Teflon was used for the stopcocks and for the sleeves of the standard taper joints.

A sample of purified N_2O_4 was distilled into a graduated sample bulb from a glass/Teflon storage container. The bulb was then attached to the reaction chamber. A weighed sample of iron powder and a glass-covered magnetic stirring bar were then placed in the chamber. The system was evacuated and thermostatted water was circulated around the reaction chamber (21 C) and

the pipette (0 C). The reaction was initiated by opening the stopcock of the N_2O_4 sample bulb and allowing the N_2O_4 to enter the reaction chamber. Simultaneously, the constant-speed magnetic stirrer and timer were activated. At appropriate time intervals, a sample of N_2O_4 was drawn into the cooled pipette (being filtered as it passed through fritted glass within the reaction chamber). The sample was expelled into a flask containing cold distilled water. After hydrolysis of the N_2O_4, the solution was neutralized with NH_4OH and the iron content was determined colorimetrically (Appendix A).*

Several problems were encountered with this system, and it was abandoned in favor of the ampoule technique. The difficulties with this apparatus were (1) the possibility of leakage, (2) excessive contact of the N_2O_4 with Teflon, (3) the required capacity of the cooling system, and (4) mechanical problems with the method of temperature control employed.

Ampoule Technique

The sealed ampoule technique had the advantage of eliminating the possibility of leakage and contamination, which was particularly important for long-term experiments. A schematic of a typical ampoule is presented in Fig. 2 . The ampoules were constructed of Pyrex, and the fritted glass disk had a pore size of approximately 15 microns.

All glassware was cleaned thoroughly with hot HCl, rinsed with 1:1 HCl/demineralized water, rinsed with demineralized water, and dried for 24 hours at 200 C. With the ampoules in the position shown in Fig. 2 , powdered samples were weighed into the upper compartments, and a series of approximately 10 ampoules was sealed directly to a common vacuum manifold. The liter storage bulb containing the purified N_2O_4 was attached to the manifold with a Teflon-sealed joint and valve. The vacuum system was evacuated and then warmed with a heat gun to complete outgassing. Approximately 10 grams of N_2O_4 were distilled into one ampoule at a time while the lower

*The methods employed to determine the total iron concentration are described in Appendixes A through C.

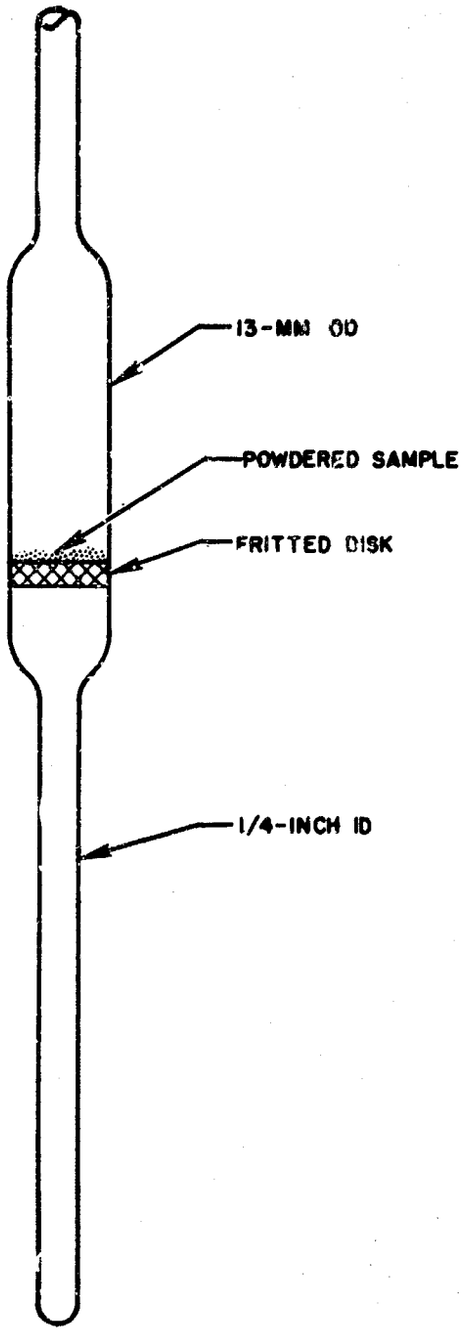

Figure 2. Pyrex Ampoule

ampoule compartment was cooled with LN_2. The coolant was then raised above the sintered disk and the system was evacuated through LN_2 traps. The ampoule was sealed shut with a torch and removed from the manifold. This procedure was repeated successively for each ampoule. The lower tube was warmed to 0 C, and the height of the liquid column was measured to determine the quantity of N_2O_4 in the ampoule, which was previously calibrated.

The ampoule was then inverted, and the larger diameter compartment was cooled in LN_2 to draw the N_2O_4 through the fritted disk into contact with the powder. The ampoules were then immersed in a constant-temperature bath for the required time. At the conclusion of the heating period, they were withdrawn, inverted, and the lower tip was cooled in LN_2 to draw the liquid through the sintered disk, thereby filtering out the solid powder. The tube containing the frozen N_2O_4 was broken from the ampoule, and its contents were hydrolyzed in 40 milliliters of water. The sample was then analyzed for total iron.

Materials

Materials used for these dissolution experiments were:

1. Iron Powder. Baker Analyzed Reagent, lot No. 26209 (98.2 percent Fe).
2. Iron Oxide Powder. Baker Analyzed Reagent, lot No. 30245 (99.3 percent Fe_2O_3).
3. Steel Alloys. The alloy disks were the same as those used for the Inhibited Nitrogen Tetroxide Program under Contract AF04(611)-10809. The disks were degreased by rinsing with high purity trichloroethylene and dried in a stream of hot, dry air. Two of the carbon steel disks were cleaned and passivated by immersing in 20-percent hydrochloric acid until the surface was clean and free of rust and scale. The disks were then rinsed with a 0.02 w/o citric acid solution and immediately immersed in a passivating solution containing 0.5 w/o sodium hydroxide, 0.5 w/o sodium nitrate, 0.25 w/o monosodium phosphate, and 0.25 w/o disodium phosphate. After 30 minutes at room temperature, the disks were removed from this solution and dried with a stream of hot, dry air.

4. Nitrogen Tetroxide. The removal of water and coluble iron from N_2O_4 was accomplished by fractional distillation through a 30-section bubble plate column (removal ratio: 20:1). Water was removed by the addition of phosphorous pentoxide prior to the distillation. The gaseous N_2O_4 was in contact with the atmosphere through a calcium sulfate drying tube, thus preventing any subsequent contamination by water. Teflon sleeves were used at all ground-glass connections.

Addition of Water to N_2O_4

A Pyrex storage bulb fitted with a Teflon stopcock was cleaned with hot concentrated hydrochloric acid and rinsed with demineralized water. After drying at 200 C for 2 days, a measured quantity of demineralized water was added to the bulb by means of a microliter syringe. Anhydrous N_2O_4 was distilled into the bulb after freezing the water with liquid nitrogen. The weight of N_2O_4 was determined by weight difference. Upon warming the frozen mixture, a visually homogeneous green solution was obtained. This liquid was transferred by means of gravity into ampoules which were clean, dry, and evacuated. The N_2O_4 was then froze in the ampoule and sealed under vacuum.

DISCUSSION AND RESULTS

Initial experiments were conducted with anhydrous iron-free N_2O_4 (< 0.1 ppm Fe and < 0.01 ppm water, by n.m.r. analysis).

Dissolution of Iron Powder

An experiment was conducted at 21 C in a glass/Teflon reaction cell using the aliquot technique that was described in detail in the Experimental Procedure Section. Five grams of iron powder and 113 grams of anhydrous

iron-free N_2O_4 were stirred continually with a glass-coated magnetic stirrer. One-milliliter aliquots of N_2O_4 were withdrawn through a sintered glass filter at 0.5, 6, 96, and 240 hours, respectively, and were analyzed for total iron (Appendix A). The results obtained are presented in Fig. 3. The total concentration of iron in the N_2O_4 increased to approximately 1.5 ppm within a period of a few hours and then remained nearly constant.

A number of difficulties were encountered with the glass/Teflon apparatus including (1) the possibility of leakage, (2) problems with temperature control, and (3) inability to use higher reaction temperatures (excessive vapor pressure). However, there is no basis for rejecting the experimental results reported in Fig. 3. To circumvent the preceding problems, the ampoule technique, described in detail in the Experimental Procedure Section was adopted.

Samples of iron powder and N_2O_4 were sealed in one end of an ampoule which contained a fritted glass disk at the center. In this procedure there was no agitation of the sample. At the conclusion of each experiment, the N_2O_4 was filtered through the disk to separate it from the iron powder, hydrolyzed with water, and analyzed for total iron. Using this technique, each ampoule provided one datum point.

Two series of experiments were conducted at 30 C in which 0.5 gram of iron powder was placed in contact with 10 grams of anhydrous iron-free N_2O_4 in each ampoule. The results are shown in Fig. 4 (Series I and II). The same trend appeared as in the preceding experiment, i.e., a rapid increase in the total concentration of soluble iron to a relatively constant value. However, the final iron concentrations were lower (approximately 0.5 and 1.0 ppm, respectively) than in the similar experiment in the glass/Teflon apparatus, and the presumably identical series of experiments shown in Fig. 4 did not yield the same final iron concentration.

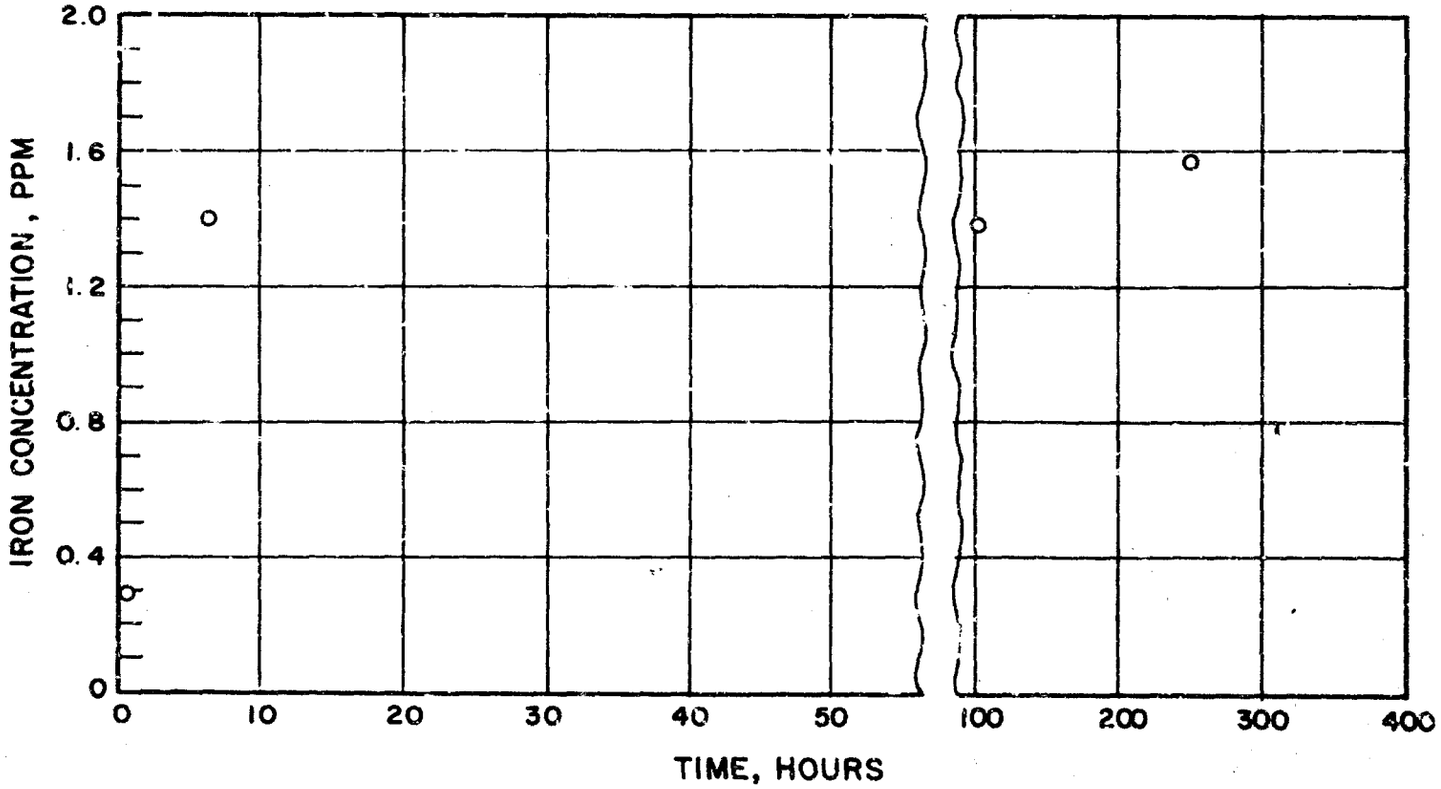

Figure 3. Dissolution of Iron Powder in Anhydrous N_2O_4 at 21 C.
(Glass/Teflon Apparatus, 5 grams Fe/113 grams N_2O_4)

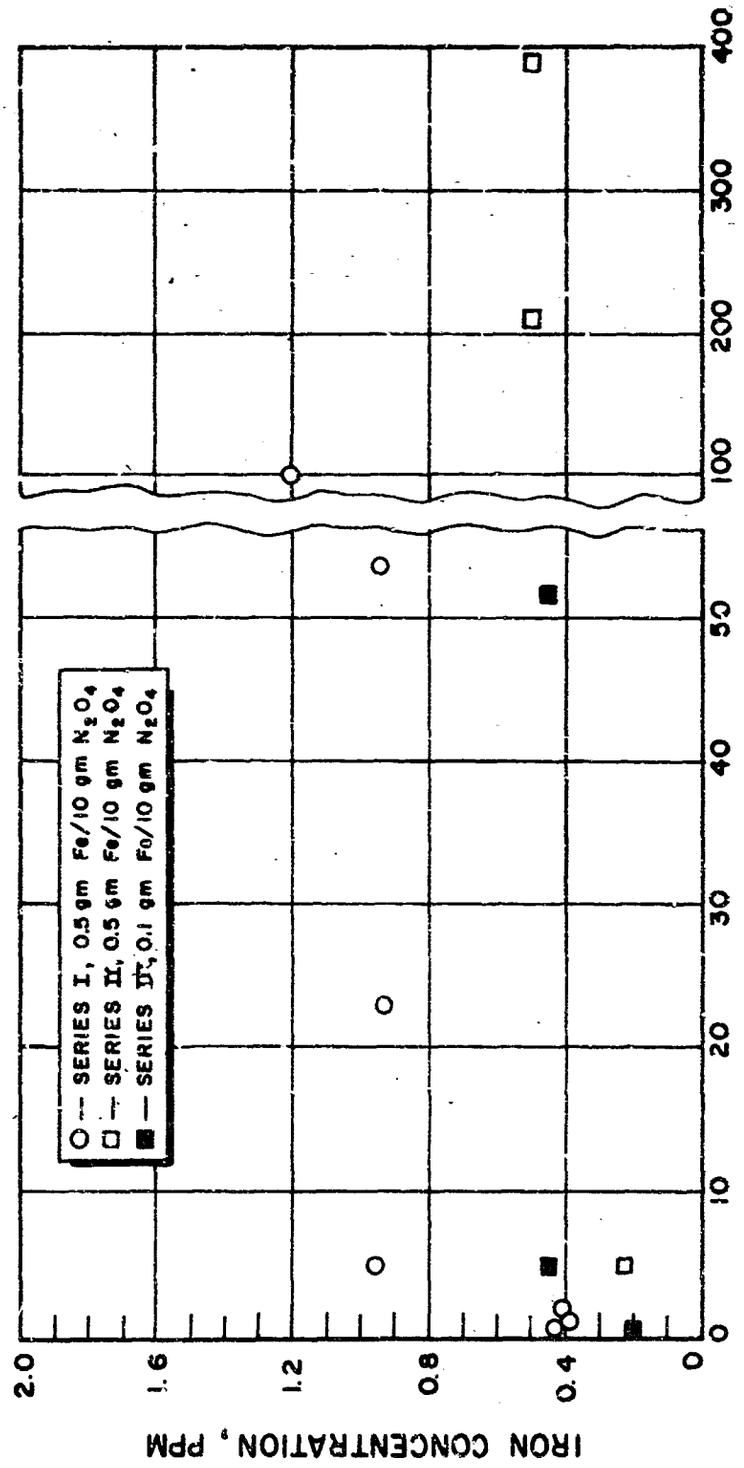

Figure 4. Dissolution of Iron Powder in Anhydrous N_2O_4 at 30° C. (Ampoule Technique)

A series of experiments was then conducted in which only 0.1 gram of iron powder was exposed to the 10 grams of N_2O_4. The results, shown in Fig. 4 (Series III), indicated that a reduction of the available surface area of the iron powder by a factor of five did not affect the final concentration of soluble iron when compared with the Series II experiments, or diminished it by only a factor of two if compared to the Series I experiments (Fig. 4). The method of analysis used to obtain all of the iron concentrations reported in Fig. 4 is presented in Appendix B.

A series of experiments was also conducted at 50 C in which 0.5-gram samples of iron powder were each exposed to 9 grams of anhydrous N_2O_4 in sealed ampoules. The hydrolyzed N_2O_4 solutions were analyzed directly for iron both by atomic absorption spectroscopy (Appendix C) and by the colorimetric 1,10-phenanthroline method (Appendix B) In addition, atomic absorption analyses were performed after the sample had been analyzed by the colorimetric technique. The results obtained are presented in Table 1. The reproducibility of this series of experiments was within the expected accuracy of the analytical methods, i.e., $\pm$0.2 ppm. Comparison of these results with those obtained at 30 C does not indicate any marked effect of temperature on the solubility of iron powder in anhydrous N_2O_4.

TABLE 1

DISSOLUTION OF IRON POWDER IN ANHYDROUS N_2O_4 AT 50 C

Contact Time, hours	Soluble Iron, ppm		
	Atomic Absorption Before Colorimetric Analyses	Colorimetric	Atomic Absorption After Colorimetric Analysis
0	---	< 0.1	---
41	0.6	0.4	0.3
41	0.3	0.1	0.1
70	0.2	0.1	0.1
70	0.5	0.6	0.6

In all of the experiments conducted with iron powder, the concentration of soluble iron leveled off with time. This behavior is compatible with several mechanisms:

1. An impurity or surface coating which is readily soluble in N_2O_4 is present initially in the metal powder, and the rate of dissolution of the metal itself is very slow.
2. The metal dissolves rapidly until a passive film is formed.
3. The iron species formed reaches a solubility limit in N_2O_4.

Mechanisms 1 and 2 would exhibit a proportionate decrease of the final concentration of iron as the size (total surface) of the iron sample was decreased. However, because this effect of sample size was not observed, it is probable that Mechanism 3 is actually operative in this reaction.

To establish the mechanism more firmly, an investigation was conducted of the possible formation of a passive film by successively exposing a single sample of iron powder to fresh portions of anhydrous iron-free N_2O_4. These experiments were conducted with a reaction cell that was identical to those used for the sealed ampoule experiments, with the exception that a Fischer-Porter Teflon metering valve was attached to the end opposite the iron sample. The results obtained with a single 0.5-gram sample of iron powder and successive 10-gram portions of N_2O_4 are presented in Table 2.

These results show conclusively that the low solubility of iron powder in anhydrous N_2O_4 cannot be attributed to the formation of a passive film. Combined with the previous data, they confirm the existence of a solubility limit which in this experiment was 0.7 ±0.2 ppm. The change in the solubility limit from experiment to experiment may have resulted from the presence of some unmeasured species, such as NOCl, the concentration of which varied in the N_2O_4 used for each series of experiments. The previous observation that the solubility is not appreciably affected by temperature is also substantiated.

TABLE 2

IRON POWDER SOLUBILITY* IN ANHYDROUS N_2O_4

Contact Time, hours	Temperature, C	Soluble Iron, ppm
18.5	30	0.7
7.5	30	0.7
17.0	30	0.9
72.0	30	0.9
167.0	30	0.9
22.0	30	0.8
24.0	30	0.8
4.0	30	0.7
102.5	30	0.7
7.0	50	0.5
66.0	50	0.7
4.5	50	0.5

*Determined by contacting an iron powder sample with successive portio of anhydrous N_2O_4

Dissolution of Iron Alloys

The rate of dissolution of steel disks in anhydrous N_2O_4 was measured using a modification of the sealed ampoule technique. The disks were 1/16 inch thick and 3/8 inch in diameter and weighed approximately 2.3 grams. Each disk was degreased with trichloroethylene and sealed in an ampoule containing 11 to 14 grams of purified N_2O_4. Because the disks could be readily removed from the N_2O_4, a fritted glass filter was not incorporated into these ampoules. The results presented in Table 3 were obtained at 30 C utilizing the analysis method described in Appendix B.

TABLE 3

DISSOLUTION OF STEEL IN ANHYDROUS N_2O_4

Sample	Contact Time, weeks	Soluble Iron, ppm
None	-	< 0.1
304 Stainless Steel	1	0.3
304 Stainless Steel	2	1.2
304 Stainless Steel	3	0.6
316 Stainless Steel	1	0.3
1018 Carbon Steel	1	2.7

A second set of experiments was conducted to determine if the high solubility of 1018 carbon steel in N_2O_4 (Table 3) was reproducible. Ampoules of the same type used in the repetitive washing experiments (containing a fritted glass filter) were used in this case. Two disks were degreased with trichloroethylene and the other two were cleaned and passivated by a tank passivation procedure recommended for this material (described in the Experimental Procedure Section). The disks were heated at 50 C for 265 hours in 20 to 25 grams of anhydrous N_2O_4. The results (employing atomic absorption analysis) are presented in Table 4.

TABLE 4

DISSOLUTION OF 1018 CARBON STEEL IN ANHYDROUS N_2O_4 AT 50 C

Pretreatment of Disks	Soluble Iron, ppm	Final Condition of Disk Surface
Cleaned and passivated	0.6	Tarnished
Cleaned and passivated	0.7	Tarnished
Degreased	0.6	Bright
Degreased	0.6	Bright

The discrepancy between that results and that presented in Table 3 is most likely caused by the absence of a fritted glass filter during the earlier experiment, which may have permitted small particles from the surface to remain in the N_2O_4. The results in Table 4 further support the existence of a solubility limit.

Dissolution of Iron Oxide Powder

The solubility and rate of dissolution of ferric oxide was studied because of the possibility of the presence of an initial oxide coating, or the formation of such a coating during the exposure of iron-containing alloys to N_2O_4. A series of ampoule experiments was conducted in which 0.05 gram of Fe_2O_3 powder was placed in 10 grams of anhydrous N_2O_4 at 30 C and then filtered out before analysis (Appendix B). The results are presented in Fig. 5. These data suggest that the concentration of soluble iron increases to a maximum and then decreases with time. However, because of the uncertainty of the chemical analysis ($\pm$0.2 ppm), the concentrations are equal within the experimental limits (i.e., 0.3 $\pm$0.2 ppm).

Addition of Water

The effect of the addition of 0.9 w/o water to the N_2O_4 on the rate of solution of iron powder was investigated at 30 C using the sealed ampoule technique. The results obtained from nine ampoules (0.5 gram iron/8 grams N_2O_4) are presented in Table 5 (Analysis Method in Appendix C).

A comparison of these results with those obtained with anhydrous N_2O_4 indicated that the rate of solution and the solubility limit were both increased in wet N_2O_4. During the last two experiments of the series, however, the iron powder was observed to be wetted with a viscous yellow liquid at the end of the experiment. In the case of the 354-hour experiment, the yellow liquid was observed to transfer across the glass frit

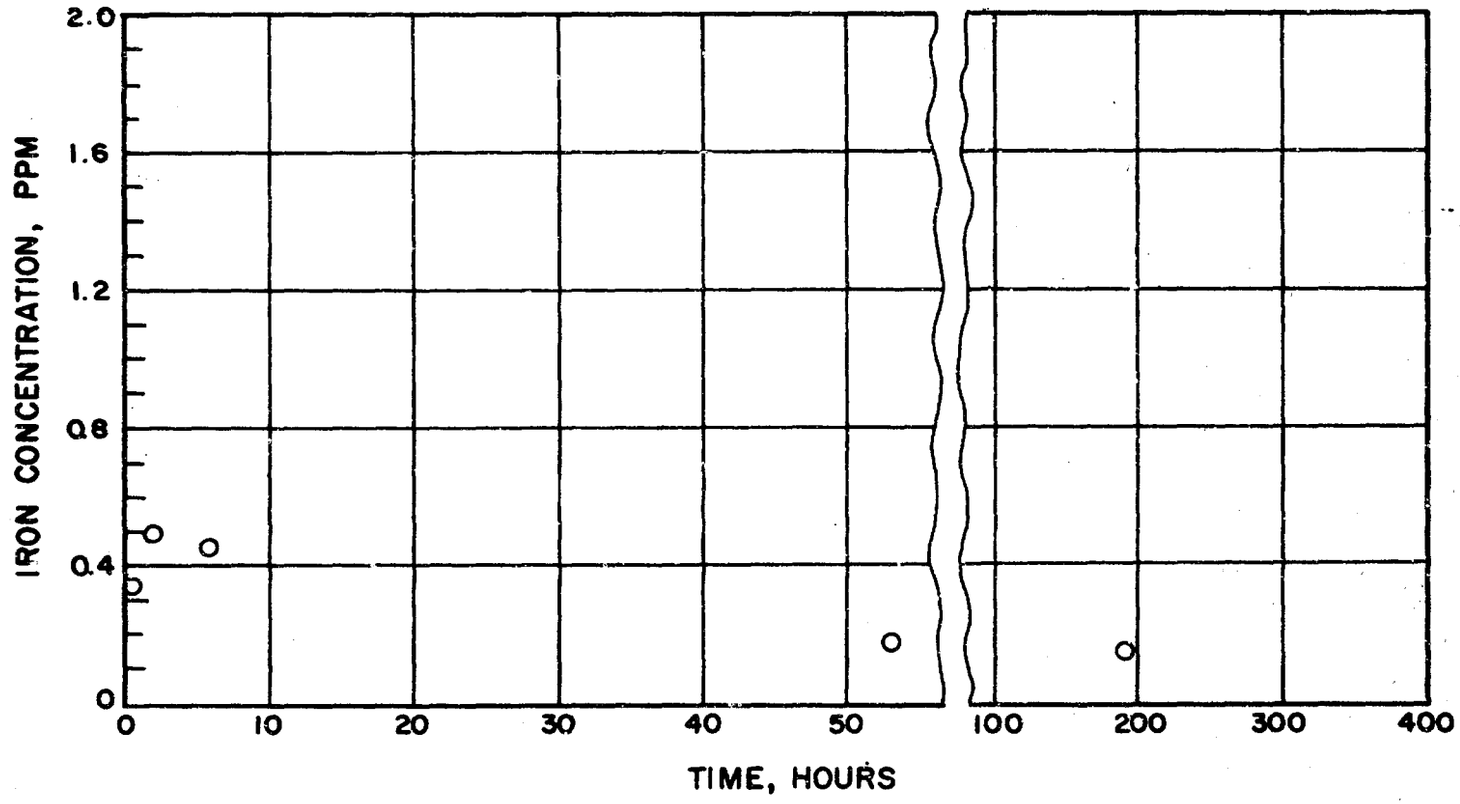

Figure 5. Dissolution of Iron Oxide Powder in Anhydrous N_2O_4 at 30 C. (Ampoule Technique, 0.05 gram Fe_2O_3/10 grams N_2O_4)

with the N_2O_4. This second liquid phase was observed only during the two longer experiments with wet N_2O_4. An aqueous phase could arise by the adsorption of water on the metal surface (or metal nitrate surface) in the form of concentrated nitric acid and would thus possess a very high concentration of ferric nitrate. Therefore, the iron concentrations listed in Table 5 may include iron which passed through the frit in the aqueous phase. This would explain the apparently high concentrations of iron after 188 and 354 hours.

TABLE 5

DISSOLUTION OF IRON POWDER IN WET (0.9 W/O WATER) N_2O_4 AT 30 C

Contact Time, hours	Soluble Iron, ppm	
0	0.01	0.06 (in duplicate)
0.1	0.7	1.4 (in duplicate)
0.5	1.0	1.0 (in duplicate)
2.0	1.8	2.0 (in duplicate)
19.0	1.8	
188.0	4.5*	
354.0	6.7*	

*Second phase observed

Effect of Filtering and Heating on Iron Content of Propellant Grade N_2O_4

To further explore possible effects of temperature soaking, two samples of propellant grade N_2O_4 [previously analyzed as containing 1.6 to 1.9 ppm soluble iron (Appendixes B and C)] were filtered through a glass frit (10 to 15 microns) and heated at 50 C in sealed ampoules for 25 hours. Upon hydrolysis and analysis (Appendix C), the samples were found to contain 0.6 and 1.0 ppm iron, respectively. A series of experiments was then conducted to distinguish the possible effects of filtration and

temperature on the amount of soluble iron. A portion of the same propellant grade N_2O_4 was filtered through a glass frit (10 to 15 microns) and separated into five 7-gram fractions each of which was sealed in a glass ampoule. Six other 7-gram samples of unfiltered N_2O_4 also were sealed in ampoules. Three ampoules of each set were maintained at room temperature for 72 hours while the remainder were heated to 50 C for 72 hours. The residue on the frit was dissolved in hydrochloric acid and analyzed for iron. The results are presented in Table 6.

TABLE 6

EFFECT OF FILTERING AND HEATING ON PROPELLANT N_2O_4
(Test Period: 72 Hours)

Filtered	Temperature, C	Soluble Iron, ppm
No	21	1.6
No	21	0.7
No	21	1.4
No	50	1.3
No	50	1.6
No	50	1.6
Yes	21	1.7
Yes	21	1.8
Yes	21	1.7
Yes	50	2.1
Yes	50	2.3

Note: Residue on frit: 115 micrograms/42 grams N_2O_4

No significant differences in iron concentration were observed among the samples which had received the various treatments. These results indicate that the filtering technique employed removes only the large iron-containing particles which occasionally exit from the container with the propellant grade N_2O_4, and that heating does not reduce the concentration of soluble iron. No explanation is apparent for the loss of iron during the first two experiments reported in this section.

CONCLUSIONS

The amount of iron which can be dissolved in anhydrous N_2O_4 from iron powder, iron oxide powder, or steel alloys at 30 or 50 C is 0.5 to 1.5 ppm. The iron concentration is apparently limited by the solubility of the iron compound(s) which forms in N_2O_4; a completely insoluble passive film does not form on the iron surface. The addition of 0.9 w/o water to the N_2O_4 may increase the iron solubility limit and a second liquid phase is formed after prolonged contact of the "wet" N_2O_4 with iron powder.

A sample of propellant-grade N_2O_4 which had been stored in a small steel laboratory container for more than 1 year was repeatedly found to contain approximately 1.5 ppm soluble iron. Filtering and heating of this propellant-grade N_2O_4, under the limited conditions employed in this study, did not affect the concentration of soluble iron.

The results obtained in this task, combined with those reported in Phase III from the solubility studies of synthetically prepared N_2O_4-solvated iron nitrate, indicate that the flow-decay deposit must result from an iron species which is present in N_2O_4 at low concentrations.

PHASE II: COMPOUND IDENTIFICATION

INTRODUCTION

The objective of this task was to determine the structure of species involved in the flow-decay process. The various techniques available were evaluated and five approaches were investigated. Model compounds and "synthetic flow-decay material" (synthesized under Phase III of this program) were studied with the goal of developing methods to determine the structure of the iron-containing species that can exist in N_2O_4, and the structure of the actual flow-decay deposit when it became available again.

The n.m.r. spectrum of solid $Fe(NO_3)_3 \cdot N_2O_4$ was investigated first. The primary difficulty with this approach was that single crystal samples were not available. N^{14} n.m.r. requires a single crystal because of the large crystallite-angle-dependent splitting of the N^{14} resonance; in a powder, this results in too broad a spectrum. Therefore, the approach attempted was detection of resonances of N^{15} which has a natural abundance of only 0.365 percent. N^{15} has spin 1/2 and no quadrupole broadening resulting in n.m.r. spectra with very low signal-to-noise ratios.

The second approach was the construction of a nuclear quadrupole resonance (n.q.r.) spectrometer for detection of N^{14} quadrupole resonance frequencies. Because pure quadrupole resonance spectrometry is accomplished in the absence of a magnetic field, the N^{14} spectrum (which is normally too broadened for powdered samples because of random orientation of electric field gradients) would be resolvable, and various kinds of nitrogen could be identified. This approach had the potential of allowing observation of separate resonances for NO_3^-, NO_2^+, NO^+, N_2O_4, and NO_2 groups, but considerable further effort probably would have been required. The instrument was nearly completed, but the spectra of $Fe(NO_3)_3 \cdot N_2O_4$ samples were not taken because of a shift of emphasis in the program.

The third approach was an initial study to determine the effect of water on the iron species formed in N_2O_4. Military specification N_2O_4 may contain up to 0.1 percent water, and it is important to establish whether this water could enter into the coordination sphere of iron in the iron nitrate species. To this end, broad-line H^1 n.m.r. studies were made to determine: (1) if water is indeed incorporated into dry $Fe(NO_3)_3 \cdot N_2O_4$ on exposure to "wet" N_2O_4, and (2) the actual state of this water, i.e., whether it exists in the crystals as -OH, HNO_3, or H_2O.

The fourth approach was to investigate the possibilities of using e.p.r. spectrometry to determine structural parameters of both solid and dissolved iron nitrate. The final approach of this phase was that of using Mossbauer spectrometry to determine the structure of the solid compounds of interest. (The use of infrared spectrophotometry and X-ray diffraction for compound identification is reported under Phase III.)

When it was found, in other tasks of the program, that iron compounds had only a very low solubility in N_2O_4, it became apparent that none of the techniques investigated, except possibly e.p.r., was sufficiently sensitive to determine the structure of the iron species as they exist in solution in N_2O_4. It was found, also, that the e.p.r. method was not suitable because the resonance for ferric iron is apparently masked by the NO_2 resonance at approximately the same g value. As for identification of the actual flow-decay compound, none of the techniques investigated were developed to the point where they would be suitable without further work.

DISCUSSION AND RESULTS

Nitrogen 15 Resonance Studies

The large chemical shifts of N^{15} resonances (large enough that the first observation of the chemical shift phenomenon was made on the two nitrogen isotopes in H_4NO_3) make attractive the possibility of determining the

structural components of iron nitrates by running a spectrum at the N^{15} resonance frequency. Although N^{14} is the more abundant isotope, the large electric quadrupole splittings result in too broad an n.m.r. spectrum of a powder sample (thousands of gauss), whereas N^{15} (S = 1/2) has no quadrupole moment and does not broaden the spectral features. Thus, a potentially useful spectrum can be obtained from N^{15}.

The C^{13} resonance was observed in compounds containing C^{13} in natural abundance. In this case, a Varian high-resolution RF unit and a Varian lock-in amplifier were used. Based on this experience, a study of N^{15} resonance was initiated. Because a high-resolution RF unit was not available for the N^{15} frequency, a variable-frequency Varian RF unit was employed, together with a Princeton Applied Research lock-in amplifier (PAR). The latter has approximately 10 times the sensitivity of the Varian lock-in amplifier. No resonances were observed even in a single crystal of $NaNO_3$ (which contained N^{15} in natural abundance). It was concluded, therefore, that the variable-frequency Varian RF unit had a much lower sensitivity than the high-resolution unit, which could not be compensated for by the very high sensitivity of the PAR. It was believed, however, that because of the expected narrow N^{15} lines, the problem would not be solved entirely by changing the RF unit, and that a higher sensitivity was necessary. Conversion of the variable RF unit to a high-resolution unit was initiated, and a new technique was developed to increase the sensitivity of narrow n.m.r. lines. At the same time, considerable enhancement of resolution was achieved.

It is believed that narrow N^{15} lines will result from some of the nitrogen species in $Fe(NO_3)_3 \cdot N_2O_4$ because they are largely surrounded by oxygen atoms which have no magnetic moment and, therefore, give no nuclear magnetic dipolar broadening of the adjacent N^{15}. Under these conditions, there are very long relaxation times. It is well known that long relaxation times are best controlled by lock-in amplifier techniques; however, when an n.m.r. line is sharp, existing high-frequency lock-in amplifier methods do not give high sensitivity.

The basis of the new technique is that an n.m.r. signal will have maximum intensity when the width of the modulating magnetic field used for lock-in amplifier detection is comparable to the natural n.m.r. line width. To test the sensitivity of the PAR, which can operate as low as 1.5 Hz, and remain compatible with any conceivable N^{15} line width (whether in solution or in a solid), the following study was conducted on the H^1 spectrum of ethyl alcohol at 60 MHz.

With the Varian high-resolution RF unit operating at 60 MHz, the magnetic field homogeneity coils were adjusted by running with regular high resolution so that the adjustments could be made on the oscilloscope (such adjustment cannot be made while using the lock-in amplifier because the spectral line is not displayed on the oscilloscope). The output of the RF receiver was then connected to the PAR through the recorder outlet with the recorder level set at 1000. This connection was necessary to optimize the impedance match of the RF receiver output circuit to that of the PAR input circuit. The internal sinusoidal voltage of the PAR was connected to the Varian probe Helmholtz coils through a 600-ohm series resistor, with the reference attenuator and vernier of the PAR set at maximum resistance. This was done to achieve a modulating magnetic field width slightly less than the frequency of the modulating field used for detection (PAR set at minimum of 1.5 Hz). The sensitivity of the PAR was set at 20 millivolts, the phase at 0, the time constant 300 seconds at 12 decibels, and Q=25. The RF power level was down 70 decibels from 0.25 watt. The receiver gain was set at position 5, and the RF phase detector frequency response in the 4 position.

Using the above technique, the following spectra were obtained. The entire ethyl alcohol spectrum is shown in Fig. [illegible] This spectrum is identical in resolution to that obtained on a Varian A-60 spectrometer. The spectrum is the second derivative of the absorption mode, which accounts for the deep wings on each side of a spectral line. These wings cause the progressive deepening of the apparent base line toward the middle of a multiplet.

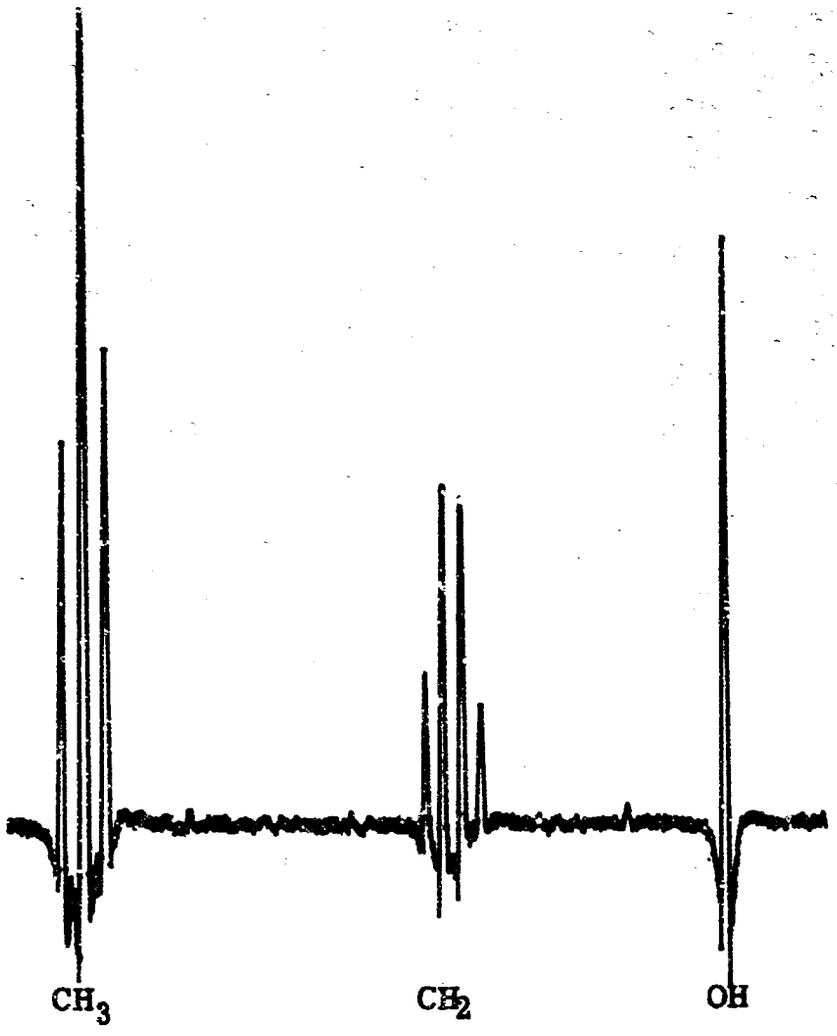

Figure 6. Spectrum of Ethyl Alcohol Obtained With New Rocketdyne Technique. Second Derivative Recorder Display

The spectrum of the ethyl alcohol quartet is presented in Fig. 7 , employing a slower passage than for the complete spectrum (Fig. 6). Immediately prior to running the spectrum of the quartet shown in Fig. 7 , an ordinary high resolution spectrum was run (Fig. 8). It is evident that the PAR method effects considerable enhancement in splitting of the individual lines of the quartet into their fine structure components. Comparing Fig 7 and 8 , it is seen that the method yields a better resolution than the ordinary high-resolution technique. An additional advantage of the new Rocketdyne method is that line voltage surges and other instabilities caused by opening of laboratory doors (with attendent pressure change effect on electronic components) can be damped with the larger output time constants available through use of the PAR. The high-resolution spectrum displayed in Fig. 8 is the best one selected from approximately 15 successively run spectra. However, the spectrum in Fig. 7 was obtained repeatedly without noise spikes and distortions.

In addition to eliminating noise-generated spectral distortions, the PAR method has another advantage. As summarized by Challice and Clark (Ref. 2), there is considerable literature dealing with the subject of resolution enhancement of spectra by means of second derivative recording. Resolution is easily doubled, while an isolated doublet which visually shows no splitting can be mathematically resolved into two spectral lines by comparing a function of the ratio of central peak height to wing depth of the second derivative-displayed spectrum. This procedure gives approximately a factor of eight in improved resolution over that obtained from the direct absorption mode display.

This is the first time that the use of broad-line techniques has been applied to the observation of high-resolution spectra. Thus, the difference between the two techniques has been reduced to a semantic one.

Sensitivity enhancement can be achieved by using a low-frequency lock-in amplifier such as the PAR. Improvement in signal-to-noise ratio by a factor of approximately 350 over that available with ordinary high-resolution absorption mode display is easily achieved. However, the

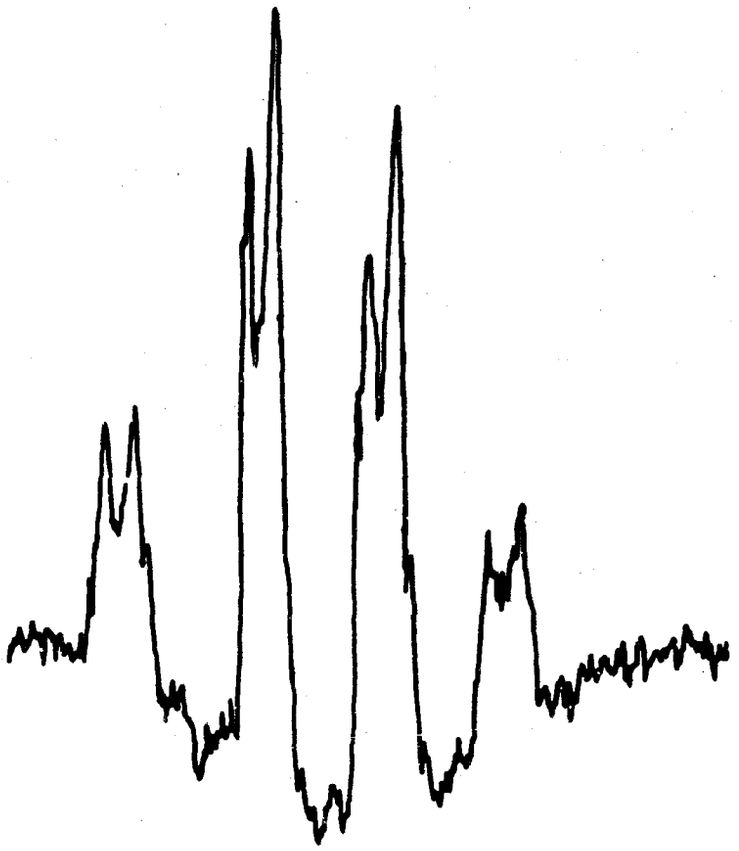

Figure 7. Spectrum of Ethyl Alcohol Methylene Group Quartet Obtained With New Rocketdyne Technique. Second Derivative Recorder Display

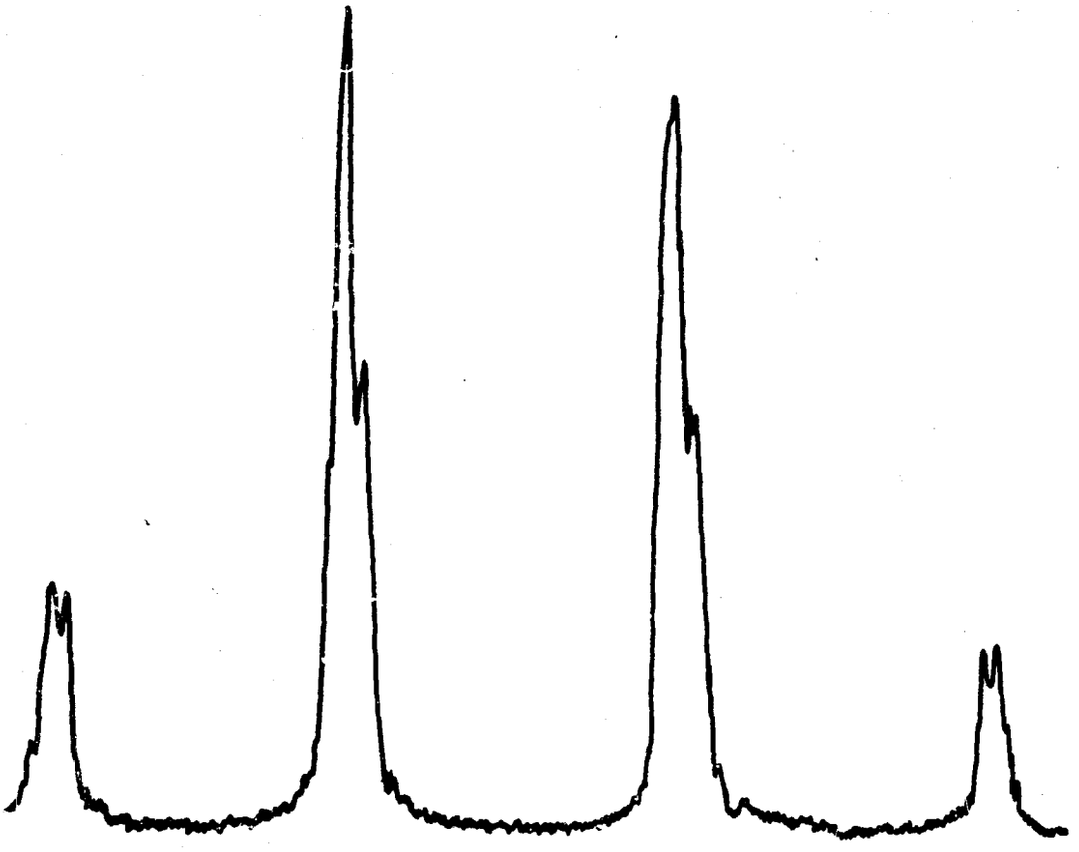

Figure 8. High-Resolution Spectrum of Ethyl Alcohol Methylene Group Quartet Run Just Before the Spectrum of Fig. 7 so as to Show Comparison of Resolution Obtainable by the Two Techniques

spectrum must be run much slower than those reported here; it would take 24 hours to optimize the PAR spectrum, but considering the number of high-resolution scans (approximately 15 minutes per scan) required for a computer-averaging technique to duplicate such an enhancement, i.e., 350 squared = 120,000, it would take approximately 3-1/2 years. Further N^{15} resonance studies related to the identification of the flow-decay species are recommended.

Broad-Line H^1 n.m.r. $Fe(NO_3)_3 \cdot N_2O_4$ Studies

The available data on the structure of the flow-decay material indicate that it is an N_2O_4 solvated iron nitrate. However, because of the normal presence of small amounts of water in the propellant, and the extremely strong coordinating reaction between water and iron nitrate, (Ref. 3 through 8) it was believed important to consider the posibility of partial hydration of the solvated iron nitrate.

Accordingly, a nuclear magnetic resonance H^1 study was conducted. There was some doubt that protons could be detected when close to the paramagnetic iron. To ascertain whether the protons could be detected by n.m.r. techniques in hydrated paramagnetic iron compounds, a sample of $Fe(NO_3)_3 \cdot 9H_2O$ was studied. The proton spectrum in Fig. 9 , which consisted of three lines, each of 25-gauss half-widths, for the particular crystal orientation employed, showed that the protons in the water of hydration could be seen. The spectrum was obtained using a Varian Associates high-resolution 60 MHz radio frequency unit coupled with a lock-in amplifier. A 4-gauss-width modulating field was employed with 0.5-watt radio-frequency power. The field sweep was the fastest rate of the magnet flux stabilizer. The multiplicity of the spectrum ruled out the possibility that saturated solution trapped in crystal cavities was responsible for the signals, because such a solution would yield a single broad line.

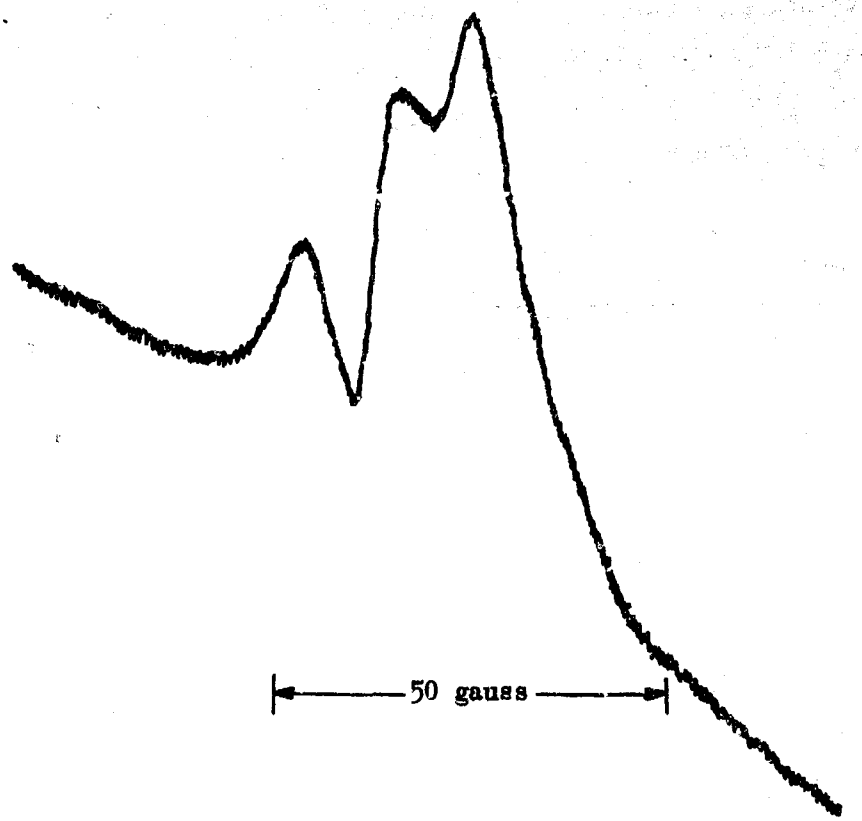

Figure 9. Proton n.m.r. Spectrum of Single Crystal $Fe(NO_3)_3 \cdot 9H_2O$ at 60 MHz and 25 C

The broad-line H^1 n.m.r. technique was improved further and used (1) in an attempt to determine the presence of water in synthetic $Fe(NO_3)_3 \cdot N_2O_4$ which had been refluxed in "wet" N_2O_4, and (2) to ascertain the structure of the solid formed. These studies were made using a modulating field of 1 gauss at 40 cycles, and a PAR lock-in amplifier. The RF receiver output to the lock-in amplifier was connected to the high-resolution recorder output so it would match the impedance with that of the lock-in amplifier better than can be done with the regular Varian cathode follower output used for the Varian output-control unit.

Figure 10 shows the spectra of the empty sample tube, a single crystal of iron nitrate nonahydrate, and 0.5 gram of synthesized anhydrous iron nitrate (solvated with N_2O_4) which had been refluxed for 48 hours with 30 milliliters of N_2O_4 containing 0.2 percent added H_2O. Comparison of the spectrum of the refluxed sample with that of the empty tube (by subtracting the background signal algebraically) shows a signal in the same position as is seen for the (much larger) sample of known iron nitrate hydrate, and roughly in proportion to the known weights of the samples. On the basis of these spectra alone, it is possible to determine only that water is present in some amount but not how many water molecules are present per iron molecule. Reference to the e.p.r. studies in this report confirm that a change occurs on refluxing the synthesized anhydrous iron nitrate in wet N_2O_4.

e.p.r. Studies of Iron Nitrates

Solids. To investigate the possibilities of using e.p.r. techniques to determine structural parameters of the iron nitrate compound which causes flow stoppage in valves, four samples of iron nitrate were studied. All spectra were run at room temperature with a 9.5×10^9 Hz spectrometer on samples contained in 5-millimeter OD Pyrex tubes.

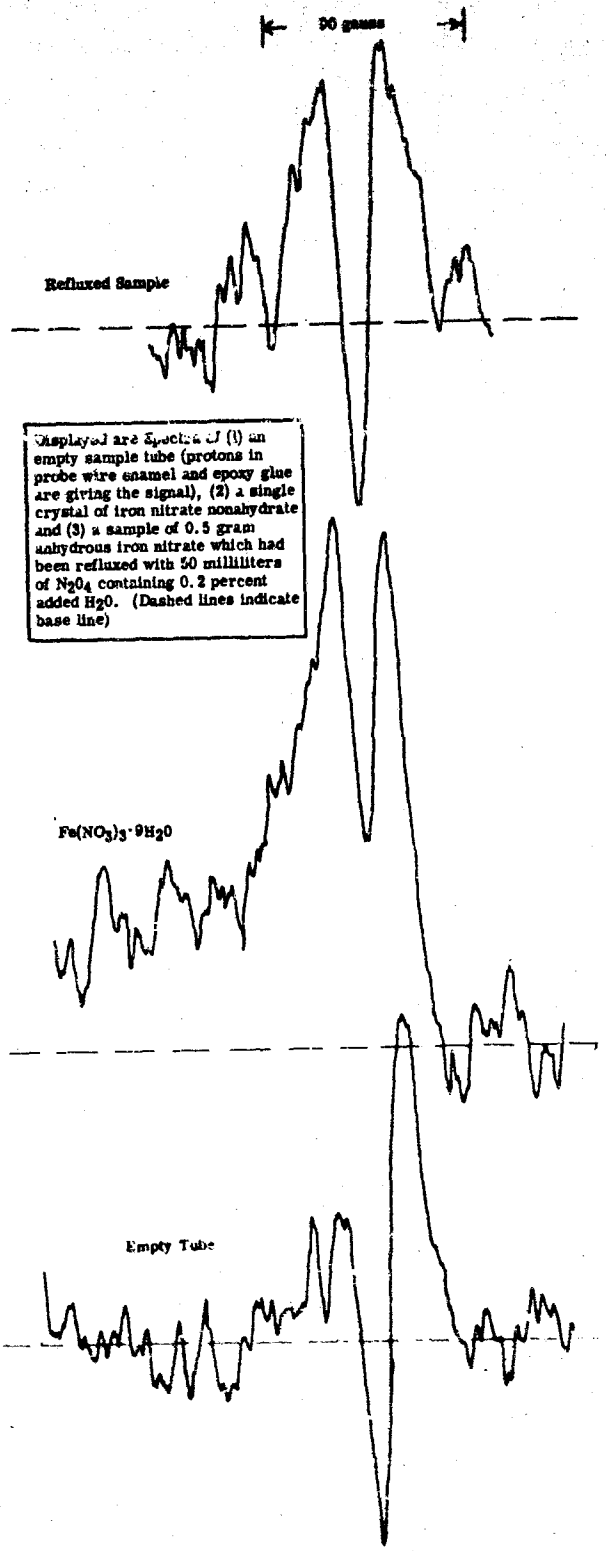

Figure 10. Broad-Line H^1 n.m.r. Spectra at 60 MHz, RF Power 0.5 Watt, Modulating Field 1 Gauss at 40 Cycles, PAR Lock-in Amplifier, Varian DP-60 High Resolution Spectrometer

The spectrum of a sample of $Fe(NO_3)_3 \cdot 9H_2O$ is shown in Fig. 11. The sample was a large, single crystal. It is expected that if a powdered sample were studied, the spectral structure at the higher fields would be broadened to correspond more closely in appearance to the spectra of the refluxed and purified samples displayed below it. The spectrum of a sample of $Fe(NO_3)_3 \cdot N_2O_4$, which had been purified (in Phase III) by precipitation of crude $Fe(NO_3)_3 \cdot N_2O_4$ dissolved in ethyl acetate by the addition of dry N_2O_4, is shown in the same illustration. For comparison, the spectrum of the same material is shown after a 0.5-gram sample had been refluxed with a 30-milliliter sample of N_2O_4 containing 0.2 percent H_2O. It is clear that the treatment with wet N_2O_4 caused structural changes. This evidence is compatible with the hypothesis that $Fe(NO_3)_3 \cdot N_2O_4$ powder in equilibrium with wet N_2O_4 contains some water of hydration.

Solution. The e.p.r. spectrum of propellant-grade N_2O_4 containing 1.5 ppm Fe and 0.1 percent H_2O is shown in Fig. 12. The sample was taken from a carbon steel cylinder in which the N_2O_4 had been stored for several months. The large truncated central dispersion mode line is caused by NO_2 (Ref. 9), but the source of the asymmetric peak on the left of the spectrum is unknown. Although normally coordinated ferric iron would be expected to be under the large NO_2 peak at $g = 2$, it was hoped that the smaller peak would be that of some iron-containing species of interest to the current program.

The spectrum of distilled iron-free N_2O_4 was found to be the same as that of Fig. 12, indicating that the observed peaks were not caused by iron species. The smaller peak apparently results from some impurity in the N_2O_4 which is not removed during distillation. This small peak at $g = 2.7$ is not the expected position for NO (Ref. 10), and addition of NO to an N_2O_4 sample did not increase the magnitude of this peak.

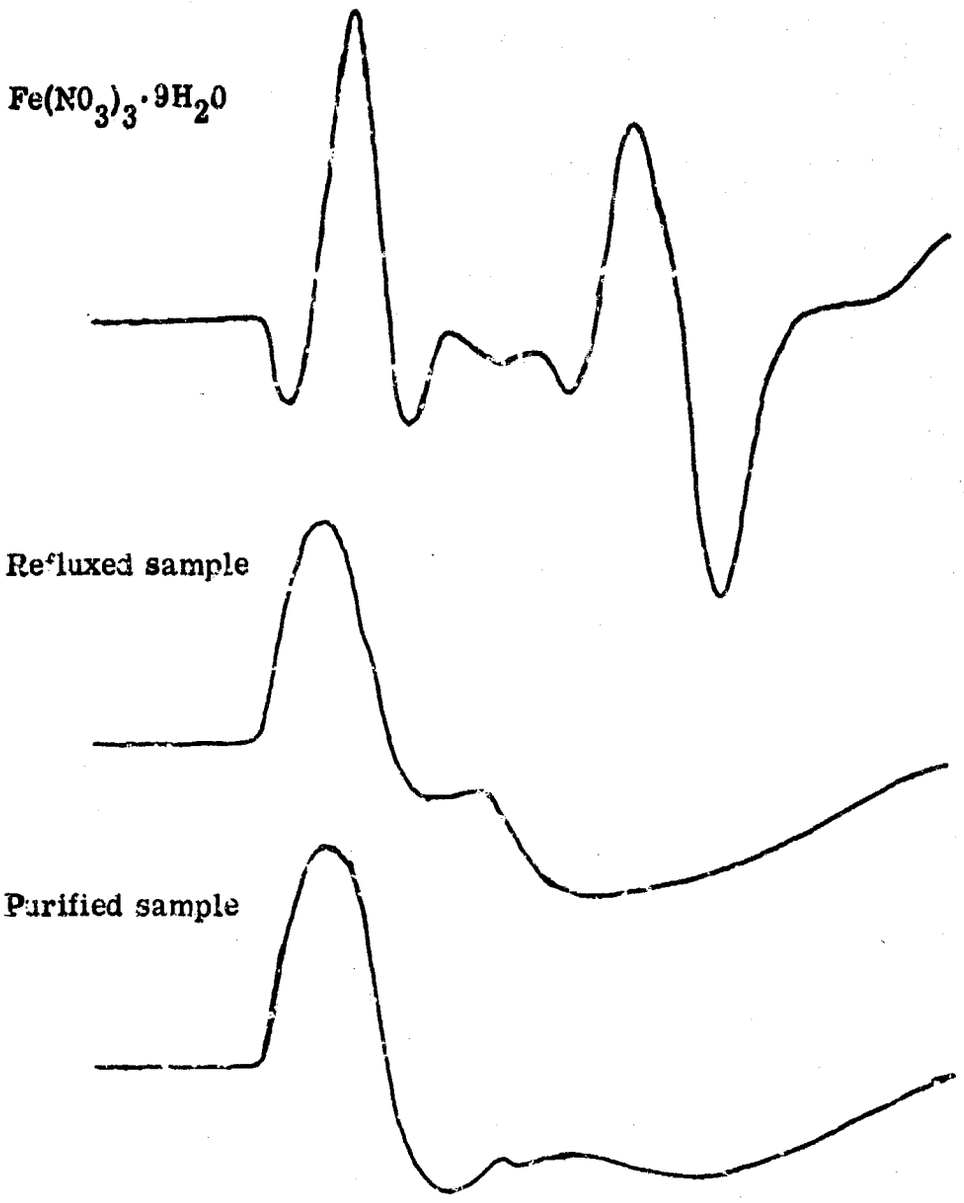

Figure 11. e.p.r. Spectra of a Single Crystal of Nonahydrous/Iron Nitrate, Purified $Fe(NO_3)_3 \cdot N_2O_4$, and Purified Material Which had Been Refluxed with N_2O_4 Containing 0.2 Percent H_2O. Ordinates are 0 to 6600 Gauss

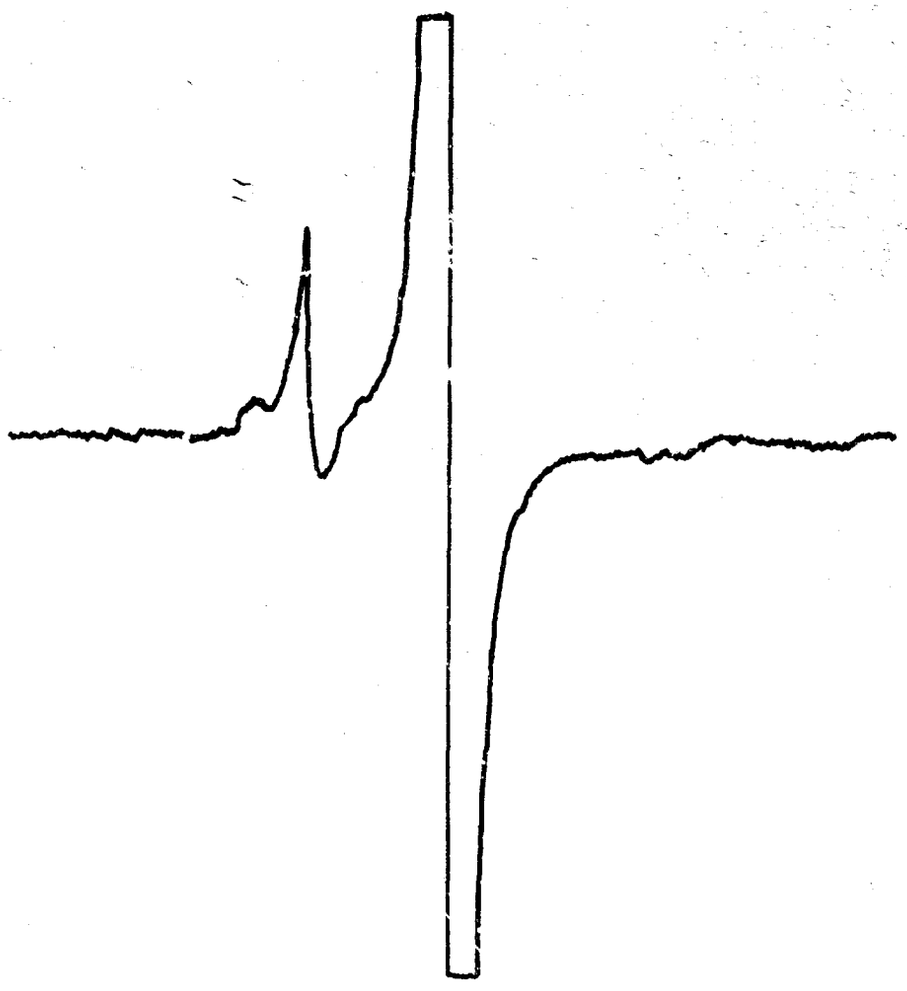

Figure 12. e.p.r. Spectrum of N_2O_4 Containing 1.5 ppm Fe and 0.1 Percent H_2O. Ordinates are 0 to 6000 Gauss. Truncated Central Dispersion Mode Line is Due to NO_2, and the Asymmetric Peak on the Left is Also Found in Fe-Free N_2O_4

Mossbauer Spectroscopy

A Mossbauer spectrum was taken of the anhydrous synthetic $Fe(NO_3)_3 \cdot N_2O_4$ (prepared in Phase III) to characterize this material more fully and to determine if this technique would be useful in determining the structure of the actual flow-decay material. The spectrum (Fig. 13) was obtained using a single line Co^{57} in Cu source at room temperature and a room-temperature sample. The sample was carefully handled and stored in an inert N_2 atmosphere while preparing the absorber and during the experiment. The isomer shift observed in Fig. 13 is ~0.25 mm/sec. The broad line width is probably caused by a fairly long spin-spin relaxation time. The absence of a sizable quadrupole splitting in Fig. 13 suggests that the iron site (or sites) has essentially undistorted octahedral or tetrahedral symmetry. If more than one site exists, the sites must be quite similar.

The spectrum observed for $Fe(NO_3)_3 \cdot N_2O_4$ is quite different from that of $Fe(NO_3)_3 \cdot 9\ H_2O$, which has a shift ~ 0.1 mm/sec less than the $Fe(NO_3)_3 \cdot N_2O_4$ and has a line width approximately twice as broad. The spectrum does not resemble spectra of the simple iron oxides, at least in bulk form.

If sufficient quantities of the actual flow-decay material can be obtained, a Mossbauer analysis would indicate if it has the same symmetry around the iron site(s) as does the synthetic $Fe(NO_3)_3 \cdot N_2O_4$. If it were found to be unsymmetrical, further evidence could be obtained regarding the nature of the species bound to the iron atoms.

CONCLUSIONS

The N^{14} n.m.r. spectrum of solid $Fe(NO_3)_3 \cdot N_2O_4$ is too broad to be useful, unless a single crystal of the material is available. The N^{15} n.m.r. spectrum may give useful information on the structure of the flow-decay solid material. Techniques have been partially developed that will

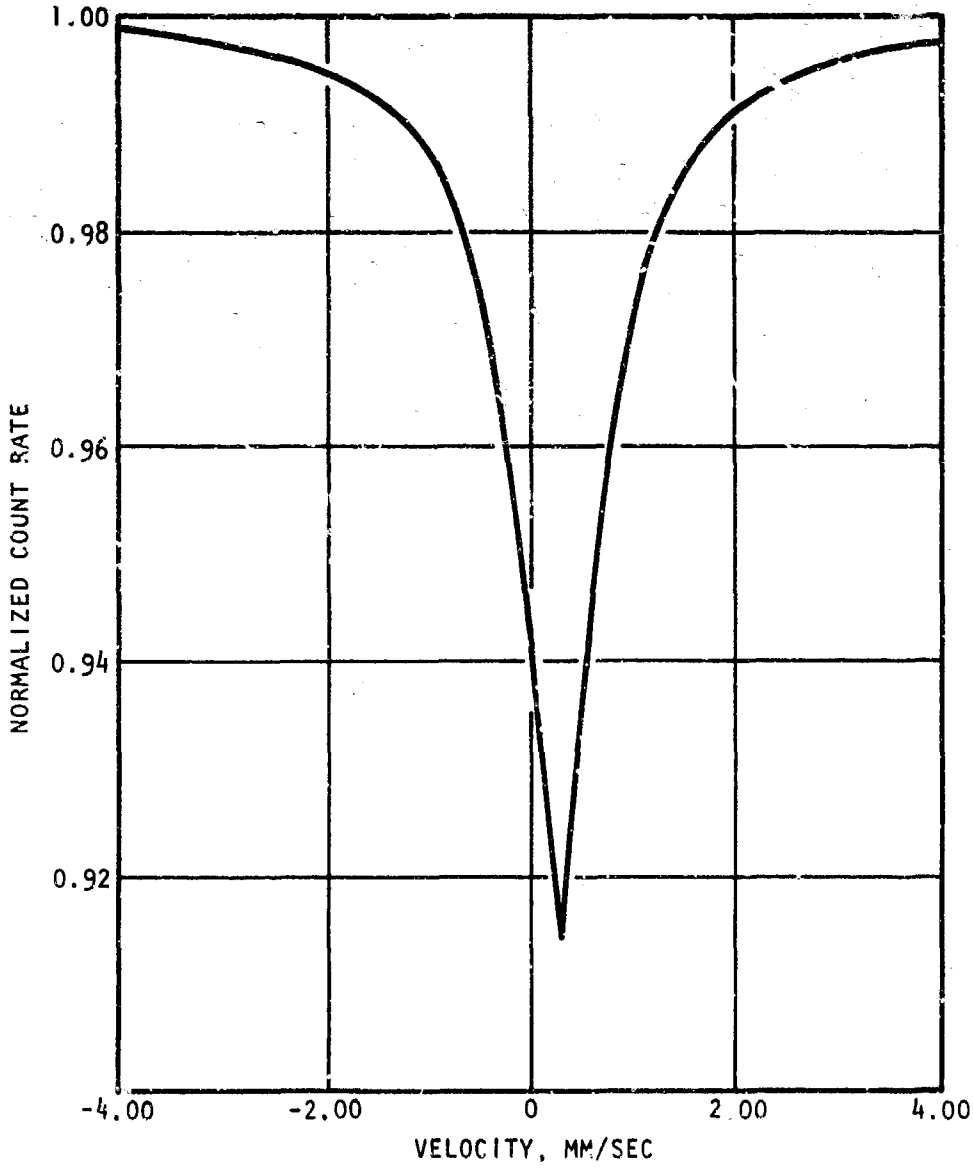

Figure 13. Mossbauer Spectrum of Solid Synthetic $Fe(NO_3)_3 \cdot N_2O_4$

probably permit the sensitivity of the N^{15} n.m.r. technique to be increased to the point where the natural abundance of N^{15} in the solid becomes observable. The n.q.r. spectrum of N^{14} may permit the various kinds of nitrogen-containing groups to be identified in solids. Considerable additional effort would be required to increase the signal-to-noise ratio of the broad-line H^1 n.m.r. spectrum of iron nitrates to a useful level for detailed structural studies of water-containing iron nitrates. The technique of e.p.r. spectroscopy is apparently sensitive enough for structure studies of iron nitrate species even in dilute solution. Unfortunately, the iron resonance is masked by the NO_2 resonance in N_2O_4, precluding the use of e.p.r. in these studies. Mossbauer spectrometry has shown that the iron site(s) in synthetic anhydrous $Fe(NO_3)_3 \cdot N_2O_4$ has essentially undistorted octahedral or tetrahedral symmetry, and that all of the iron sites are quite similar. This technique is capable of determining if the iron atoms in the actual flow-decay material exist in environments similar to those in the synthetic flow-decay material.

PHASE III: COMPOUND SOLUBILITY

INTRODUCTION

The objectives as outlined in the statement of work have been successfully met. A compound of the composition $Fe(NO_3)_3 \cdot N_2O_4$ [structurally: $NOFe(NO_3)_4$] was shown to be identical with the flow-decay deposit isolated at the USEFF facility (Ref. 1) and was successfully prepared and purified in sufficient quantities to meet the needs of all of the phases of the program. When, subsequently, the actual flow-decay material (flow bench, Phase V) was isolated, it was possible to establish unequivocally the identity of this synthetic material [$NOFe(NO_3)_4$] with the actual flow-decay compound. Infrared and X-ray spectroscopy have clearly established this identity.

When sufficient quantities of the iron nitrate had been prepared, solubility studies with N_2O_4 were conducted in freshly distilled, anhydrous, iron-free N_2O_4, over the temperature range 0 to 37.8 C (32 to 100 F). Solubility studies of the iron nitrate in N_2O_4 in the presence of small concentrations of nitric oxide (0 to 1 w/o) and water (0.1 and 0.5 w/o) were also conducted. Significant data have been obtained which tend to refute earlier projections that the solubility of iron species in N_2O_4 were much higher than have actually been found.

EXPERIMENTAL DETAILS

Preparation of (NO^+) $[Fe(NO_3)_4]^-$

Nitrogen tetroxide (>300 millimoles) was condensed in one bulb of a two-bulb reactor equipped with Fischer-Porter needle valves. Iron pentacarbonyl (9.2 millimoles) which had been purified by fractional condensation was then condensed into the second bulb. N_2O_4 was added slowly to the $Fe(CO)_5$ by opening a needle valve between the two bulbs. The reaction was stirred magnetically and maintained in the vicinity of -20 C while the

N_2O_4 was being added. A rapid reaction occurred with the formation of a brown solid and the evolution of a considerable amount of gas. The gas was pumped off using a Sprengel system and was measured. The amount of carbon monoxide collected was 43.2 millimoles (theory = 45.9 millimoles). The solid was left in the excess N_2O_4 overnight at room temperature. A light brown solid (2.5 grams) was isolated when the excess N_2O_4 and NO were extracted under a vacuum. Analysis of this crude material yielded the following results: Fe, 11.7 w/o; NO_3^-, 35.9 w/o; N_2O_4, 48.1 w/o; and unknown impurities, 4.3 w/o.

A second run (approximately a tenfold scale-up) was conducted under similar conditions, but no attempt was made to collect the evolved gases. This reaction yielded approximately 20 grams of the identical light brown product.

Purification of $Fe(NO_3)_3 \cdot xN_2O_4$

Purification of the crude material was attempted by recrystallization from purified N_2O_4. A Soxhlet extraction apparatus was modified for this purpose. Finely ground crude material (0.5 gram) was placed in a glass thimble and the complete apparatus was assembled in a dry box. The extraction apparatus was evacuated on the high vacuum system and N_2O_4 (75 milliliters) was condensed into it. A small deposit of a solid was noted in the pot after 1 day of extraction. After 1 week of extraction, 20 milligrams of the purified material were collected. The following analytical results were obtained for the purified material: Fe, 15.5 w/o; NO_3^-, 54.9 w/o; N_2O_4, 26.1 w/o and unknown impurities, 3.5 w/o. The theoretical values for (NO^+) $[Fe(NO)_4]$ or $Fe(NO_3)_3 \cdot N_2O_4$ are: Fe, 15.7 w/o; NO_3, 55.7 w/o and N_2O_4, 27.6 w/o). It should be emphasized that the value for unknown impurities is obtained by difference. Therefore, it includes the summation of all errors which may be present in the analytical scheme in addition to any impurities which actually may be present in the sample. A mass balance of greater than 95 percent is generally considered acceptable for this type of analysis.

The second method of purification which was investigated was the recrystallization from ethyl acetate. Approximately 2 grams of the crude material was placed in ethyl acetate and the small amount of undissolved impurities was filtered off. The filtrate was then concentrated by removing the solvent under evacuation. To the resulting reddish brown syrup, a large excess of N_2O_4 was added. An immediate precipitation of a solid occurred. The mixture was filtered and then the solid was washed several times with fresh N_2O_4. The following analytical results were obtained for the purified material: Fe, 16.0 w/o; NO_3^-, 55.2 w/o; N_2O_4, 27.2 w/o; and unknown impurities, 1.6 w/o.

A larger sample of crude iron nitrate (6.5 grams) was similarly purified. The analytical results on a sample of this second batch of purified material were as follows: Fe, 16.5 w/o; NO_3^-, 55.2 w/o; N_2O_4, 26.9 w/o; and unknown impurities, 0.4 w/o.

The infrared spectra, as mulls in halocarbon oil, of the purified materials were identical. Their physical appearances (pale brown powders) and their reactivities with moisture (rapidly becoming wet and the evolution of gases accompanied by bubbling effect) were also identical.

Analysis of $Fe(NO_3)_3 \cdot xN_2O_4$

The following analytical procedure has been used in the analysis of the iron nitrate-N_2O_4 complex.

The weighed sample was dissolved in water. Each N_2O_4 forms one NO_3^- and one NO_2^- ion. The percent N_2O_4 was obtained by determining the nitrite ion in the aqueous solution. An aliquot was introduced into a volumetric flask and acidified. Sulfanilic acid was added to form the diazo intermediate. After adjusting the pH, α-naphthylamine was added to produce the red colored α-naphthylamine-azobenzene-p-sulfonic acid. The concentration of the red azo dye was measured spectrophotometrically at 520 millimicrons. A calibration curve was obtained using known amounts of sodium nitrite.

The iron content was determined by extracting a portion of the sample, acidifying with H_2SO_4, and boiling to remove nitrous and nitric acids. Stannous chloride was added to reduce iron (III) to iron (II). 1, 10-phenanthroline was added and the red-colored tris-1, 10 phenanthroline-iron (II) chelate was measured spectrophotometrically at 510 millimicrons. A calibration curve was obtained with standard iron (II) solutions.

The total nitrate ion was determined by first removing the iron with acetylacetone and reducing the nitrate with zinc amalgam to nitrite. The resulting nitrite was determined as described previously

The original nitrate in the material was obtained by difference.

Flow-Decay Compound Characterization

The flow test facility sight valve with its flow-decay deposit (Fig.14) was emptied of its liquid N_2O_4 content using the high vacuum system. To prevent exposure of the solid deposit to moisture, a completely enclosed system was required. The sight valve was dismantled in an inert atmosphere (gloved box) and the solid deposit was removed. All subsequent handling of the solid was accomplished in an inert atmosphere.

An infrared spectrum of the solid (Fig.15) was obtained as a mull in halocarbon oil. Sodium chloride plates and the infrared spectrophotometer Infracord 337 (Perkin-Elmer) were used.

X-ray diffraction powder patterns were obtained from two different sources. One set which was derived using FeK_α radiation was obtained from the Science Center, a Division of North American Aviation. The other using CuK_α radiation was obtained at Rocketdyne. The dimensions of the two cameras used were identical. From the films of the powder patterns, it was possible to calculate the d-spacings using the film measuring device and Bragg's Law: $\lambda = 2\ d\ \mathrm{Sin}\ \theta$. The d-spacing was calculated using the procedures outlined in the Norelco pamphlet "Instructions For Operation

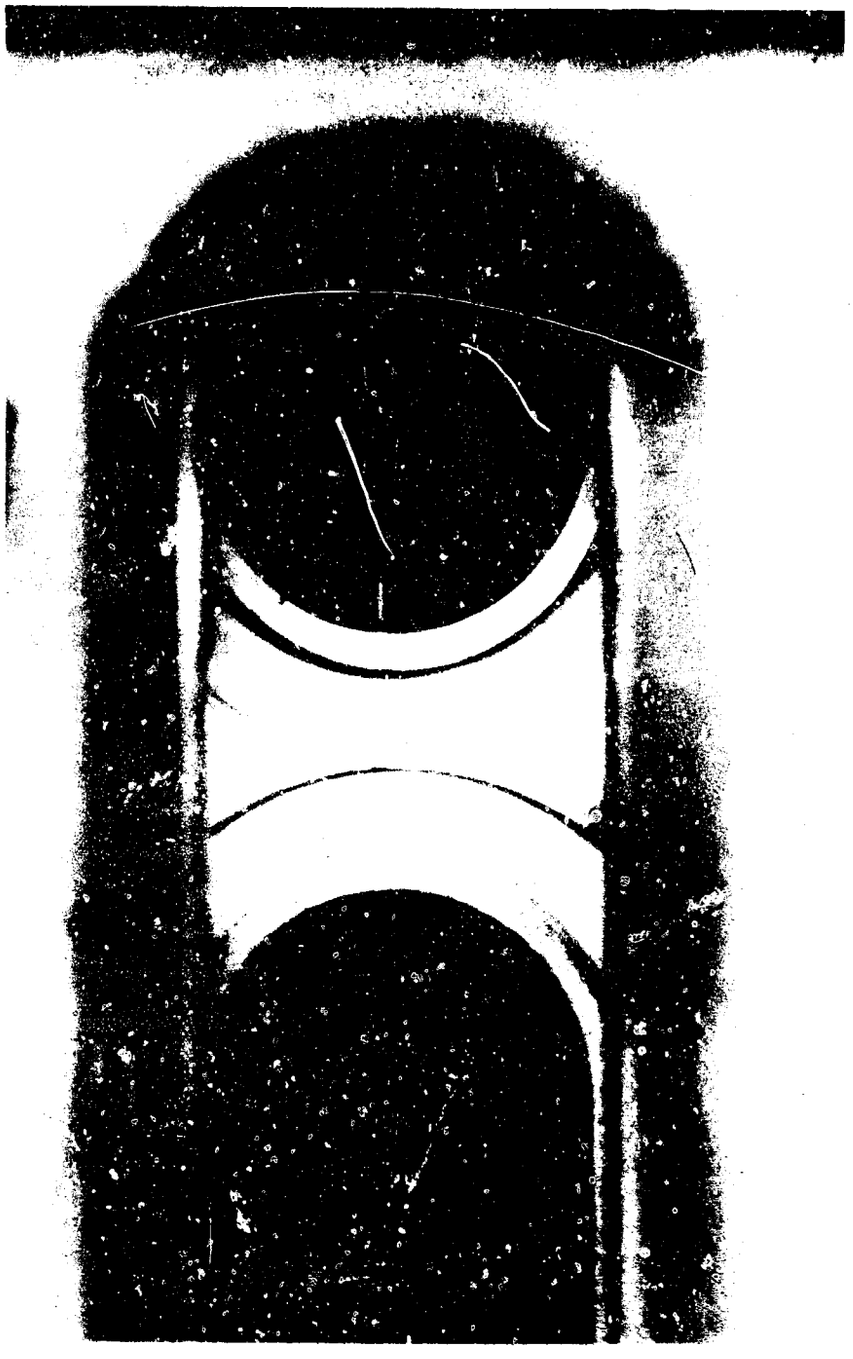

Figure 14. Sight Valve From N_2O_4 Flow Test Facility

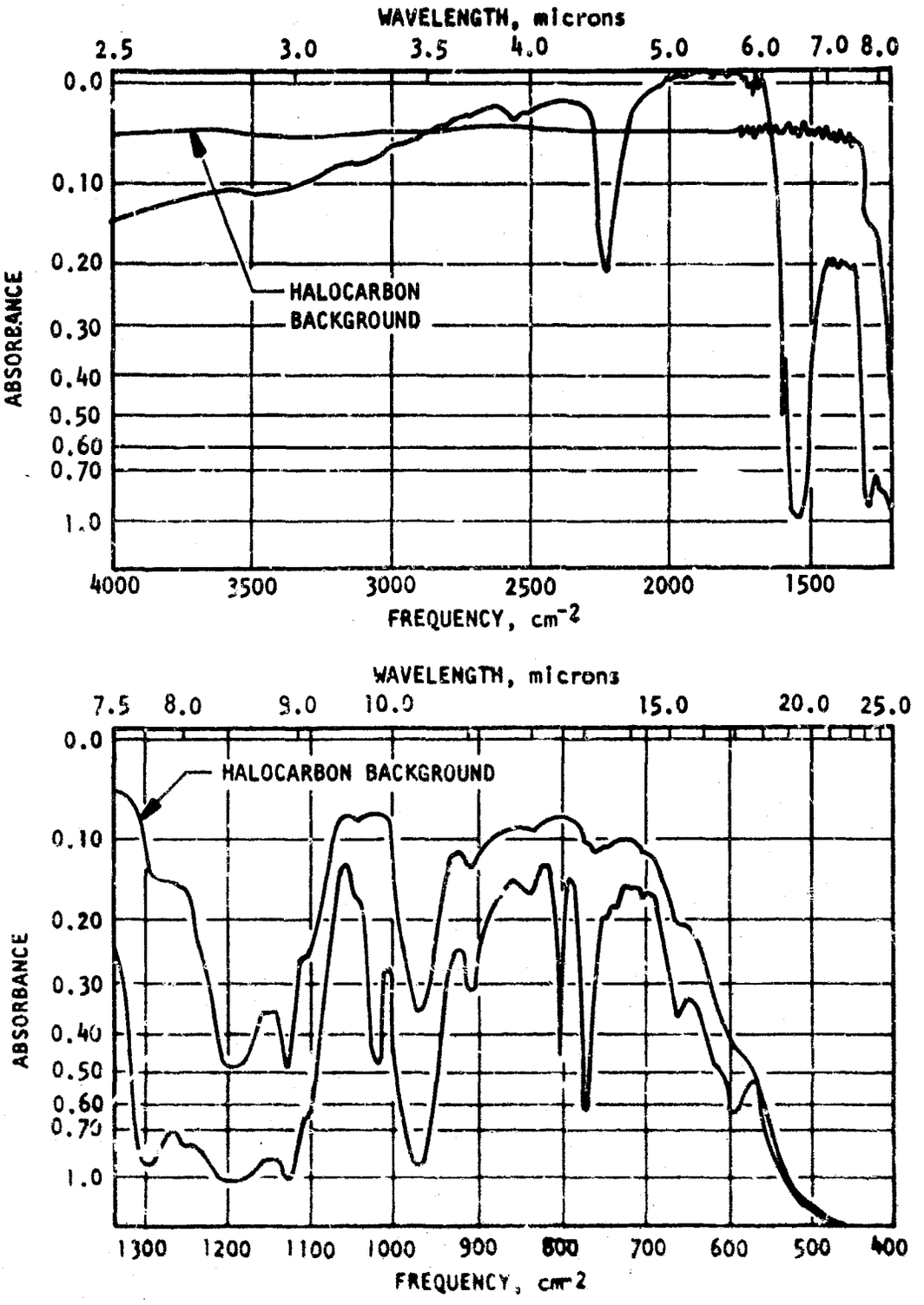

Figure 15. Infrared Spectrum of Flow-Decay Compound (N_2O_4 Flow Test Facility)

of Large and Small Powder Cameras," (Ref. 11) and the appropriate radiation wavelengths; $\lambda = 1.539$ Å for CuK_α and $\lambda = 1.934$ Å for FeK_α. The calculated values of some of the major lines are recorded in the second and fourth columns of Table 7. There are many additional lines; however, a match between major lines is believed sufficient. Columns 1 and 3 are obtained from reading the films on the scales available for CuK_α radiation. However, a close match has been obtained between these values (columns 1 and 3) and the corresponding calculated values. It should also be noted that no corrections have been made for film shrinkages.

The comparisons of the values of d-spacings have indicated that the actual flow-decay compound was identical to the synthetic $Fe(NO_3)_3 \cdot N_2O_4$ in crystalline structure.

The crystalline form of the material recrystallized from ethyl acetate - N_2O_4 mixture was shown to be different from the flow-decay compound by both sources of X-ray diffraction work. These data (Table 7) were obtained in the same manner as described previously.

Solubility of $Fe(NO_3)_3 \cdot N_2O_4$ in Distilled N_2O_4

The solubility apparatus consisted of a glass vessel equipped with a Teflon-covered stirring bar and two Teflon needle valves (Fig. 16). The apparatus was calibrated and dried thoroughly prior to use. The solid $Fe(NO_3)_3 \cdot N_2O_4$ was placed in the apparatus through needle valve A in an inert atmosphere (dry box). The N_2O_4 was distilled into the solubility apparatus through valve A using a glass vacuum system. The apparatus was then immersed in a constant-temperature bath in such a fashion that only the valves remained above the liquid level of the bath. The N_2O_4 - iron nitrate mixture was stirred by means of a magnetic stirrer. Sampling was accomplished by means of a U-shaped glass vessel equipped with Teflon needle valves (Fig. 16). The sampler was directly attached to the solubility apparatus through an O-ring joint. A Teflon or a Viton O-ring was used for this purpose. The section between valve B and valve D was evacuated and then refilled with dry nitrogen. The presence of the nitrogen

TABLE 7

X-RAY DIFFRACTION POWDER PATTERN OF $NOFe(NO_3)_4$

Synthetic Compound Recrystallized From N_2O_4 CuKα (Rocketdyne)		Actual Flow Decay Compound (Flow Facility) FeKα (Science Center)		Synthetic Compound Recrystallized From Ethylacetate-N_2O_4 Mixture			
				CuKα (Rocketdyne)		FeKα (Science Center)	
d-Spacing, angstroms	Intensity	d-Spacing, angstroms	Intensity	d-Spacing, angstroms	Intensity	d-Spacing, angstroms	Intensity
7.5	s	7.51	s	6.3	vvs	6.34	vvs
7.0	vs	7.17	vs	5.8	vvs	5.70	vvs
6.2	vs	6.28	vs	5.3	s	5.21	s
5.6	s	5.61	s	4.20	m	4.20	m
5.1	m	5.16	m	3.70	s	3.66	s
4.58	vvs	4.58	vvs	3.48	s	3.33	s
4.35	w			3.20	s	3.21	s
4.10	m	Many additional lines		3.10	vs	3.08	vs
3.75	s			3.00	vs	2.99	vs
3.43	s			2.44	m		
3.25	s	Refer to Experimental Section for Calculations		2.35	w	Many additional lines	
2.80	m			2.28	m		
2.60	w			2.17	w	Refer to Experimental Section for calculations	
2.44	m			1.98	w		
2.30	w			1.88	w		
2.18	m			1.78	w		

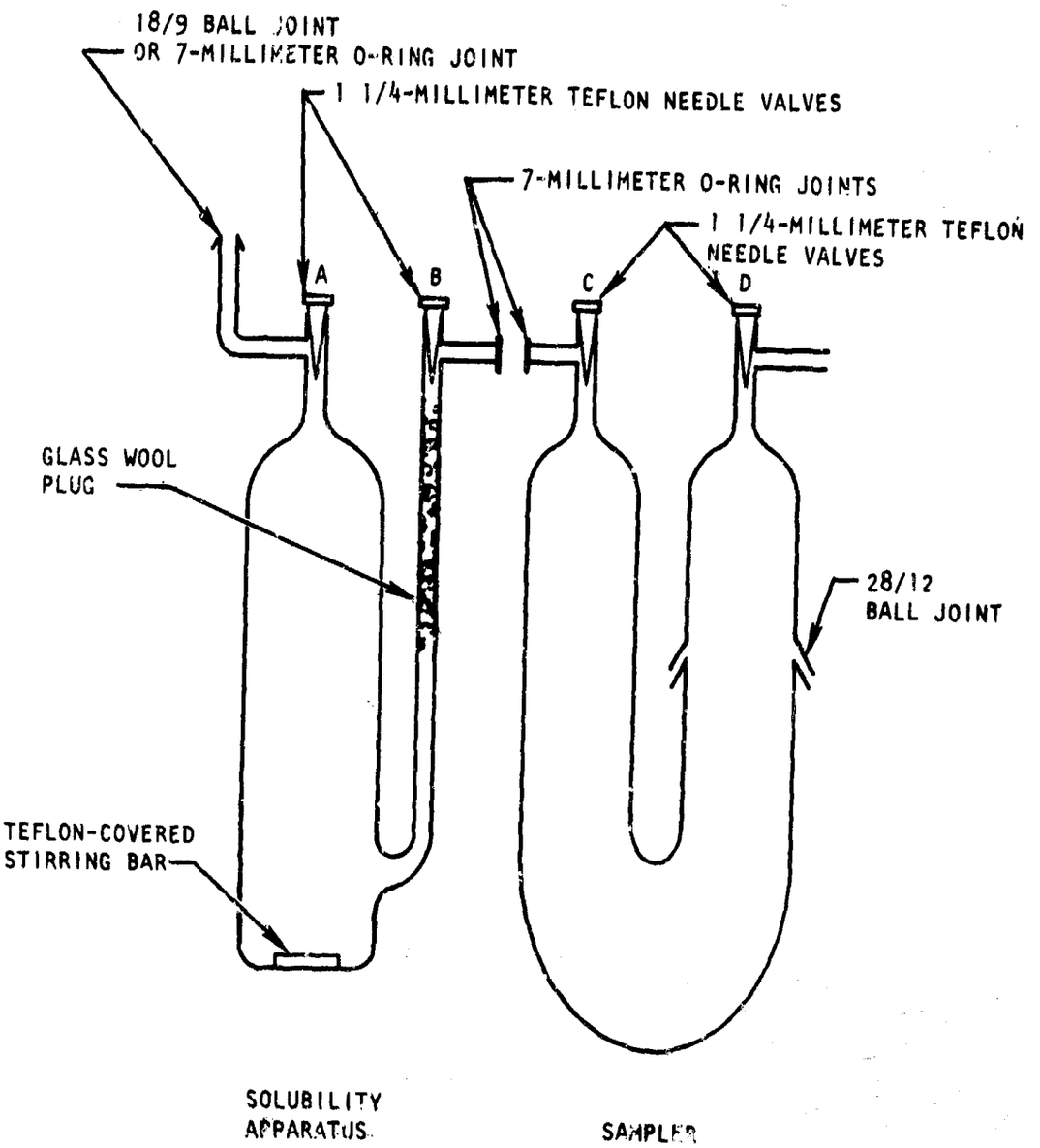

Figure 16. Solubility Apparatus and Sampler

provided back pressure and thus minimized the vaporization of the N_2O_4. The sampling was accomplished with a -78 C bath around the sampler. At low temperatures, pressurization of the solubility apparatus with dry nitrogen was necessary to force the liquid out through the opening in valve B. A glass wool plug prevented any solid particles from being carried over into the sampler. During the sampling, the solubility apparatus was maintained in the constant-temperature bath, thus assuring that a truly representative liquid sample was being taken. The weights of the N_2O_4 samples were obtained by the difference in the weights of the U-sampler before (evacuated) and after (GN_2 removed) the sampling and the hydrolyses of the N_2O_4 samples were accomplished directly in the U-tube sampler, by the addition of ice-cold water (deionized). Aliquots of these hydrolysates were then submitted for iron analyses.

A modification in the method of loading the solubility apparatus with N_2O_4 was made after the first few experiments. Originally, the N_2O_4 was distilled into the apparatus. By means of a specially constructed adapter which permitted the N_2O_4 to be flowed directly into the apparatus, the loading process was greatly facilitated. This adapter arrangement is shown in Fig.17. The section between valve A and B was initially evacuated through valve C. Then with valve C closed and valve B opened, the N_2O_4 was flowed into the apparatus by opening valve A. Upon completion of the transfer of the liquid N_2O_4, valve B was closed and the excess vapor recondensed into the glass bulb by tipping the entire setup over and placing the bulb in a dry-ice bath. The weight of the N_2O_4 that was transferred was easily obtained by determining the weight of the bulb before and after the transfer.

Solubility determinations were made at controlled temperatures of 0, 25, 30, and 37.8 C (32, 77, 86, and 100 F) and the results are presented in Table 8.

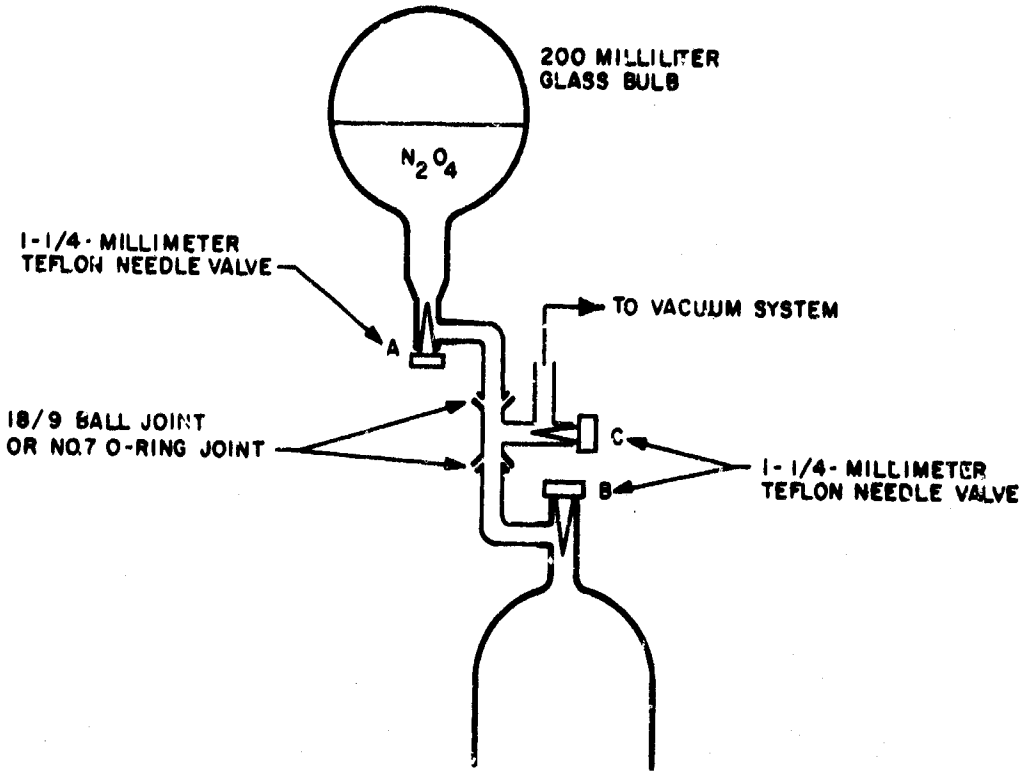

Figure 17. N_2O_4 Transfer Apparatus

TABLE 8

SOLUBILITY OF $NOFe(NO_3)_4$ IN N_2O_4

Temperature, C	Method of Analysis	Iron Concentration, ppm Duration of Studies, days						
		2	5	9	14	24	28	38
0	1				0.5		0.6	
	2	0.2	0.3	0.5	0.2			
	3	0.2	0.8	0.6	0.3			
25	1	*	1.6					
	2			0.1	0.1			
	3		0.3	0.1	2.6			
30	1	0.6	*			1.4		0.6
37.8	1	0.9	0.1	0.5	0.3	1.8		
	3	*	1.2	*	*	1.9		

NOTE: 1: Colorimetric method using o-phenanthroline

2: Atomic absorption spectrophotometric method at Rocketdyne

3: Atomic absorption spectrophotometric method at Space Division

*Results were discarded because they were exceptionally high

NO Additive to N_2O_4-Iron Nitrate Mixture

Nitric oxide was purified by passing it through a -156 C trap several times, the purity was checked by infrared and mass spectometry and by vapor pressure measurements. The solid $Fe(NO_3)_3 \cdot N_2O_4$ (63 milligrams) was placed in the solubility apparatus in the manner described previously. The gaseous NO (162.5 cc) was then placed in the apparatus by condensing it in a narrow sidearm added to the apparatus shown in Fig.16. The N_2O_4 (100.7 grams) was loaded into the apparatus using the adapter shown in Fig.17 and a cooling bath of ice-brine mixture. With the completion of the addition, the sidearm was slowly warmed, thus allowing the NO to vaporize and dissolve in the N_2O_4. The apparatus was then placed in a constant-temperature bath maintained at a temperature of 25 C.

Solubility determinations were made at 25 C (77 F) and at the following NO concentrations: 0.22 w/o, 0.46 w/o, and 0.99 w/o. The results are presented in Table 9.

Water Additive to N_2O_4-Iron Nitrate Mixture

Water (0.10 gram) and N_2O_4 (97.0 grams) were mixed in a 200-milliliter glass bulb equipped with a Teflon needle valve. This mixture was directly added to the solubility apparatus containing the solid $Fe(NO_3)_3 \cdot N_2O_4$ This was accomplished by affixing the bulb containing the mixture to the solubility apparatus by means of the special adapter (Fig. 17).

The investigations were conducted at 25 C (77 F) and at the water concentrations of 0.1 and 0.47 w/o. The experimental results are presented in Table 10. During the first experiment (0.1 w/o H_2O) the fine particles of $NOFe(NO_3)_4$ remained as discrete separate particles whereas during the second experiment the particles conglomerated into a small ball.

TABLE 9

SOLUBILITY OF $NOFe(NO_3)_4$ IN N_2O_4 IN THE PRESENCE OF NITRIC OXIDE AT 25 C (77 F)

NO Concentration, weight percent	Method of Analysis (Ref. Table 8)	Iron Concentration, ppm			
		Duration of Studies, days			
		2	5	9	14
0.22	1	0.6	*	*	*
	3	1.0			
0.46	1	0.7			
	2	Nil	0.2	0.3	0.3
	3	1.9	0.6	0.6	0.4
0.99	2	1.0	0.6	0.4	
	3	1.2	0.8	0.6	

*The use of dilute HF solution (5 percent) as a rinse solution has invalidated these results. Such a solution has been shown to definitely leach out iron from Pyrex.

TABLE 10

SOLUBILITY OF $NOFe(NO_3)_4$ IN N_2O_4 IN THE PRESENCE OF WATER AT 25 C (77 F)

H_2O Concentration, weight percent	Method of Analysis (Ref. Table 8)	Iron Concentration, ppm			
		Duration of Studies, days			
		2	5	9	14
0.10	1	0.1	0.2		
	2	1.5	2.2	Nil	0.4
	3	0.2	0.3	0.3	0.6
0.47	2	2.9	3.2	3.5	3.6
	3	3.8	3.5	3.8	4.1

DISCUSSION AND RESULTS

The primary objective of the investigation was the preparation of $Fe(NO_3)_3 \cdot xN_2O_4$, identical in all respects with the flow-decay deposit. The first step toward such a "standard" $Fe(NO_3)_3 \cdot xN_2O_4$ was a more detailed examination of reaction 1, primarily to ensure that no carbonyl species were retained in the product. This was easily accomplished by measuring

$$Fe(CO)_5 + (3 + x)N_2O_4 \longrightarrow Fe(NO_3)_3 \cdot xN_2O_4 + 5CO + 3NO \qquad (1)$$

where

x = 1 or more

the CO evolved in a controlled reaction. It was satisfactorily demonstrated that no carbonyl species were retained in the product by the fact that essentially quantitative evolution of CO (94 percent of theory) was observed and the fact that no carbonyl band was evident in the infrared spectrum of the product. The empirical formula of the crude material thus produced was determined to be $Fe(NO_3)_{2.8} \cdot 2.5N_2O_4$.

The secondary objective was to develop a method of purification for the crude $Fe(NO_3)_3 \cdot xN_2O_4$. Previous work (Ref. 1) had indicated that a series of iron nitrate-N_2O_4 compounds existed and attempts to purify them by sublimation converted them into an entirely different type as demonstrated by gross changes in the infrared spectra. Observations very similar to these have been reported by C. C. Addison and co-workers at Nottingham University (Ref. 8). These authors have recently prepared several iron nitrate-N_2O_4 compounds, to which they have assigned the structure (NO^+) $[Fe(NO_3)_4]$ and (NO_2^+) $[Fe(NO_3)_4]$. The second "compound" was prepared by subliming the first, and structural assignments were made on the basis of infrared spectra.

A review of parallel work on this system indicates that Addison's conclusions are an oversimplification. The first crude product prepared at Rocketdyne shows an infrared spectrum identical with Addison's first product, and the structural assignment (NO^+) $[Fe(NO_3)_4]^-$ is believed to be

correct. However, upon repeated sublimations, a series of changes occurred in the material and the species that Addison identified as (NO^+) $[Fe(NO_3)_4]^-$, by comparison of infrared spectra, appears to be a partially changed mixture rather than a discrete compound. Spectral data at Rocketdyne indicate that in addition to the simple change in cation (NO^+ to NO_2^+) that Addison suggests, there are also at least one and perhaps several changes involving the rest of the molecule. Infrared absorptions appear that are not attributable to any of the usual forms of the cations, nitryl (NO^+) or nitrosyl (NO_2^+); the anions, nitrite (NO_2^-) or nitrate (NO_3^-); the ligands, nitrito ($-ONO$) or nitrato ($-ONO_2$); and do not arise from the degradation product $FeO(NO_3)$. Possibilities include the participation of NO_3 groups in a new form of bridging, tridentate coordination of NO_3 to the metal, or the formation of new $FeO_x(NO_3)_y$ species. The flow-decay deposit has been found to be essentially identical to the crude compound of Addison's nitrosonium salt structure, (NO^+) $[Fe(NO_3)_4]^-$ (Ref. 1).

Because sublimation could not be used as a purification method, investigations involving recrystallization from nonaqueous solvents, including N_2O_4 itself by cyclic extraction techniques, were undertaken. The cyclic extraction technique using N_2O_4 involved a Soxhlet extraction apparatus which was modified to exclude moisture and the use of stopcock grease. Recrystallization did occur and after 1 week of extraction, 20 milligrams of a pale yellowish solid material was collected. Analytical results showed this material to have the empirical formula $Fe(NO_3)_{3.19} \cdot 1.03\ N_2O_4$. This purified solid material was found to match more closely the flow-decay deposit in certain properties than the crude material. The purified material was much lighter in color, approaching that of the flow-decay deposit. Its reactivity in moist air also more closely approximated that of the flow-decay deposit. The infrared spectrum of the purified material was identical to that of the crude and thus to that of the flow-decay deposit.

Because the extraction technique using N_2O_4 appeared extremely time consuming and the yield of the purified material appeared very low, other methods of recrystallization were investigated. A second method, which

involved solubilizing the crude material in ethyl acetate and then precipitating the solid by the addition of N_2O_4, proved to be quite convenient. A large amount of a pale brown colored solid was obtained which was identical by infrared spectrum and elemental analyses with the previously purified material (by cyclic extraction techniques using N_2O_4). Two separate purification runs produced materials with the following empirical formulae: $Fe(NO_3)_{3.1} \cdot 1.03\ N_2O_4$ and $Fe(NO_3)_{3.1} \cdot 0.99\ N_2O_4$; on 98 to 99 percent mass balances.

During the latter half of the program, with the flow test facility (Phase V) in full operation, an opportunity arose whereby the actual flow-decay material could be isolated, characterized, and directly compared with the synthetically prepared material. Flow stoppage was accomplished in a glass sight valve which permitted the viewing of the actual deposition of the flow-decay material. The sight valve was then isolated and attempts were made to collect the deposited material. The sight valve was photographed with the N_2O_4 removed and an enlarged version is shown in Fig. 14 in which the deposition on the needle and seat is clearly visible. However, the deposition was present not only on the needle and seat but on the entire metallic surfaces. The needle with the heaviest concentration of deposit was removed from the valve in an inert atmosphere and also photographed (Fig. 18). The photograph reveals an obvious coating of a solid material along the shaft. It was then possible to scrape off the deposit in an inert atmosphere and collect it for further characterization. The pale brown solid appeared to be a dry, hard, crystalline material which when exposed to the atmosphere reacted rapidly with moisture and evolved gases accompanied by bubbling. Other investigators of N_2O_4 propellant systems, have reported that the clogging of control valves and filters was caused by the formation of gelatinous material "reddish in color, slimy, and extremely viscous to the touch" (Ref. 12). These workers may have accidentally exposed the solid to moisture, which would explain their observations. X-ray diffraction study of the present flow-decay material indicates that it is definitely crystalline. The d-spacings from the powder pattern of the flow-decay deposit are presented in Table 7.

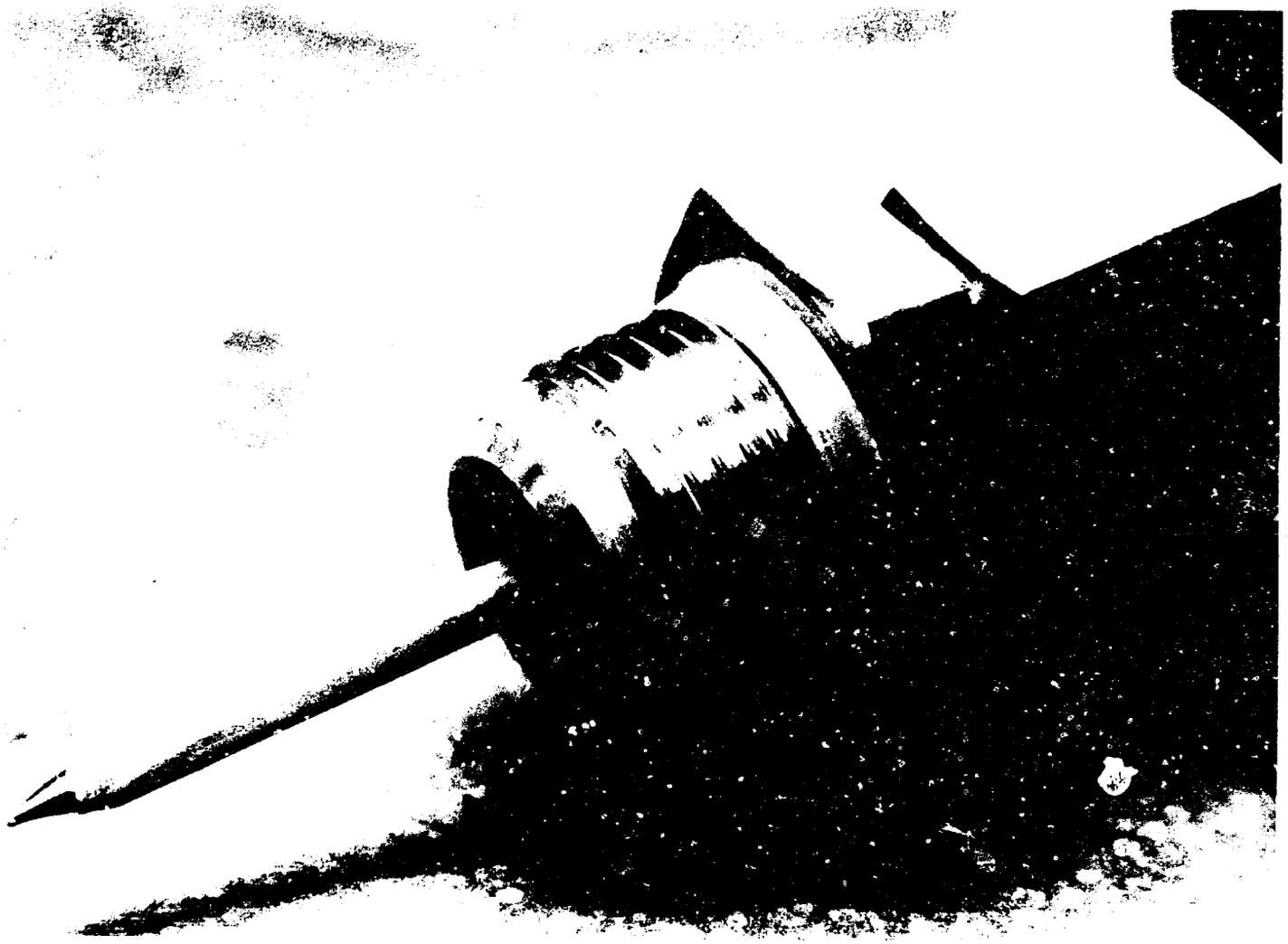

Figure 18 . Valve Needle From Sight Valve N_2O_4 Flow Test Facility

Infrared spectroscopy, (Fig.15) showed that the flow-decay compound was identical chemically to the synthetically prepared iron nitrate, $NOFe(NO_3)_4$. X-ray diffraction studies have shown that the flow-decay compound was also identical to the synthetic $NOFe(NO_3)_4$ in crystalline structure. The iron nitrate, $NOFe(NO_3)_4$, recrystallized from pure N_2O_4 has the same infrared spectrum and X-ray powder pattern as the flow-decay compound. X-ray diffraction studies, in addition, have indicated that $NOFe(NO_3)_4$ can exist in at least one other crystalline form. When $NOFe(NO_3)_4$ was recrystallized from ethyl acetate-N_2O_4 mixture, it had a different powder pattern than that of the material recrystallized from pure N_2O_4. These materials had been shown previously to be chemically alike (infrared and elemental analyses). The d-spacings from the powder pattern of this second crystalline form is also recorded in Table 7.

With the preparation of sufficient quantities of pure "synthetic flow-decay compound", solubility studies in N_2O_4 were initiated. To establish a reference point of solubility and for purposes of comparison with propellant-grade N_2O_4, freshly distilled anhydrous iron-free N_2O_4 ($<$ 0.1 ppm Fe and 0.01 ppm water) was utilized. The N_2O_4 was also pretreated with oxygen to preclude the possible presence of traces of NO.

The solubility determinations were made in specially constructed glass apparatus. Solubility runs were conducted at controlled temperatures (constant-temperature baths) of 0, 25, 30, and 37.8 C (32, 77, 86, and 100 F). Solubility was established by withdrawing liquid samples periodically and then analyzing the samples for iron. The analytical results have been somewhat erratic, probably because of inherent errors in the sampling procedures and the procedures involved in the analysis of a component which is in very low concentrations.

From the results of these studies, it can be concluded that the solubility of $NOFe(NO_3)_4$ in pure N_2O_4 over the temperature range 0 to 37.8 C (32 to 100 F) is quite low, on the order of 0.1 ppm to 2 ppm (in terms of Fe concentration). A positive temperature coefficient of solubility apparently

exists over the range of study as shown in Fig. 19. This is indicated by the positive slope of the line drawn through the average values of the solubility data (Table 8) at the respective temperatures.

The data presented in Table 8 are analytical results derived from identical unknown samples (aliquots) utilizing three different methods. The first set of results (1) resulted from the utilization of the standard colorimetric iron procedure using o-phenanthroline as the complexing agent (Appendix B). The second set (2) was derived from the iron analysis using the atomic absorption spectrophotometer (Appendix C) (AAS) at Rocketdyne. The third set (3) resulted from a similar AAS work, using, however, another instrument and involving another operator at the Space Division of North American Aviation.

During the latter part of the solubility studies, the colorimetric method was abandoned in favor of the AAS method because of the increased accuracy of the AAS technique.

Investigation of the effect of the presence of small amounts of nitric oxide on the solubility of the flow-decay compound in N_2O_4 was conducted at 25 C (77 F). The results, presented in Table 9, indicate that nitric oxide in small concentrations (up to 1 w/o) has little or no effect on the solubility of the flow-decay compound in N_2O_4. Iron concentration was in the 0 to 2 ppm range.

The effect of the presence of small amounts of water on the solubility of the flow-decay compound in N_2O_4 was also investigated. The results of this study (Table 10) indicate that water in small concentrations (0.1 w/o or less) has little or no effect on the solubility of $NOFe(NO_3)_4$ in N_2O_4 at 25 C (77 F). Only at a higher concentration of water (0.47 w/o) is there a noticeable increase in the solubility. This increase is small (twofold) in comparison with the increase in the water concentration (fivefold). This water concentration exceeds the limit allowable by military specifications for propellant uses.

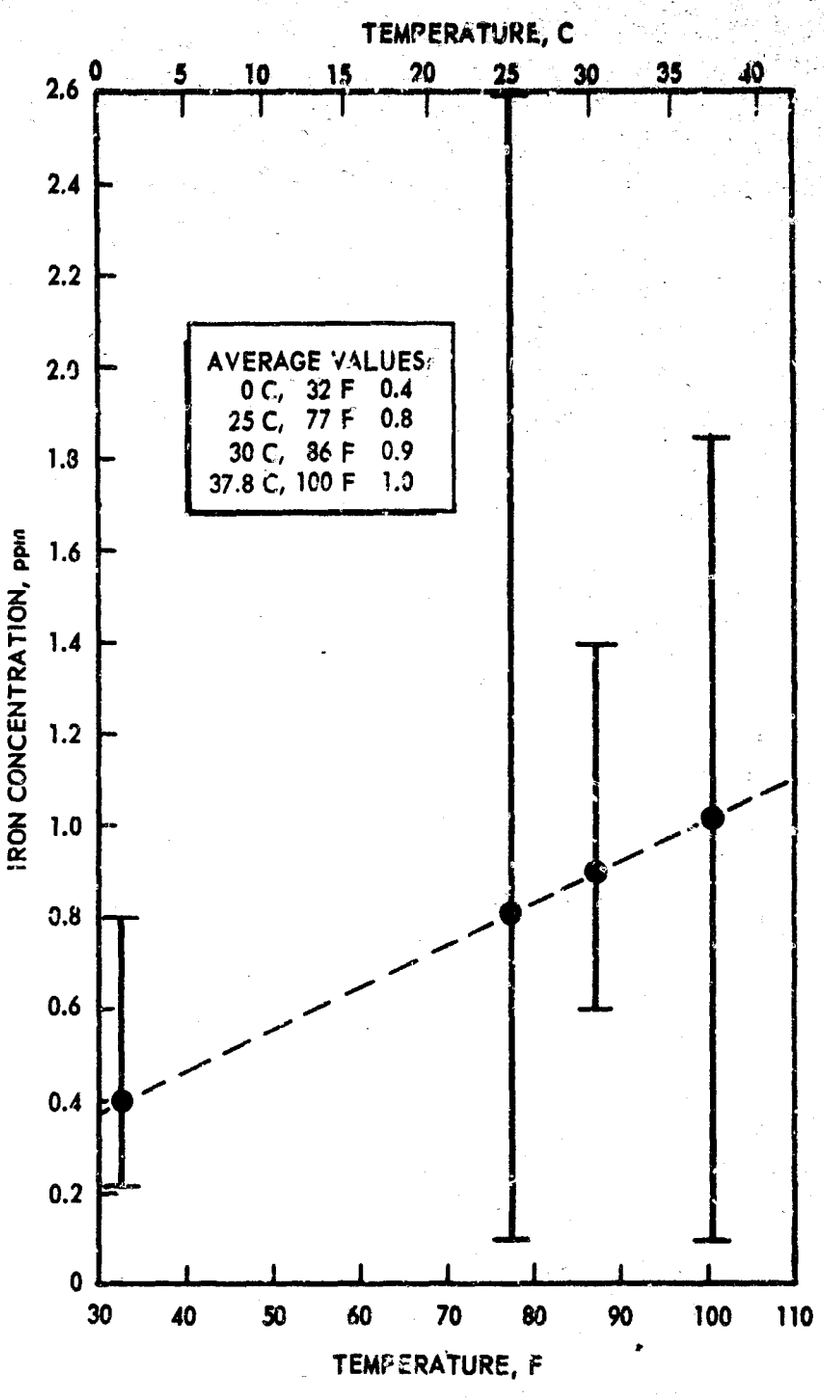

Figure 19. Solubility of $NOFe(NO_3)_4$ in N_2O_4 as a Function of Temperature

The solubility studies presented in this report would necessarily require many duplicate determinations to ensure sound statistical bases for the conclusions. Such work, however, would have entailed considerable time and effort which were beyond the scope of this program.

CONCLUSIONS

The anhydrous iron nitrate $NOFe(NO_3)_4$ has been successfully prepared and purified in sufficient quantities to meet the needs of the entire program. Evidence has been obtained to establish unequivocally the identity of this material with the actual flow-decay (N_2O_4 corrosion product) deposit.

The solubility of the flow-decay compound in freshly distilled N_2O_4 over the temperature range 0 to 37.8 C (32 to 100 F), and in the presence of small concentrations of nitric oxide and water has been found to be quite low, on the order of 1 to 4 ppm in terms of iron concentration.

PHASE IV: COMPOUND ELIMINATION

INTRODUCTION

Investigation of appropriate coordinating agents as additives for eliminating flow decay was the major task of this phase of the program. The additive approach was based on the concept that it would never be practical to remove the flow-decay compound completely from N_2O_4. In such a case, its effect might be eliminated if it could be converted to a more soluble species, thus preventing its deposition. It is known that molecules with basic functions can substitute for the coordinate N_2O_4 molecules in complexes of the type metal nitrate$\cdot N_2O_4$ (Ref. 13). The flow-decay compound $NO^+[Fe(NO_3)_4]^-$ may be formulated as $Fe(NO_3)_3 \cdot N_2O_4$.

The investigations in the laboratory have produced a number of candidate additives for the elimination of flow decay. Some of these were subsequently made available to the flow test facility (flow bench, Phase V) for actual testing in flow situations. The results of the laboratory tests and the elimination of flow decay in the flow bench have clearly demonstrated the feasibility of the principle of the additive (coordinating agents) approach.

In addition to the additive work, a small flow system for the study of flow decay on a laboratory scale has been developed. This device could prove very useful in any future study.

EXPERIMENTAL

Reactivity of $NOFe(NO_3)_4$ With Additive Reagents

A small amount of the $NOFe(NO_3)_4$ was placed in a vial and the test reagent was added to the solid by means of a syringe. The reactivity was noted visually. All operations were carried out in a dry atmosphere box. The results are recorded in Table 11.

TABLE 11

INVESTIGATIONS OF COMPOUND ELIMINATION AGENTS

Agent	Solubility of $NOFe(NO_3)_4$ in Agent	Reaction With N_2O_4	Thermal Stability
Acetonitrile	Sol	App NR	NR
Acetylacetone	Sol	R	X
Nitromethane	Insol	R	X
Perfluoro-acetic Anhydride	Insol	App NR	--
Nitrobenzene	Sol	App NR	Mod R
Ethylacetate	Sol	App NR	NR
Hexafluoro-acetylacetone	Sol	R	X
Pentane	Insol	App NR	X
Freon 113	Insol	App NR	X
Silicone Fluid XF6100	Insol	R	X
Trifluoroacetonitrile	Insol	App NR	--
Benzaldehyde	Sol	App NR	--
Benzophenone	Sol	App NR	--
Benzonitrile	Sol	App NR	NR
Acetone	Sol	App NR	Mod R
Hexafluoroacetone	Insol	App NR	--
Pentafluorobenzaldehyde	Sol	App NR	--
Heptafluorobutyraldehyde Ethyl Hemiacetal	Insol	--	--
Pentafluorobenzonitrile	Sol	App NR	NR
Perfluorobutyronitrile	Insol	App NR	NR
p-Dioxane	Sol	App NR	Sl R
Tetrahydrofuran	Sol	R	X
Monoglyme	Sol	App NR	Mod R
Diethyl Ether	R, precipitate	X	X
Tolylene 2, 4-Diisocyanate	R, precipitate	X	X

TABLE XI

(Concluded)

Agent	Solubility of $NOFe(NO_3)_4$ in Agent	Reaction With N_2O_4	[illegible]
Morpholine	Fumed	X	X
N, N, N^1, N^1 - Tetramethylene 1, 3 Butanediamine	Flashed, precipitate	X	X
Pyridine	R, precipitate	X	X
Tri-n-Butylamine	R, tar	X	X
Triethylene Glycol	Sol	R	X
Diglyme	Sol	App NR	Mod R
Dimethylsulfoxide	R, precipitate	X	X
n-Butyl-p-Toluene Sulfonate	Sol	--	--
Diethylcarbonate	Sol	App NR	NR
Diethylmalonate	Sol	App NR	Sl R
Diethyloxalate	Sol	App NR	--
Quinoline	Sol	R	X
Benzaldoxime	R, tar	X	X
Piperidine	Fumed	X	X
Adiponitrile	Sol	App NR	NR
Ethylene-dinitrilo-tetracetic acid	X	Insol	X
(1, 2-cyclohexylene-dinitrilo) - tetraacetic acid	X	Insol	X
2, 2' Bipyridine	X	Insol	X
1, 10-Phenanthroline	X	R	X
Cupferron	X	R	X
Dimethylglyoxime	X	R	X
N-phenylbenzo-hydroxamic acid	X	R	X
Decafluorobenzophenone	X	App NR	--
Acetophenone	Sol	App NR	Mod R

NOTE: Sol = the compound readily dissolved in the reagent

Insol = the compound was insoluble in the reagent

R = reaction was observed

App NR = no apparent reaction (visual)

NR = analyses (pressure, mass spectral, visual) indicated no reaction

Mod R = moderate reaction, reaction products were observed

Sl R = slight reaction

X = indicates no test was planned

- = incomplete

Reactivity of Additive Reagents With N_2O_4

A small amount of the reagent was placed in a vial and the N_2O_4 was added to it from a small supply bulb (50 cc) equipped with a Fischer-Porter Teflon needle valve. The reactivity was noted visually. All operations were carried out in an inert atmosphere glove bag. In cases where the reagent was a gas at room temperature, the reagent was condensed in a small ampoule and then a small amount of N_2O_4 condensed over it. When it warmed to room temperature, the reactivity was observed visually. The results are presented in Table II.

The Solubility of $NOFe(NO_3)_4$ in N_2O_4 in the Presence of Candidate Additive

The solubility of the iron nitrate in N_2O_4 in the presence of a candidate coordinating reagent (i.e., acetonitrile) was carried out in the following manner. The solid $NOFe(NO_3)_4$ was placed in a small glass bulb equipped with a Teflon-covered stirring bar and a Teflon needle valve. The weight of the solid was obtained by the difference in weights of the evacuated bulb before and after the addition of the solid. N_2O_4 was then condensed over the solid. The mixture was allowed to warm to room temperature and stirred (magnetic stirrer) overnight. Most of the solid was observed to be insoluble over this period. The reagent (acetonitrile, 0.2 w/o) was then condensed into the bulb and the mixture allowed to warm to room temperature. After 1 hour of stirring, the amount of insoluble solid decreased considerably. After overnight stirring, all of the solid had dissolved. The resulting solution was subjected to a temperature cycling by immersion in 0 to 37.8 C (32 to 100 F) baths.

The Thermal Stability Tests

The thermal stability tests were conducted in a small stainless-steel bomb which was equipped with a valve and a gage. The mixture (25 to 50

milliliters) of N_2O_4 and additive (1 w/o) was made in a glass bulb. The mixture was then transferred to the bomb with the adapter arrangement shown in Fig. 17 , with the bomb now replacing the solubility apparatus. The procedures involved are identical. The bomb was then placed in an oven, the temperature raised to 73.9 C (165 F), and kept at this temperature for 24 hours. Any pressure increase resulting from the evolution of gases was noted. After the heating cycle, the vapor above the liquid was analyzed by mass spectrometry for possible product of reactions such as H_2O, CO_2, and N_2. The liquid was then removed and observed for any visible evidence of reaction. The results are tabulated in Table 11.

Solubility of $NOFe(NO_3)_4$ in INTO

The solubility of $NOFe(NO_3)_4$ (35 milligrams) in INTO (4 w/o FNO_2) was tested in a Kel-F ampoule equipped with a stainless-steel valve. Under ambient conditions, no visual change occurred as the liquid INTO came into contact with the solid. Shaking it had no apparent effect on the mixture. The mixture was allowed to stand at room temperature for 3 days. There was no apparent change.

The INTO was then removed using the high-vacuum system and the solid isolated in an inert atmosphere. It was then noted that the solid had changed to a white solid. X-ray powder pattern showed the solid to be crystalline but unlike any fluorides reported in the literature. An attempt was made to obtain an infrared spectrum of the solid. The quantity of the solid was too small for an adequate spectrum.

The experiment was repeated using a larger amount of the solid (150 milligrams). The same observations as above were noted. The infrared spectrum of the isolated white solid showed a single peak at 4.25 microns $[(NO_2)^+]$. The elemental analysis on a sample of this solid yielded the following results: Fe, 27.9 w/o; NO_2, 28.3 w/o; F, 40.9 w/o; and unknown impurities, 2.9 w/o (theoretical for $NO_2^+FeF_4^-$: Fe, 31.40 w/o; NO_2^+, 25.87 w/o; and F, 42.73 w/o).

Reactivity of INTO With an Additive

Perfluorobenzonitrile (0.27 gram) was condensed into a stainless-steel (30 cc) bomb equipped with a stainless-steel valve. INTO (9.5 grams) was then flowed directly from the storage tank to the bomb using appropriate stainless-steel couplings. The bomb was then heated to 160 F for 24 hours. Mass spectral analysis of the vapor showed CO_2, N_2, small amounts of CF_4, and HF. Attempts to recover C_6F_5CN were unsuccessful.

Laboratory Flow-Decay Apparatus

The small flow-decay apparatus consisted of two (1-liter) stainless-steel bombs, 1/4-inch stainless-steel lines, and a small loop (U-trap) made of glass tubing (Fig. 20). The glass was joined to the metal line using Teflon sleeves. Teflon needle valves were used as part of the glass loop so that the loop could be completely isolated, uncoupled, and transferred to the dry box for the removal of the solid deposit for characterization purposes. The entire apparatus was leak checked and dried by evacuation using the high-vacuum system through valve E. Propellant grade N_2O_4 was placed in the apparatus by flowing it through valve A with valve B closed.

An operational run consisted of: heating the N_2O_4 supply to 54.4 to 60 C (130 to 140 F) using a heating tape wound around the bomb, flowing the liquid through the glass loop which was kept in a cooling bath, and receiving the N_2O_4 in a catch tank. The heating of the N_2O_4 provided a greater solubility of the iron compound (hopefully, saturation), and provided the pressure necessary for the N_2O_4 flow to take place. The temperature of the N_2O_4 before each run was estimated by reading its vapor pressure (gage I) and using the literature vapor pressure-temperature relationships. A heating tape also was used around the metal line upstream of the glass loop to prevent the premature deposition of the solid. The pressure in the line during a run was indicated by gage II. The pressure in the line was found to be quite erratic during the run. After the completion of a run,

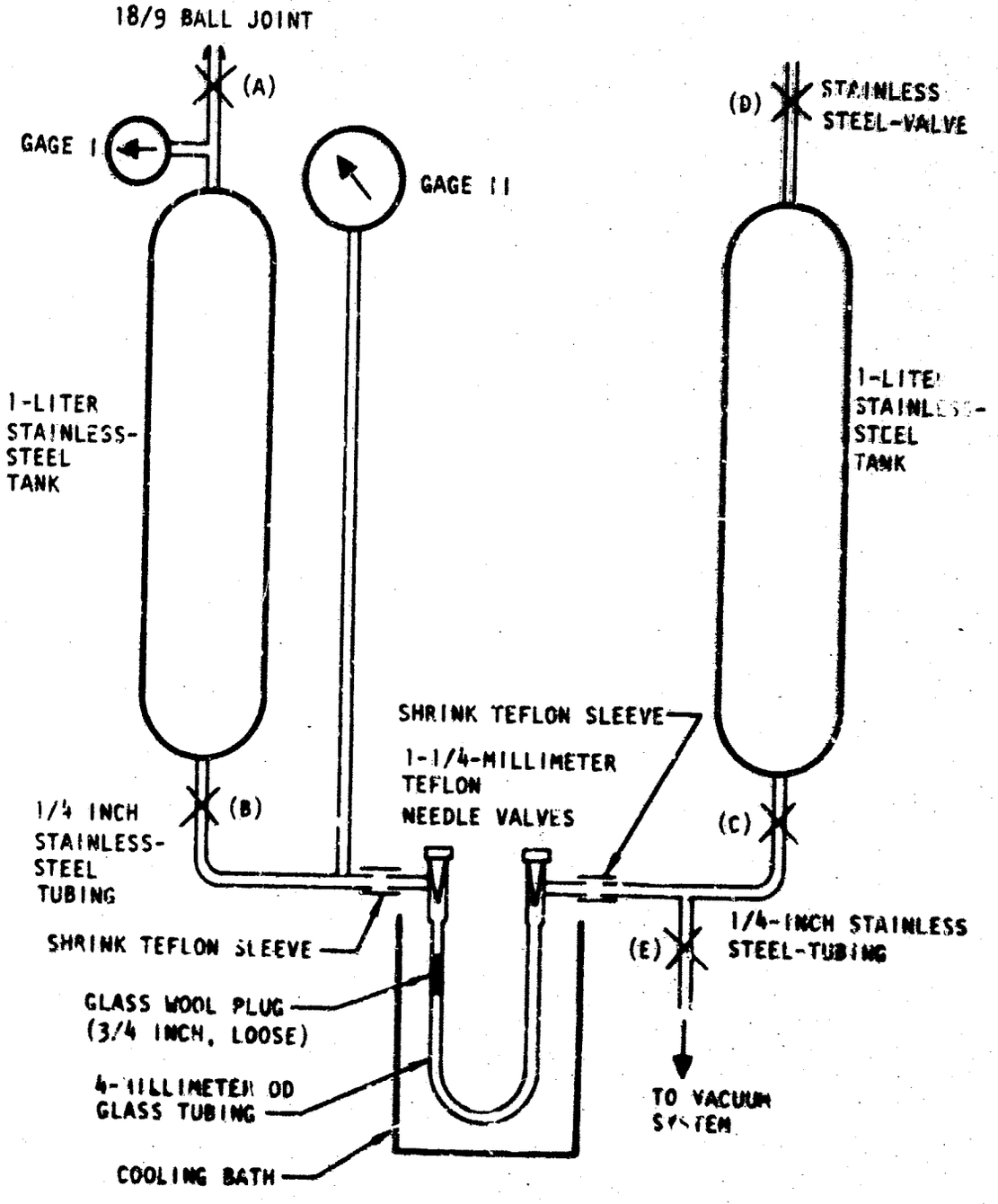

Figure 20. Laboratory Flow-Decay Apparatus

the flow of N_2O_4 could be reversed simply by transferring the heating tapes from one side to the other. A rough, average flowrate of each run was determined by knowing the starting amount of N_2O_4 and recording the time necessary for that particular run.

Several variations were carried out to determine the best conditions for solid deposition. Some of these variations were: changes in the flowrates (10 to 25 ml/min), use of constrictions in the glass loop, use of metal surface for deposition, use of Fischer-Porter Teflon needle valves, changes in the temperature of the cooling bath -10 to 0 C (14 to 32 F), and use of a glass wool plug.

During the earlier experiments, any one single run was found to deposit only a very small amount of solid material. Several runs were, therefore, necessary to provide even the minimal amount for analysis.

The best conditions for the operation of the flow-decay apparatus were found to be: the use of a loose plug of glass wool (3/4-inch), a flowrate of roughly 15 ml/min, and preheating the N_2O_4 for several days. Under these conditions, a single run produced enough solid for positive identification. The solid thus produced was shown by infrared spectroscopy to be identical to the flow-decay compound.

The effectiveness of an additive in the elimination of the flow decay deposit was duplicated with the above laboratory apparatus. A built-up deposit was completely dissolved away by a single pass of N_2O_4 containing 0.25 w/o of acetonitrile. This same solution gave no deposit after 1 day of storage at 60 C (140 F).

DISCUSSION AND RESULTS

The search for appropriate coordinating agents for the elimination of flow decay consisted of subjecting the materials of choice to three major tests: (1) solubility of $NOFe(NO_3)_4$ in the material, (2) the

reactivity of the material with N_2O_4 at ambient temperature, and (3) the reactivity of the material with N_2O_4 at elevated temperatures, 71 to 74 C (160 to 165 F) (thermal stability test).

The first test involved the addition of the coordinating reagent to the solid iron nitrate, $NOFe(NO_3)_4$ in an inert atmosphere. Many reagents of different types, both monofunctional (unidentate ligands) and polyfunctional (multidentate ligands) have been found which readily dissolved the iron nitrate. The reagents that were tested under this program and the results of these tests are compiled in Table 11.

The reagents which passed the first test were then tested to see whether they would react with N_2O_4 under ambient conditions. The results of these tests also are tabulated in Table 11 . The reagents that reacted with N_2O_4 were eliminated from further consideration.

Investigations of the solubility of the iron nitrate in N_2O_4 in the presence of the coordinating agents which were designated candidates from the results of the first two tests were then conducted. An example of this test, a combination of the first two is illustrated by the following: when acetonitrile was added to a mixture of $NOFe(NO_3)_4$ (40 ppm of Fe) and N_2O_4 at room temperature, it was found to solubilize the solid $NOFe(NO_3)_4$ completely. Practically all of the solid was insoluble under these conditions before the addition of acetonitrile. Such a solution also was found to maintain its integrity (no visible change) during a temperature cycling over the range of 0 to 37.8 C (32 to 100 F).

Other reagents were found which did not dissolve the solid $NOFe(NO_3)_4$ by themselves, but were found to be effective in solubilizing the solid as N_2O_4 mixtures. For example, the $NOFe(NO_3)_4$ was insoluble in CF_3CN alone, but was soluble in a mixture of CF_3CN and N_2O_4.

The thermal stability of N_2O_4 with small amounts of coordinating reagents (no more than 1 w/o) was the third area of investigation. These tests were

conducted at 73.89 C (165 F) over a period of 24 hours in stainless-steel bombs. The last column of Table 11 indicates the results obtained from these tests.

The maximum amount of additives used for tests was arbitrarily set at 1 w/o of the N_2O_4 mixture because it was believed that a greater amount might cause significant changes in the propellant properties of N_2O_4.

The reagents that had passed the three tests were then considered as prime candidates for use as additives to N_2O_4. These prime candidates were finally scheduled to be tested in actual flow situation in Phase V. Four of these reagents, acetonitrile, benzonitrile, ethylacetate and perfluorobenzonitrile, were provided for this purpose. All of these reagents were effective in the elimination of flow decay (for details see Phase V).

The solubility of $NOFe(NO_3)_4$ also was tested in INTO (N_2O_4 + FNO_2) when the possibility arose that INTO could substitute for N_2O_4 itself. Visual examination indicated that the solid was insoluble in INTO under ambient conditions. Upon isolation, however, it was noted that the color of the solid had changed from light brown to pure white. Analyses (infrared and elemental) indicated that the new solid had a composition of $FeF_3 \cdot NO_2F$ (equivalent to $NO_2^+FeF_4^-$).

The reactivity of INTO with one of the prime candidate additives (pentafluorobenzonitrile) also was tested. Apparently, pentafluorobenzonitrile is not compatible with INTO. Mass spectral data indicated the formation of CF_4, CO_2, N_2, and HF. The parent compound was not recovered.

A small flow-decay apparatus was built to facilitate the study of the flow-decay phenomenon on a laboratory scale. After numerous exploratory experiments, it was possible to produce enough of the deposit for identification purposes. The infrared spectrum was found to be identical to that of the flow-decay compound (Fig. 15).

The effectiveness of an additive in the elimination of the flow-decay deposit (demonstrated with the flow bench, Phase V) was duplicated in the laboratory with the small flow-decay apparatus. The predeposited solid was wiped clean in a single pass after the addition of 0.25 w/o acetonitrile to the N_2O_4.

CONCLUSIONS

The feasibility of the principle of elimination of flow-decay deposit by the additive approach has been demonstrated. Reagents with different functional groups have been discovered as effective complexing agents in N_2O_4 and, thus, prime candidates in the elimination of flow-decay deposits. A convenient tool for the study of the flow-decay phenomenon on a laboratory scale has been developed.

PHASE V: EFFICIENCY OF ELIMINATION

INTRODUCTION

The primary objective of this task was to determine the feasibility of the chemical additive approach to eliminating flow decay. The secondary objective was to determine the influence of various operating parameters on the rate of flow decay.

EXPERIMENTAL

Experimental Flow Bench

Based on prior knowledge of the conditions which lead to the flow-decay phenomenon, an experimental flow bench was designed and built to use in studying flow decay. A basic outline of the system is shown in Fig. 21. Two 5-gallon stainless-steel tanks comprise the endpoints of the N_2O_4 flow path. The main tank or delivery tank is contained within a tempe ture-conditioned stirred water bath. No temperature control was provid for the catch tank. Both tanks were connected to a pressurization and vent system which supplied gaseous nitrogen for pressurization. The pressure control system allowed both the tank being emptied and the tank being filled to be maintained at constant pressure throughout any flow process.

Although many changes in detail were made during the course of the experimental work, the flow path remained essentially as shown in Fig. 21. After leaving the constant-temperature main tank, N_2O_4 was cooled by passing through a heat exchanger, then flowed through a turbine flowmeter before entering the test section. A remote-control metering valve was present in the line, but ordinarily was used only to start and stop flow and was completely open during the run. A bypass loop allowed the N_2O_4 to be returned to the main tank from the catch tank without flowing through the test section. The return flow could be filtered or not, as desired.

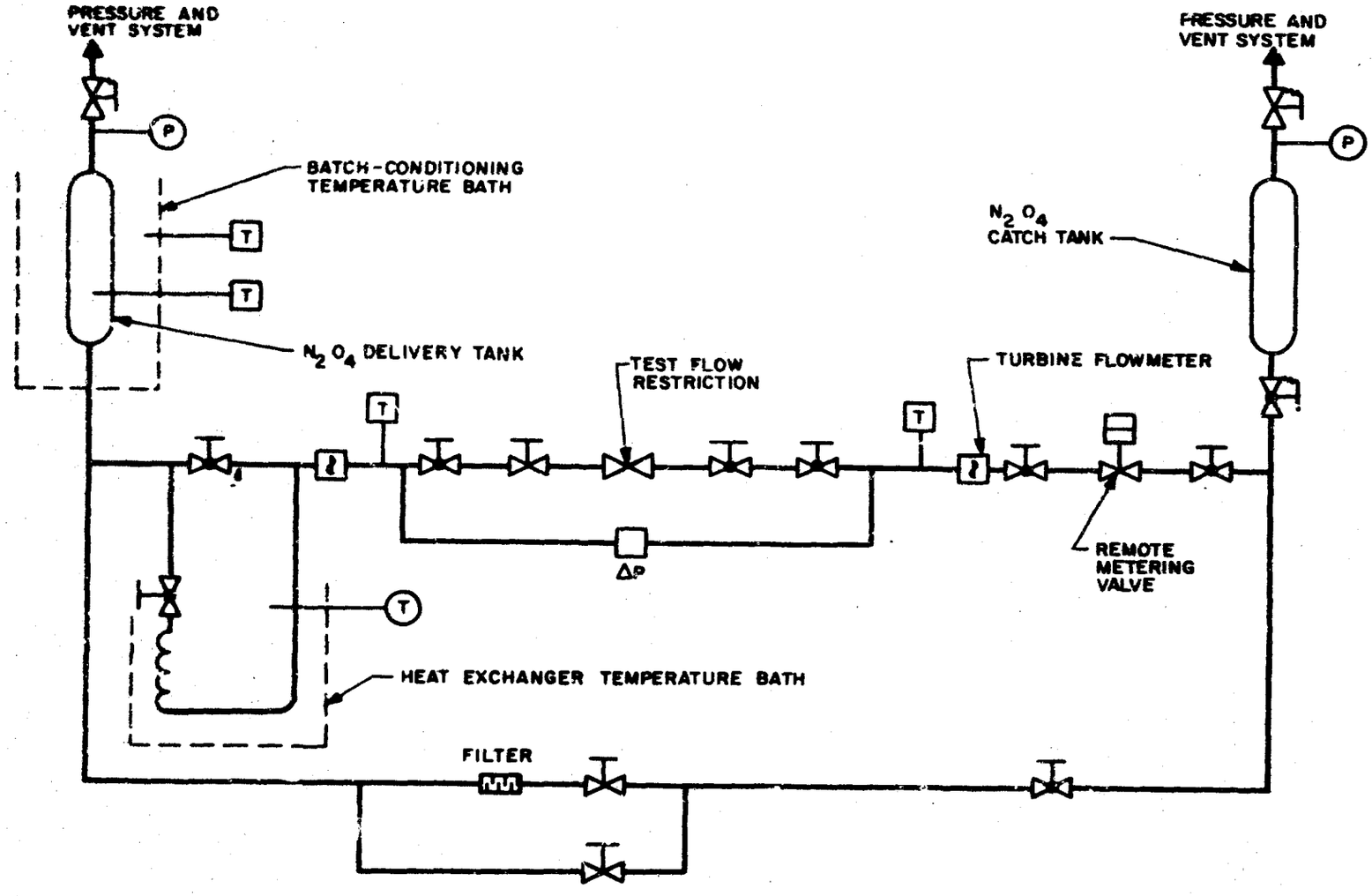

Figure 21. Propellant Engineering Laboratory N_2O_4 Flow Test Facility

All materials used in constructing the flow bench were new 300 series stainless steels, not previously exposed to N_2O_4.

Heat Exchanger Designs

The original heat exchanger design consisted of a long (100 feet) coil of 1/4-inch tubing placed inside a stirred constant-temperature bath. The purpose of the long coil was to provide sufficient heat exchange surface to ensure a constant N_2O_4 temperature at the exchanger outlet, regardless of flowrate. Although the exchanger worked well from this viewpoint, other shortcomings appeared. It became apparent that the heat exchanger surface was influencing the outcome of flow-decay experiments because some material was being precipitated within the exchanger.

The second heat exchanger design consisted of a short length of concentric tube exchanger, with N_2O_4 flowing through the annulus and cooling water flowing through the middle. This exchanger made it possible to vary the temperature during a run, a desirable test variation which was impossible with the original design. However, the small surface area meant that equilibrium temperature was not reached in flowing through the exchanger and therefore the N_2O_4 outlet temperature varied with changes in the N_2O_4 flowrate. Also, the flowrate was limited to much smaller values than it had been previously because of the small cooling capacity. With the original design, the N_2O_4 was never in contact with a temperature much below its final outlet temperature. This was not true for the small-surface-area exchanger. In summary, each design had disadvantages and no method of simultaneously achieving all the desirable characteristics could be determined.

Instrumentation

Nitrogen tetroxide flowrates were measured with Fischer-Porter radio-frequency-type turbine flowmeters. Readout appeared on a Leeds and

Northrup stripchart recorder. Some of the runs at low flowrates resulted in operating the turbine meters in an area below the manufacturer's range of guaranteed linearity. However, precise linearity was not necessary for the type of experiment conducted, providing the output was constant at a given flow.

Tank and vent pressures were obtained by observation of bourdon tube pressure gages. Differential pressure drop across parts of the test section could be obtained with two Pace differential pressure transducers having readouts on Foxboro circular chart recorders. Differential pressures were not monitored for most runs.

Temperatures were derived by means of iron-constantan thermocouples placed inside the main tank, in the constant-temperature bath, and in the line both before and after the test section. Temperatures were recorded in Fahrenheit degrees. Centigrade values are included for clarity.

Operating Procedures

Typical flow-decay runs were initiated with N_2O_4 in the main tank at the temperature of the surrounding bath. All manually operated line valves were positioned as desired before any pressurization. The catch tank vent was opened and the vent pressure regulator was adjusted to effect the desired back pressure in the catch tank. The main tank pressurization system was then set to obtain the desired tank pressure. Heat exchanger coolant flow was initiated if necessary, and the remote metering valve was opened to allow flow through the system to begin. If required, the flowrate was adjusted by changing the setting of the test valve under flow conditions.

After completing the run, the main tank was vented, the catch tank was pressurized, and the N_2O_4 returned through the filter loop.

DISCUSSION AND RESULTS

Flow Decay Behavior

Characteristic Appearance.

Slow Decrease in Flowrate. In the most commonly observed type of flow-decay behavior, the flowrate in a fixed-geometry, constant-pressure N_2O_4 flow system gradually decays toward zero. Complete stoppage of flow occurs eventually, but required several minutes at typical run conditions. The cause of the decreasing flowrate is a buildup of solid deposits at the minimum flow area in the system. Flow decay is normally induced by heating the N_2O_4 at a temperature above ambient, then cooling rapidly in a heat exchanger before passing through a flow control valve. Some typical flow bench runs, chosen to illustrate various points, are presented in Fig. 22.

For Run 148, the N_2O_4 was heated to 120 F (48.89 C) in the main tank, then cooled to 60 F (15.56 C) by passing through the heat exchanger. Pressure in the main tank was maintained at 250 psig and in the catch tank at 30 psig. Almost all of the pressure drop occurred in the test needle valve. After 19 minutes of run time, the flowrate decreased from 0.24 to 0.15 gpm.

The effect of cooling in the heat exchanger was evident in Run 134. Run temperature and pressures were approximately the same as for Run 148, but the rate of flow decay was noticeably faster, dropping from 0.22 to 0.1 gpm in 9 minutes. After 9 minutes of run time, two ball valves were actuated to shift the N_2O_4 flow path to a line bypassing the heat exchanger. Hot N_2O_4 then flowed directly from the main tank into the flow bench. The hot N_2O_4 quickly redissolved the solid deposits in the flow valve, causing the flowrate to recover to its initial value and then remain constant. Run 149 demonstrates the reversibility of the effect. During one continuous run, the N_2O_4 flow path first led through the heat exchanger, then was shunted around it, and then returned passing through the exchanger.

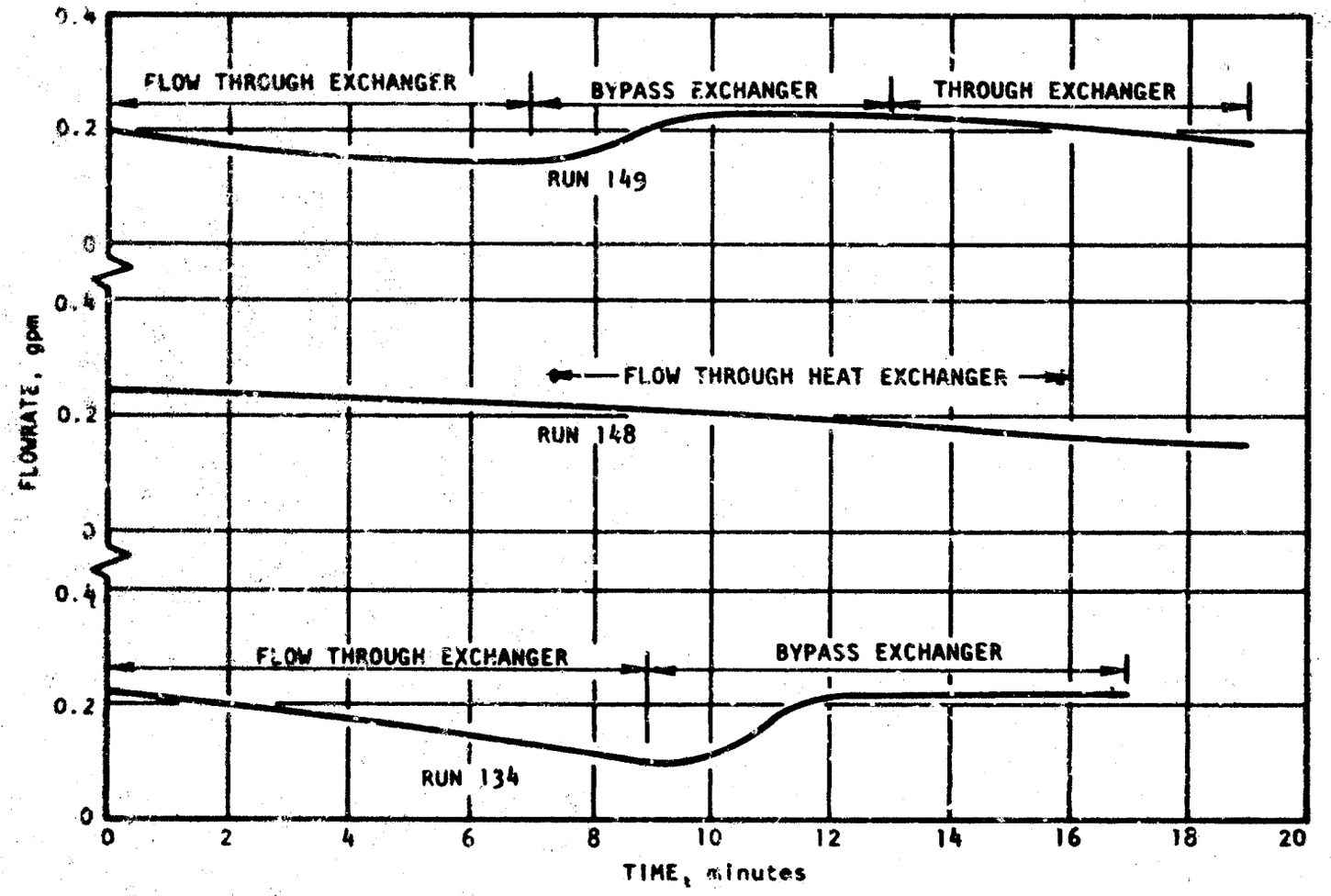

Figure 22. Flow Decay Behavior

Several other characteristics of typical flow decay are apparent in Fig. 22. The rate at which the flow-decay deposits redissolve in hot N_2O_4 is considerably faster than the rate at which they are formed. Also, although the test temperatures and pressures are approximately identical for all three runs, there are large variations in the rate of decrease in flowrate. These differences arise principally from the use of different batches of N_2O_4 and subjecting the N_2O_4 to heat soak periods of different lengths prior to the run. If these variables are also maintained constant, the run-to-run variations in rate of flow decay are small.

Some of the deposits formed in the valve during Run 148 were still present at the initiation of Run 149, approximately 1 hour later. Thus, when hot N_2O_4 was flowed through the system during Run 149, the flowrate recovered to a value greater than that at the start of the run. The slight disagreement between this value and the initial value for Run 148 is due to small changes in the run pressures. No special attempt was made to keep these conditions exactly the same during this series of runs. The initial flowrate for Run 149 was higher than the final flowrate for Run 148. This also is typical and has been observed many times. Part of the flow-decay deposit appears to redissolve on standing. Also, some of it may be removed if the main tank is emptied completely during a run and nitrogen pressurization gas is allowed to flow through the system for a short period of time.

Finally, comparing the first few minutes of each run, (Fig. 22) Run 148 is perfectly linear while Run 134 is slightly concave downward and Run 149 is convex. A considerable number of runs conducted under a variety of conditions have demonstrated that the flowrate vs time curve for flow decay under steady-state conditions is approximately linear to zero flow. An appreciable nonlinearity which is apparent in the first 2 or 3 minutes of runs conducted with the heavy sight glass valve is due to temperature changes during the time required for this component to approach the line temperature.

Flow decay is the buildup of solid deposits at the point of minimum cross-sectional area. In addition to the origin and composition of the deposit, the reasons for the deposit forming at this particular place are of particular interest. Because this is the point of highest flow velocity, it should be the point least susceptible to a buildup of solid film. However, it would be the most likely location for entrapment of solid particles large enough to bridge the annular gap in a needle valve. Inspection of the flow traces reveals that this cannot be the process occurring. The flow vs time curves are smooth and continuous. Employing Run 148 as an example, it is possible to use the pressure drop across the valve, flowrate, and density to calculate an approximate value for the minimum cross-sectional area. This, along with the known valve orifice size, indicates an annular area with an outer diameter of 0.065 inch and an inner diameter of 0.057 inch. To bridge the gap, a solid particle must, therefore, be a minimum of 0.004 inch in one dimension. The average length of the perimeter is 0.190 inch. Thus, if spherical particles are assumed, only 50 particles of the minimum 0.004-inch size would be required to completely block the flow passage. The flow trace should then decrease from its initial value to zero in no more than 50 discrete steps. Sudden changes of this magnitude were clearly not occurring during the flow tests presented.

The ability of the solid deposits to adhere to the surface at the point of minimum cross section despite the high flow velocities at that point could be expected to vary with different valve geometries and flow conditions. In some cases, pieces of the solid deposit flake off from time to time, causing sudden increases in the flowrate. A typical run illustrating this behavior is presented in Fig. 23. The sudden increases at three different points during the run result from small portions of the flow-decay deposit breaking loose. The thicker the deposited film becomes, the more susceptible it is to breaking loose. Sudden decreases in flowrate, as would be caused by solid particles bridging the annular gap, were never observed.

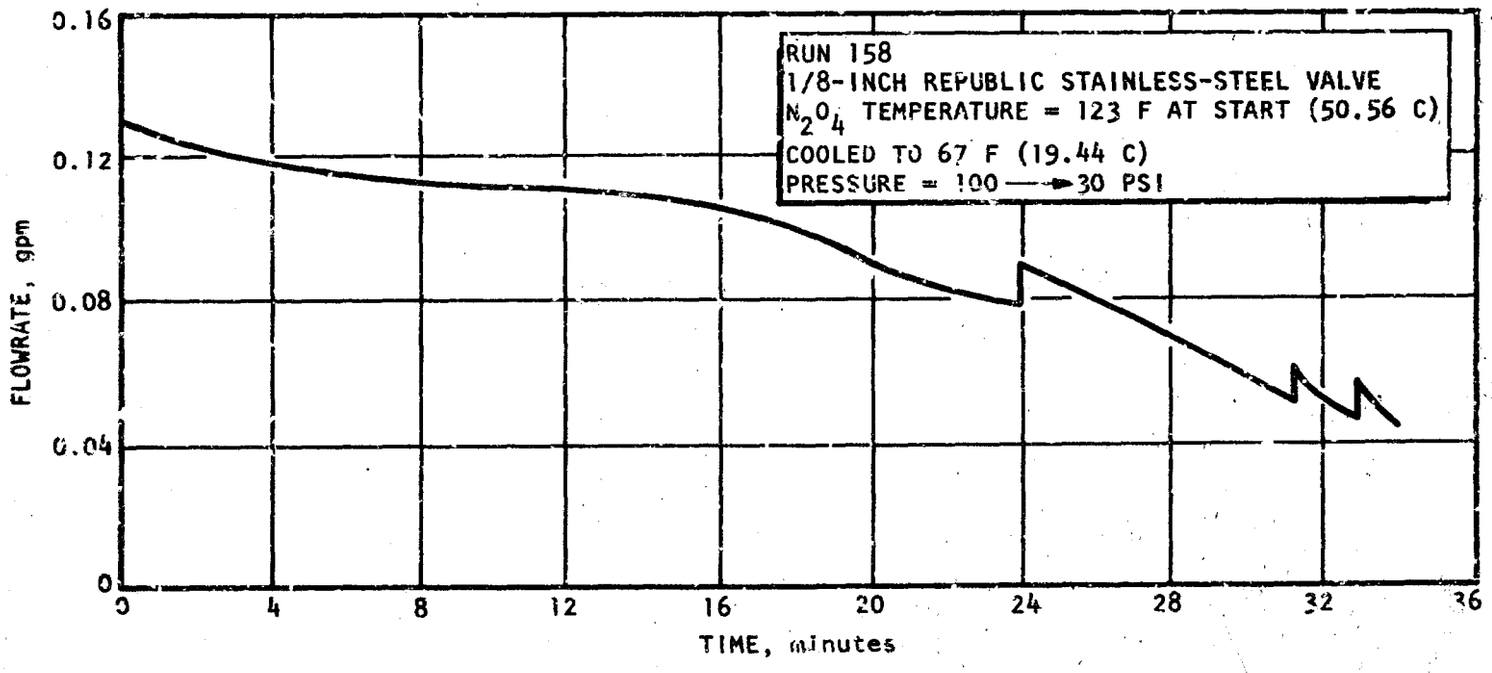

Figure 23. Flow Decay With Flaking Off of Solid Deposit

Rapid Decrease in Flowrate. The rates of decrease in flowrate during typical flow bench runs, as seen in the previous section, would obviously affect system operation but might not be considered a serious hazard in normal rocket engine applications. Total operating time of a rocket engine seldom approaches the 15 to 30 minute run times studied here. However, on certain occasions, extremely rapid decreases in flowrate can result, with complete blockage of a 0.25 gpm flow in as little time as 1 minute. This behavior has been termed "castastrophic flow decay" and is illustrated in Fig. 24. The instantaneous increases in flowrate illustrated in Fig. 24 are the result of manually widening the needle valve opening to maintain flowrate. After 26 minutes, the valve opening had been increased 14 times so that the valve minimum flow area was approximately 10 times its initial value, but flow was completely stopped. The total temperature drop from the main tank to a point downstream of the needle valve was only 10 F. Obviously, a condition which required only a 4 to 10 F temperature change for initiation and which can completely stop a 0.25 gpm flow presents a potentially extreme hazard in the operation of small rocket engines with N_2O_4 oxidizer. This "catastrophic flow decay" behavior appears to arise from a supersaturated condition, but the exact factors responsible are still unknown. Almost all possible ranges of flow-decay rate have been observed from this maximum of approximately 0.25 gpm/min to the smallest practically measurable value of approximately 0.00025 gpm/min.

Deposits observed on the valve needle after Run 113 are illustrated in Fig. 25. The deposits were typically a pale yellowish-white and disappeared rapidly when exposed to air.

Effect of Flowrate and Pressure. The flowrate vs time curves in Fig. 22 were essentially linear to zero flow. This will become more and more apparent in succeeding illustrations. These runs all involved a nearly closed needle valve with pressures on both sides of the valve held constant. The minimum flow area is annular in shape with an annular gap width that is small in proportion to the diameter. For a constant pressure

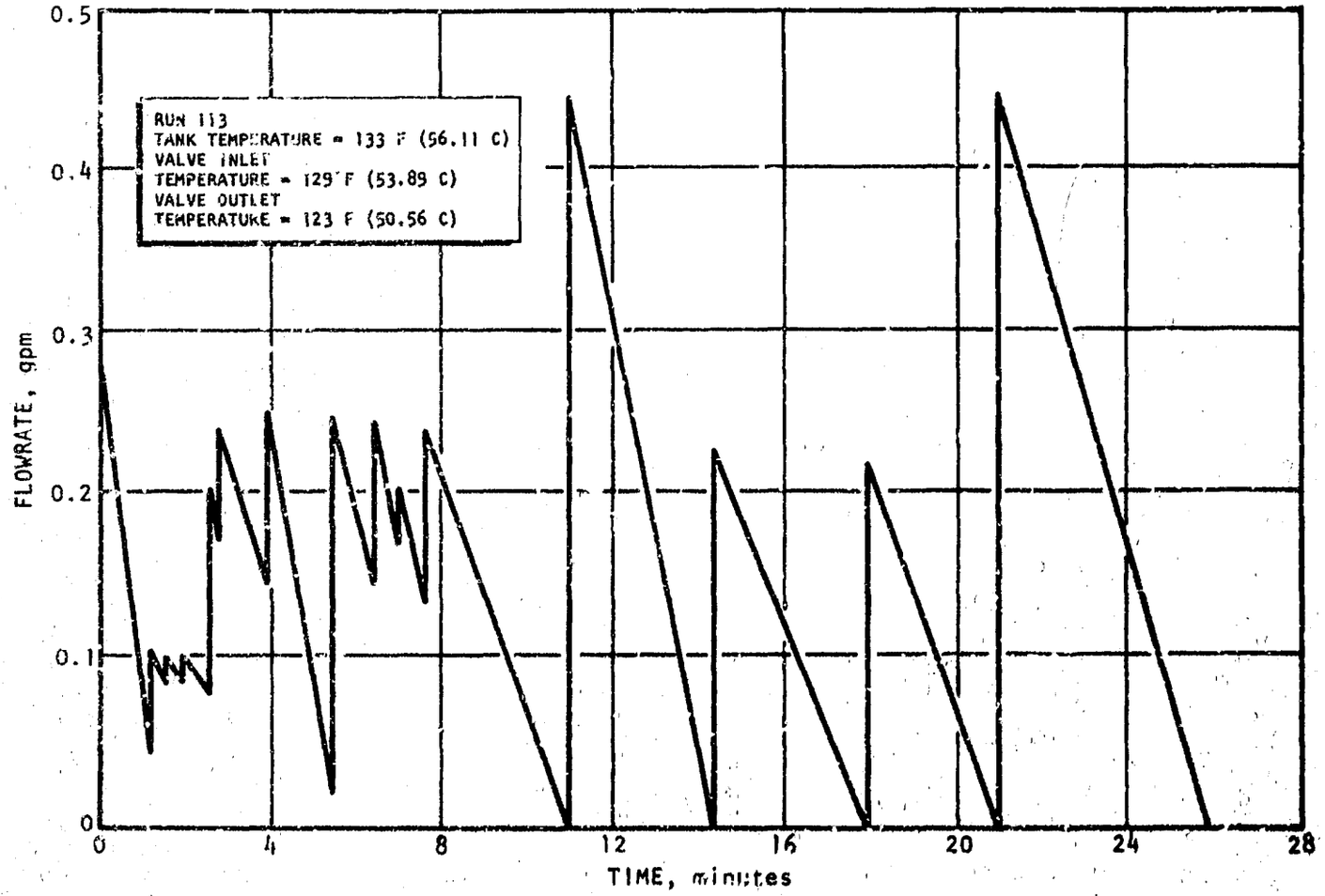

Figure 24. Catastropiic Flow Decay

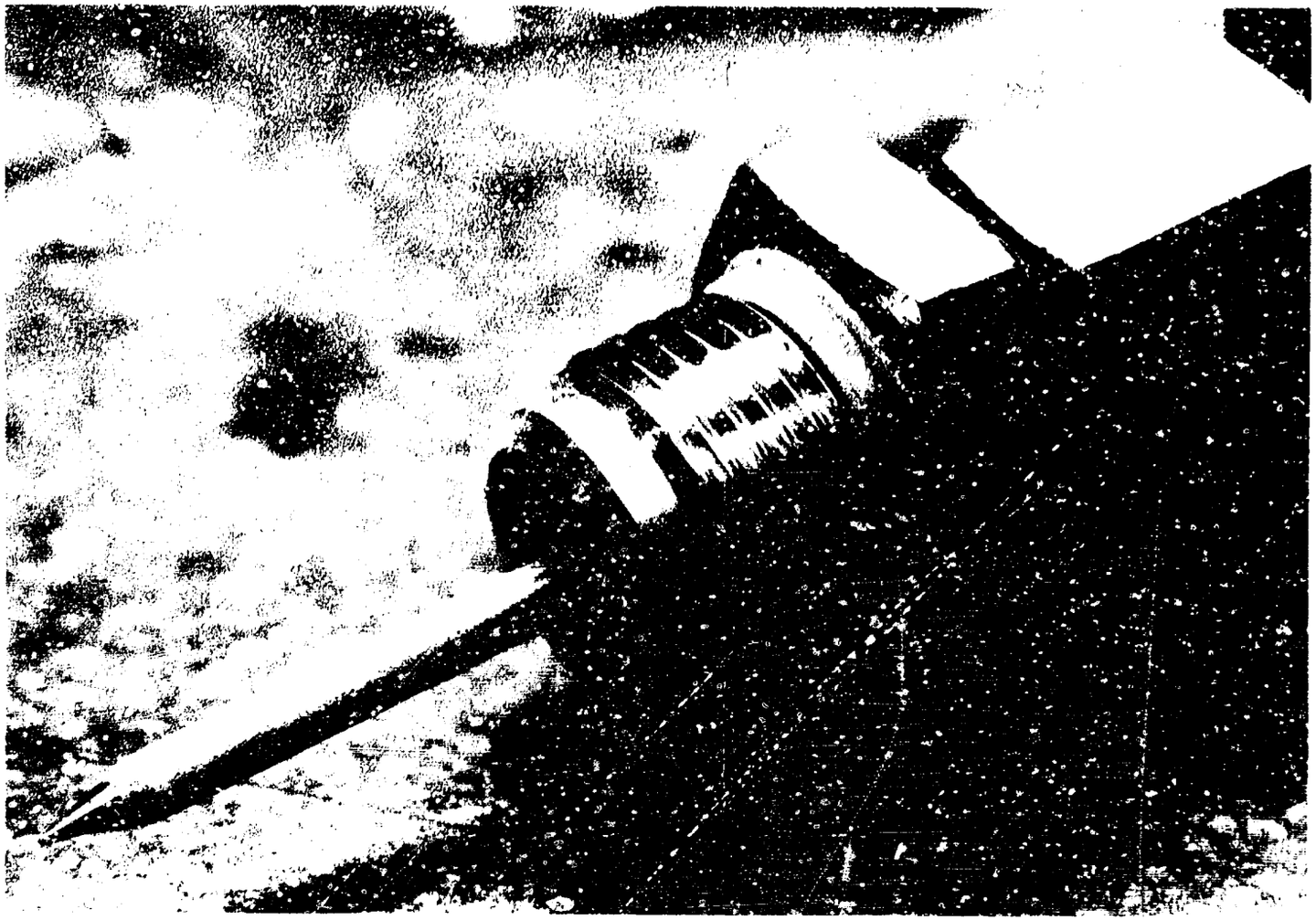

1XZ65-2/14/67-C1B

Figure 25. Flow Decay Deposits on Valve Needle

drop, flowrate is directly proportional to the area of a constriction. Therefore, a linear decrease in flowrate with time indicates a linear decrease in area and a linear increase in thickness of the film deposited at the minimum area. Because the deposition rate is constant with time and is not a function of mass flowrate, this would indicate that only a small part of the total material which could be deposited, actually accumulates at the point of minimum area and that the deposition rate is limited by local transport processes (i.e., because linear velocity is approximately constant).

The magnitude of the pressure drop across the constriction in which flow decay is occurring has an important effect on the rate, but the absolute pressure does not appear to be influential. One early hypothesis was that the absolute value of the pressure downstream of the valve would be important from the standpoint of whether or not cavitation were possible. It was thought that cavitation boiling within the valve could be responsible for the accumulation of solid deposits at that point. Numerous experimental runs were conducted to verify this hypothesis, one of which is shown in Fig. 26. Run 132 was conducted with the sight gage valve so that visual confirmation of the presence or absence of cavitation was possible. The run was initiated with 250-psig main tank pressure and 0-psig vent pressure. The N_2O_4 temperature was reduced from 125 to 60 F (51.67 to 15.56 C) by flowing through the heat exchanger ahead of the valve. Under these conditions, extensive cavitation was visible within the valve. After several minutes of flow, the pressures both upstream and downstream of the valve were increased by 100 psi. At the same time, the valve opening was increased to partially restore the flowrate. No cavitation bubbles were visible under the higher pressure conditions. However, the rate of flow decay was not significantly affected. These and similar results have established that cavitation is not of appreciable importance in producing flow decay.

The pressure drop across a valve determines the flow velocity at the minimum cross section for flow. It was expected that the velocity would

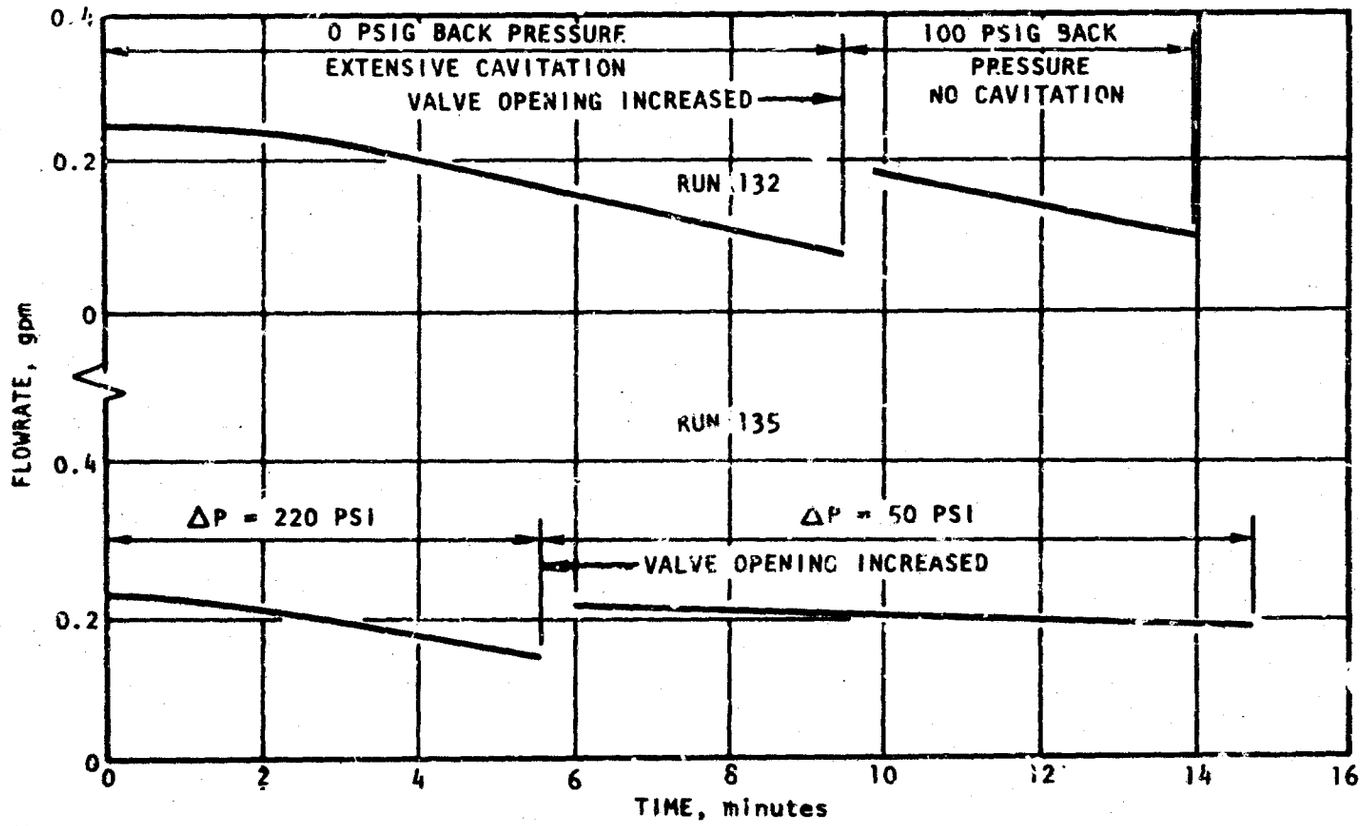

Figure 26. Effect of Pressure and Differential Pressure

influence the deposition of a solid film at this point. During Run 135 (Fig. 26) the differential pressure at start was 220 psi (30 psig downstream, 250 upstream). The differential pressure was then lowered to 50 psi by decreasing the upstream pressure while keeping the downstream pressure constant at 30 psig. The valve opening was increased as necessary to yield approximately the same initial flowrate at the lower pressure drop. A marked change in the rate of flow decay resulted. A large part of this change must be attributed to the fact that increasing the valve opening changes the ratio of the length of wetted perimeter to the cross-sectional flow area. Therefore, a much thicker film is required to effect the same fractional change in area. Because the pressure drop changed by a factor of more than 4, the area must have increased by more than 2 and the perimeter/area ratio by even more. The rate of flow decay should thus have decreased by a factor of approximately 3 because of this effect alone. However, the observed change was even greater. If the concentration of flow-decay material in the flowing stream were constant, a higher precipitation rate at the lower pressure drop would be expected because of the lower velocity through the minimum area. In fact, the decay decreased substantially indicating that the pressure drop in some way influences the actual formation of the solid material, yielding a higher stream concentration of material for higher differential pressures. This effect was not observed for differential pressures higher than those in Fig. 26.

Initiation of Flow Decay.

Initial Reaction Time. At the initiation of this investigation it was assumed that flow decay could be produced simply by heating N_2O_4 above some minimum temperature and cooling it before flowing through a valve. The flow bench and test plan were designed accordingly. After building the system and loading it with N_2O_4, a series of exploratory runs were conducted at various conditions thought to be favorable to flow decay. No evidence of the flow-decay phenomenon was observed. Over a 3-week period, runs were conducted with the N_2O_4 heated over the range of 100

to 140 F (60 C), with tank pressures of 100 to 500 psi, vent pressures of 0 to 250 psig, flows from 0.1 to 0.5 gpm, slow batch cooling rather than sudden heat exchanger cooling, and with any combination or change of variables which might possibly affect the process. No discernable decrease in flowrate occurred during any test during this period. A new batch of N_2O_4 was loaded into the system, but there was still no flow decay. Finally, after discovery of the boiloff effect (discussed in the following section), it became possible to condition the N_2O_4 for flow decay. Then it was determined that boiloff was no longer necessary. Fresh N_2O_4 could be loaded into the flow bench, be heated for 1 hour, and effect immediate flow decay at a variety of run conditions. Therefore, it appears that an initial aging or corrosion of the tank wall must occur before a system becomes subject to flow decay. During the present investigation, the time required for this process was on the order of several weeks of exposure to N_2O_4.

Boiloff Effect. After the initial period of unsuccessful flow bench operation, the investigators on this task visited the Special Propellant Flow Facility (SPFF) at Rocketdyne where the flow-decay phenomenon was first discovered and studied. A demonstration run was conducted which resulted in flow decay when using the same sight gage needle valve that had been used for the flow bench tests. During the demonstration, it was observed that the nature of the SPFF operation (short-duration flows with rapid recycling and continuous operation) resulted in the loss of significant quantities of N_2O_4 from the system. The tank pressurization and venting process carried out on each flow cycle was certain to result in some N_2O_4 loss with each tank vent, and the cumulative effect over a large number of cycles could be substantial. It was postulated that this could be the missing factor necessary to produce flow decay in the flow bench. Testing with the flow bench was then resumed after deliberately allowing an appreciable fraction (greater than 10 percent of the N_2O_4) to boil off by venting the hot main tank to the atmosphere for several minutes. This resulted in the first experimental observation of flow decay in the flow bench.

After emptying the system and loading with a new batch of N_2O_4, it was again necessary to boil off a portion of the N_2O_4 to produce flow decay. This behavior was repeated with three succeeding loads of N_2O_4. Therefore, it appears that boiling away a part of a given mass of N_2O_4 will dispose a flow system toward flow decay when it would not otherwise be susceptible. The exact mechanism by which the boiloff influences flow decay is still not known. It could be simply a concentration of some critical nondistilling chemical species of low volatility, or it could be the result of some reaction which occurs more favorably at low pressure, perhaps due to the greater dissociation into NO_2 at lower pressures. Further observations of this effect were eliminated when increased aging of the flow bench made it unnecessary to boil off any N_2O_4 before obtaining flow-decay behavior. The test history of the flow bench system, illustrating the change in behavior with increasing system age is summarized in Table 12.

Nucleation Effect. The formation of a solid precipitate from a saturated or super-saturated solution usually begins at certain microscopic nucleation sites. If the initial nucleation step is difficult or slow, there may be a possibility of utilizing this knowledge to delay or inhibit the precipitation. In the course of the experiments performed during this task, the deposition of flow-decay material was observed on steel, aluminum, glass, and plastic. For this reason, avoiding flow decay by control of construction materials does not seem promising. However, there appeared to be some differences in the ease with which the solid deposit adhered to different surfaces.

The existence of a specific surface nucleation effect was demonstrated during parallel flow tests. Identical valves were placed in a parallel flow circuit, with common inlet and outlet lines. Separate flowmeters monitored the flow through each valve. The results obtained with two needle valves, both of which were new and had been subjected to the same cleaning treatment before placing in the system, are illustrated in Fig. 27. During the first run (180), a low rate of flow decay began immediately in valve No. 1, but the initial nucleation step did not occur in valve

TABLE 12

INITIAL FLOW-DECAY CONDITIONS

N_2O_4 Batch	Runs	Result
1	1 to 48	No decay under any conditions
2	49 to 73	Decay only after extensive boil-off
3	74 to 100	Decay only after boil-off
4	101 to 112	Decay only after boil-off
5	113 to 131	Decay after soaking for 3 days at 130 F (54.4 C), no boil-off
6	132 to 145	Decay immediately after loading into system
7	146 to 167	Decay immediately after loading
8	168 to 191	Decay after soaking for 3 days at 120 F (48.89 C)
9	192 to 226	Decay immediately after loading
10	227 to 238	Decay immediately after loading
11	239 to 240	Decay immediately after loading
12*	241 to 245	No significant decay obtained
13	246 to 254	Decay immediately after loading
14	No runs	
15	255 to 259	Decay immediately after loading
16	260 to 266	Decay immediately after loading
17	267 to 268	Decay immediately after loading

*Refer to section on special tests with the Gemini engine

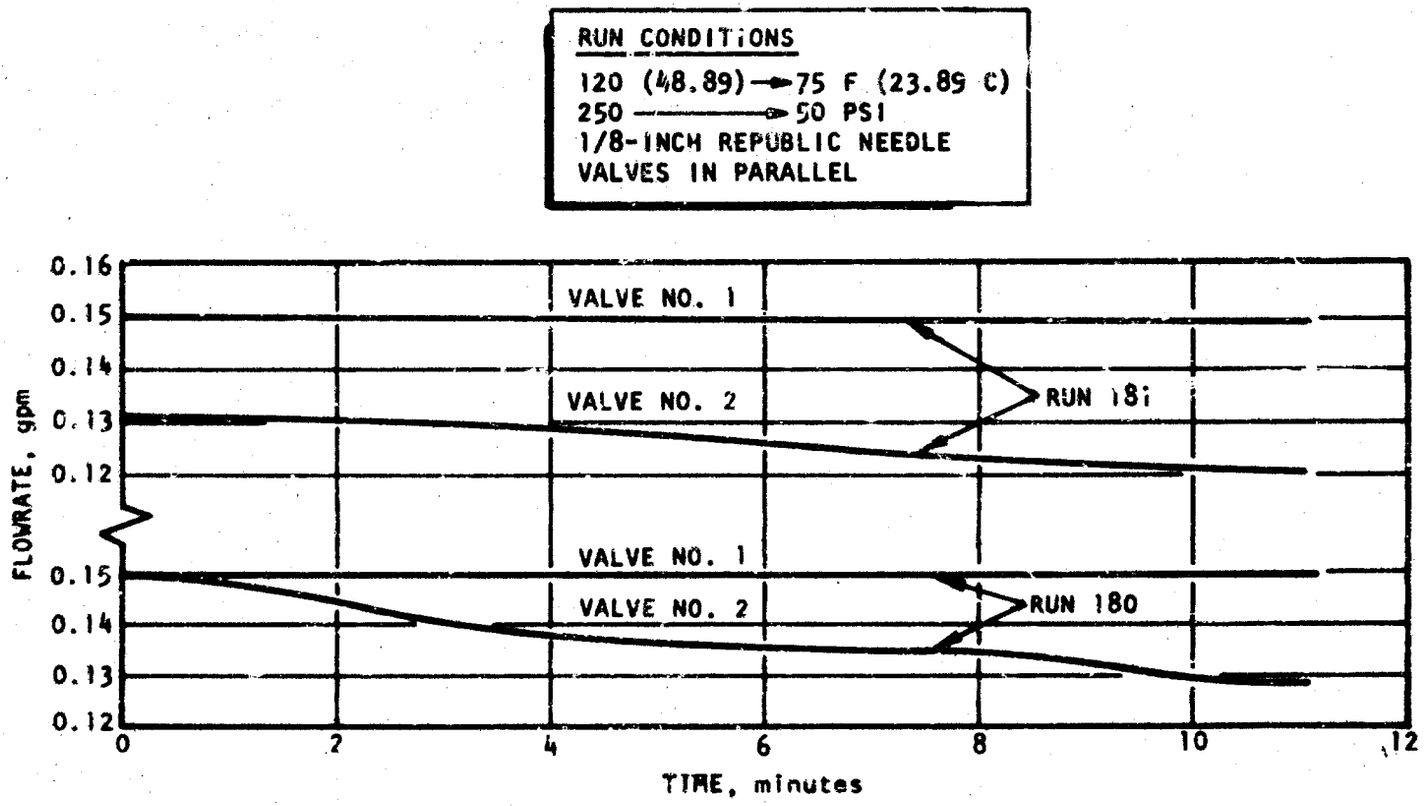

Figure 27. Delayed Nucleation Effect

No. 2 until after more than 20 minutes of flow during two separate runs. After the initial nucleation had occurred, the rate of flow decrease (rate of buildup of deposits) was the same in both valves. This is further discussed in the following section. The indications are that the initial nucleation step is influenced by microscopic factors, giving unpredictable nucleation delay times; but once nucleation has occurred, the rate of deposition of flow decay material is a function of the relevant thermodynamic variables. The rate of flow decay in Fig. 27 is very small; a long nucleation delay time was never observed for runs which resulted in appreciable rates of flow decay.

Geometric Effects.

Parallel Valve Flow Tests. The parallel flow circuit was used for a number of experiments to determine the effects of valve design on susceptibility to flow decay. With parallel flow through identical valves, approximately equal rates of flow decrease are obtained. Two such runs are illustrated in Fig. 28. In the first case, the rate of flow decay in one valve consistantly leads that in the other valve by a small amount. In the other run shown, the relative rates were reversed each time the valve openings were increased to restore a completely stopped flow. Although the rate of flow decay through two identical valves is seldom exactly identical, the variations shown in Fig. 28 are sufficiently small to allow meaningful comparisons to be made between nonidentical valves on the basis of observed differences in parallel flow decay rates.

Four miniature valves were selected for parallel flow comparisons. These valves, shown in Fig. 29, were standard commercial 1/8- and 1/4-inch size stainless-steel valves with globe-pattern flow paths. The stem design varied from a straight vee to a blunt vee to a blunt stem with a plastic insert. Since the flow tests were made with the valves almost completely closed, the minimum cross section to flow was a thin annulus in all cases and the stem design is not likely to be consequential. The orifice diameters were 0.065, 0.120, 0.170, and 0.215 inch. An example of the parallel

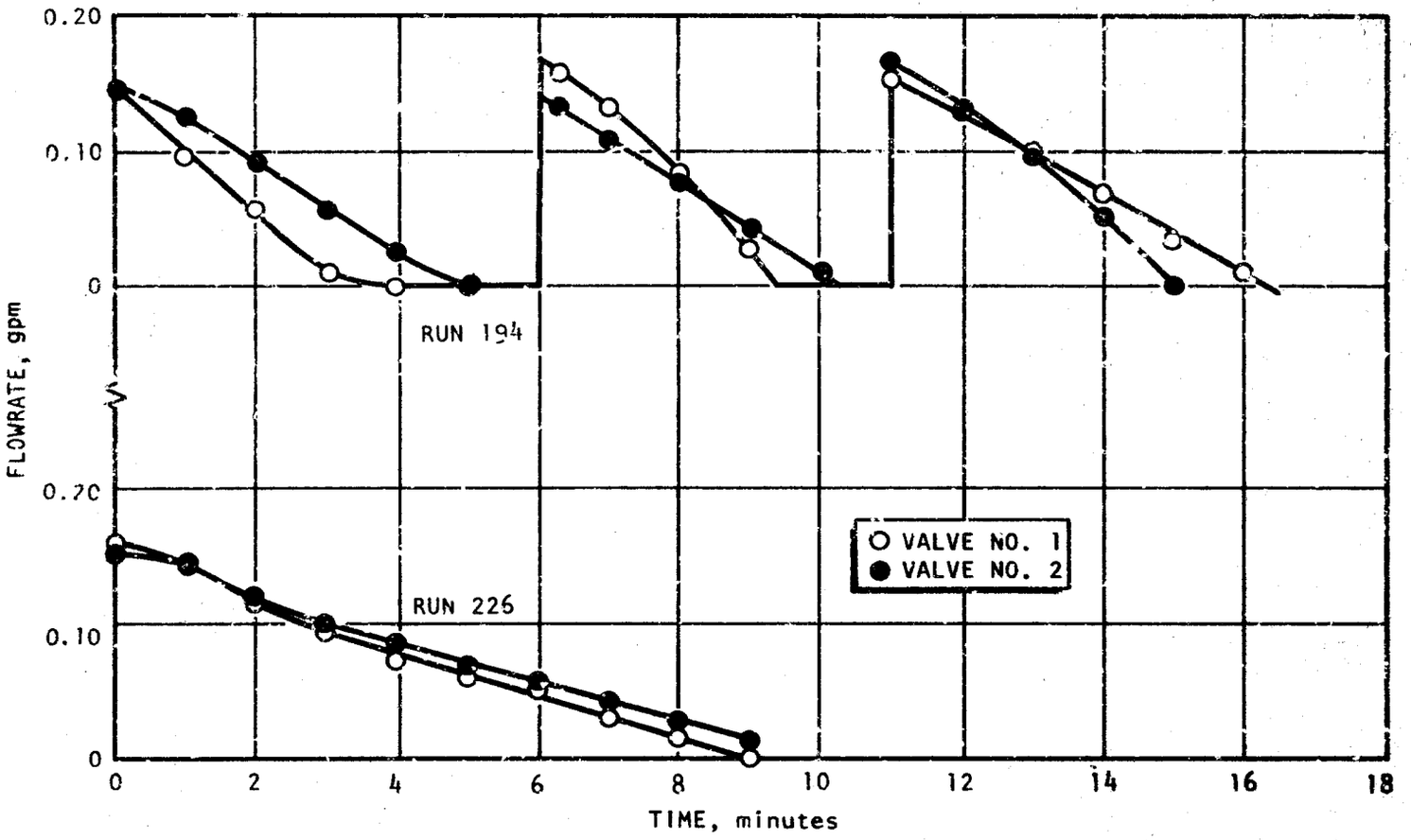

Figure 28. Parallel Flow With Identical Valves

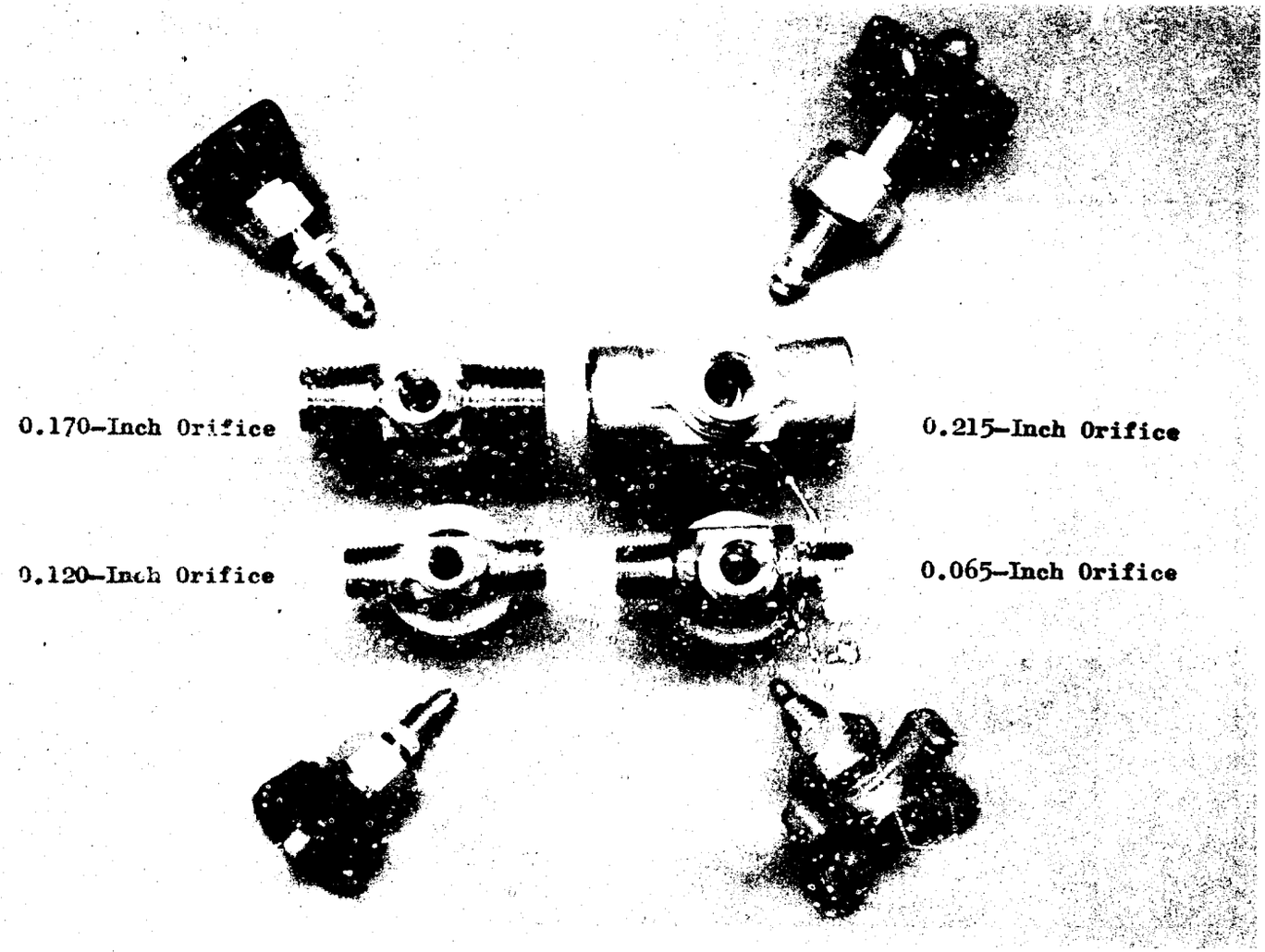

Figure 29. Needle Valves Used During Parallel Flow Tests

flow comparisons is presented in Fig. 30. Those three runs compare the 0.065-inch orifice with the 0.120-inch orifice valve. For all runs, the valve with the larger diameter orifice exhibited a faster rate of flow decay. This was ascertained for all bilateral comparisons between the valves in Fig. 29. In every case, the valve with the larger orifice diameter was the more susceptible to flow decay.

The results of these parallel valve flow tests conform to expectations based on the fact that the rate of buildup of film thickness at the minimum flow area is constant for a given set of flow conditions. The larger the diameter of the valve orifice, the larger will be the ratio of length of wetted perimeter to cross-sectional area for a given area (i.e., the smaller will be the annular gap between the orifice and the valve stem). Therefore, the same film thickness will have a larger effect on flow through the valve with the larger diameter orifice.

Variations in Valve Design. In the course of the nearly 300 experimental runs conducted with the N_2O_4 flow bench for this study, a wide variety of valve types were determined to be susceptible to flow decay. Either the specially designed sight gage needle valve or a 1/8-inch miniature steel needle valve were used for the majority of runs. However, flow decay was experienced at least once with a number of different needle valves and with such other diverse flow restrictions as were present in a pneumatically operated proportional control valve, a filter, and a complete feed system for the Gemini SE-7. It appears that any point of area constriction in an N_2O_4 feed line will be subject to flow decay if the minimum flow area is sufficiently small and a large enough pressure drop across the constriction is present.

Point of Origin of Solid Deposits. A question of prime importance concerns the point of formation of the solid flow-decay precipitate. At the start of this investigation it was not known whether the solid material was actually precipitated out at the valve or whether it was formed in the

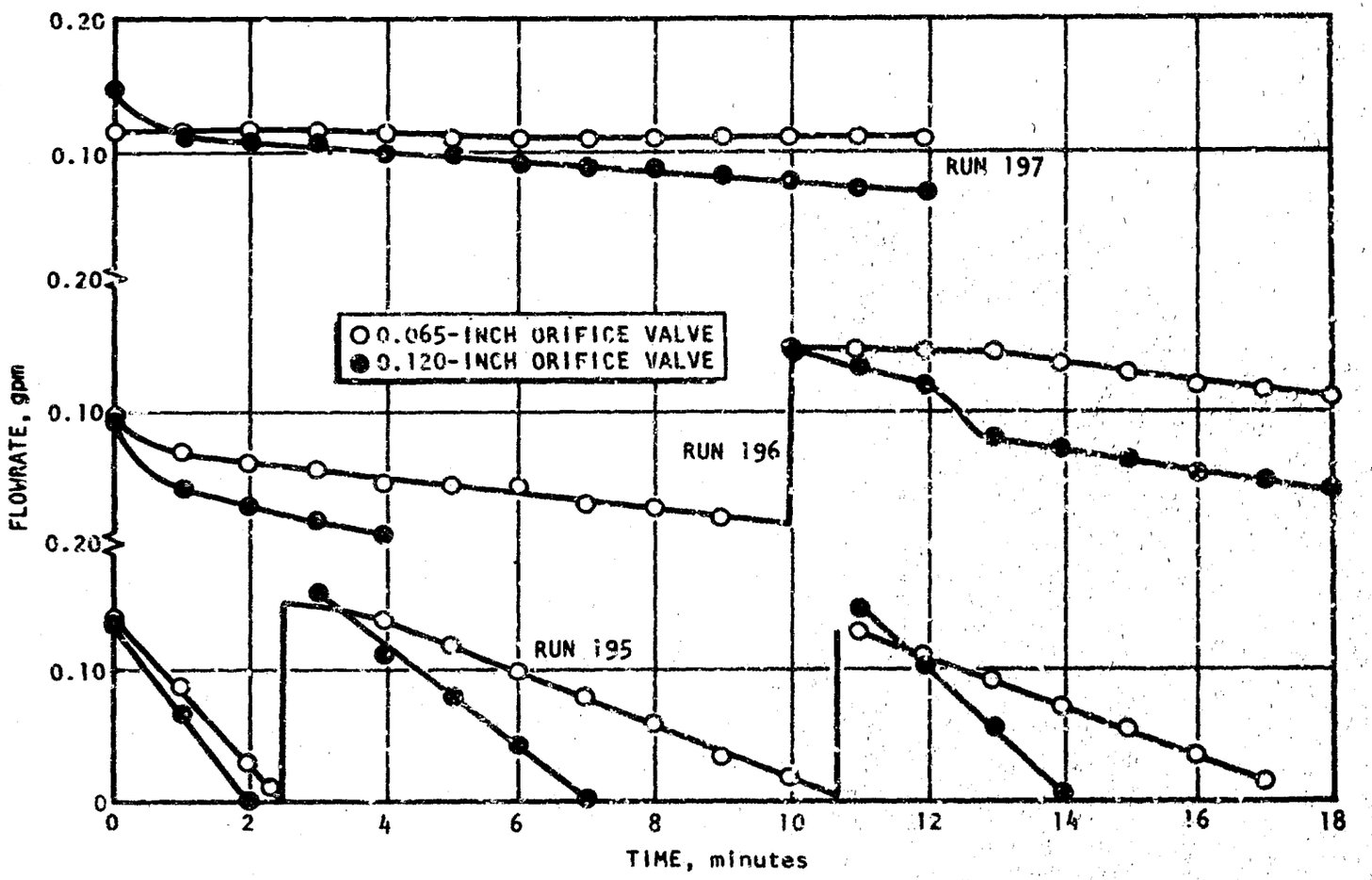

Figure 30. Parallel Flow Valve Comparison

bulk N_2O_4 as a result of temperature cycling, and merely accumulated at the valve as the N_2O_4 flowed through. Three separate types of experimental evidence help clarify this particular question.

The first and most definitive type of evidence is illustrated in Fig. 31. In runs with the glass wall valve in which a visible deposit was obtained, this deposit was always present downstream of the valve orifice, never upstream. This would seem to be a positive indication that the precipitate was being formed at the valve and was not present in the form of solid material upstream of the valve orifice.

The second set of observations resulted from a series of runs conducted with a metal cold finger placed in the flow line. Locations both upstream and downstream of the flow-controlling valve were tried. It was found that a deposit could be obtained on a cold surface upstream of the valve. This provided, for the first time, proof that a pressure drop is not necessary to form the precipitate. However, it was observed that the deposit was always heavier with the cold finger in the downstream position than in the upstream position. Because the total amount of deposit was extremely small in all circumstances, the comparisons were only qualitative, based on visual observation. Nevertheless, the large magnitude of the differences was believed to be quite significant. Thus, these experiments, while proving that a pressure drop is not essential to formation of the solid flow-decay deposits, still suggest that most of the material contributing to valve plugging is actually formed at the valve rather than upstream.

A third set of data was derived from a set of 11 runs which were conducted with two needle valves in series. The differential pressure across one of the valves was monitored as well as the pressures upstream and downstream of both valves. If solid flow-decay material were present in the flowing stream before reaching the valves, the upstream valve would be expected to plug up first. This would be indicated by a rising differential pressure across the downstream valve (pressures upstream and downstream

1XZ65-2/14/67-C1A

Figure 31. Deposits in Sight Gage Valve

of the two valves are regulated to constant values). Conversely, if solid deposits are formed only as a result of the pressure drop or some other process occurring in the valves, some of the material formed at the upstream valve could be expected to remain in the stream and contribute to plugging of the downstream valve. In this case, the downstream valve would be expected to plug up more rapidly and exhibit an increasing differential pressure.

During 6 of the 11 runs conducted with valves in series, the differential pressure across the downstream valve increased as flowrate decayed (with a corresponding decrease in the differential pressure across the upstream valve). During three runs, the differential pressure across both valves remained constant. Two runs exhibited a decrease in pressure drop across the downstream valve. Three different pairs of valves were used. The positions of each pair of valves (i.e., upstream vs downstream location) were also reversed for at least one run with each pair of valves. In the two cases where a decreasing pressure drop across the downstream valve was obtained, reversal of the valve positions resulted in either a constant pressure drop or an increasing pressure drop across the downstream valve during succeeding runs. In other cases, with increasing downstream pressure drop, reversing the valve positions had no effect on the results. One set of such data is illustrated in Fig. 32. As flowrate dropped, the pressure differential across the downstream valve increased and that across the upstream valve decreased, regardless of the position of a particular valve.

The results of the series valve flow tests, while not entirely unambiguous, tend to support the formed-at-the-valve hypothesis rather than the formed-upstream hypothesis. Because many other factors (absolute pressure and temperature levels, individual valve differences, etc.) could influence the outcome of these tests, it is not surprising that the results vary from run to run. It is apparent that either a decrease in temperature or a decrease in pressure (some decrease in temperature will also accompany a pressure drop) in a flowing stream of properly conditioned N_2O_4 can

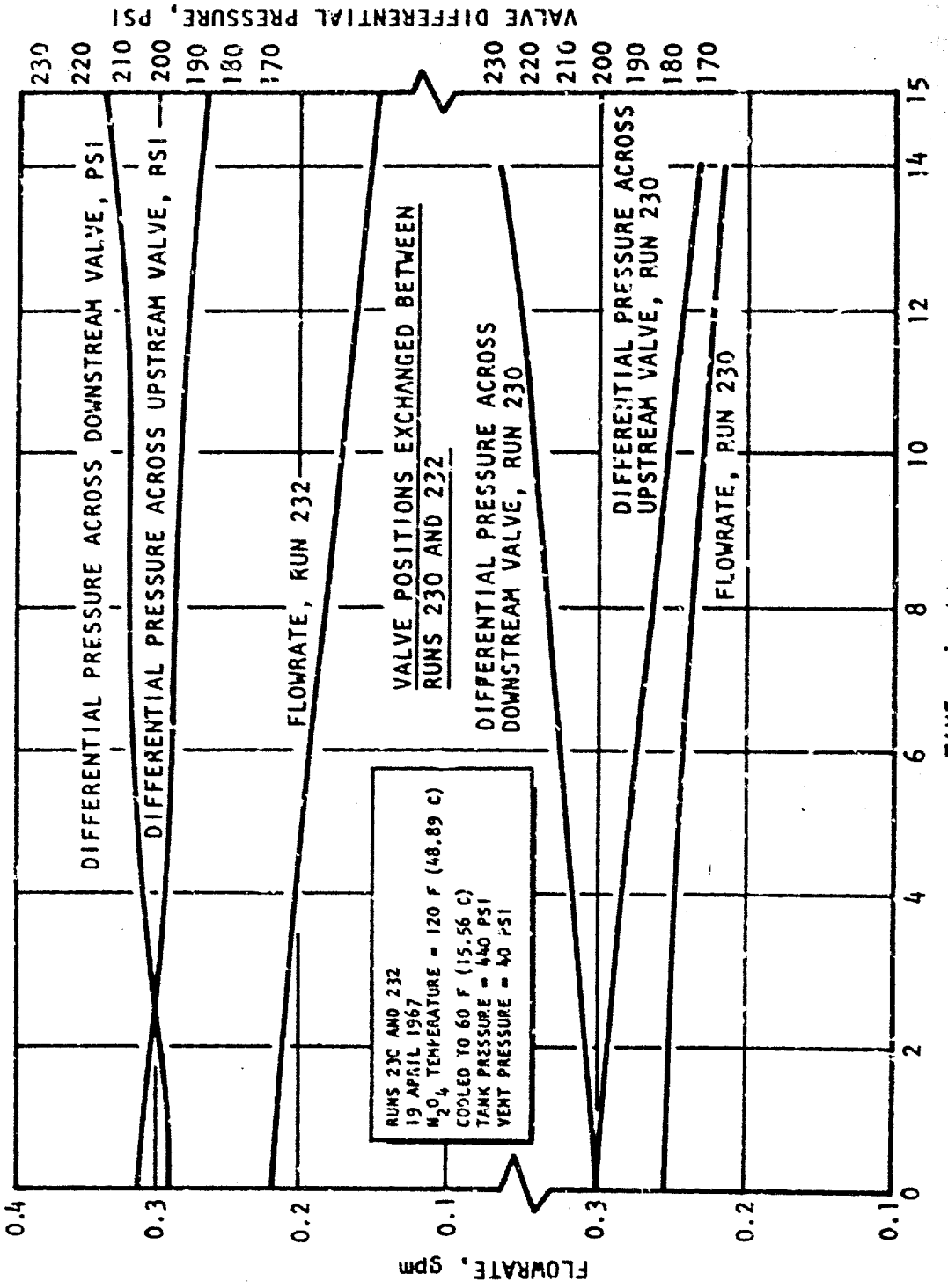

Figure 32. Flow Tests With Valves in Series

result in a precipitate at the site of the temperature or pressure change. All of the experimental evidence available to date indicates that the bulk of the material contributing to flow decay through a valve or other flow constriction comes out of solution at the point of pressure drop and does not exist as a solid, upstream of this point. This conclusion immediately infers that the flow decay cannot be prevented by means of a simple filter.

Temperature Effects.

Cold-Finger Experiments. Experiments with a metal cold finger placed in the flow line were discussed in the previous section. These experiments established that a drop in temperature alone is able to cause deposition of flow-decay material on a cold surface. This would suggest that, in any N_2O_4 storage tank subject to slow thermal cycling, a deposit would be formed on the wall surface during any decreasing temperature period. However, the extremely small bulk concentration of material, probably no more than 1 or 2 parts per million, make it unlikely that such a deposit would ever be detected. These experiments suggested the building of the laboratory-scale flow system for visual detection of deposits which was discussed under Task IV.

Minimum Temperature Requirement. It is of considerable importance to determine the minimum temperature to which N_2O_4 must be exposed to effect flow decay. If this minimum temperature were quite high, then flow decay might never be a problem in normal systems. Because the phenomenon of flow decay was first discovered during normal ambient temperature operation of a flowmeter calibration facility, excessively high temperatures are obviously not necessary. However, storage tanks exposed to the sun can easily reach temperatures well above the measured ambient air temperature and no precise knowledge of the necessary temperature was available. Conclusive evidence of flow decay starting with a bulk temperature of 90 F (32.2 C) was obtained during several runs. One such run is illustrated in Fig. 33. A new batch of N_2O_4 was loaded into the

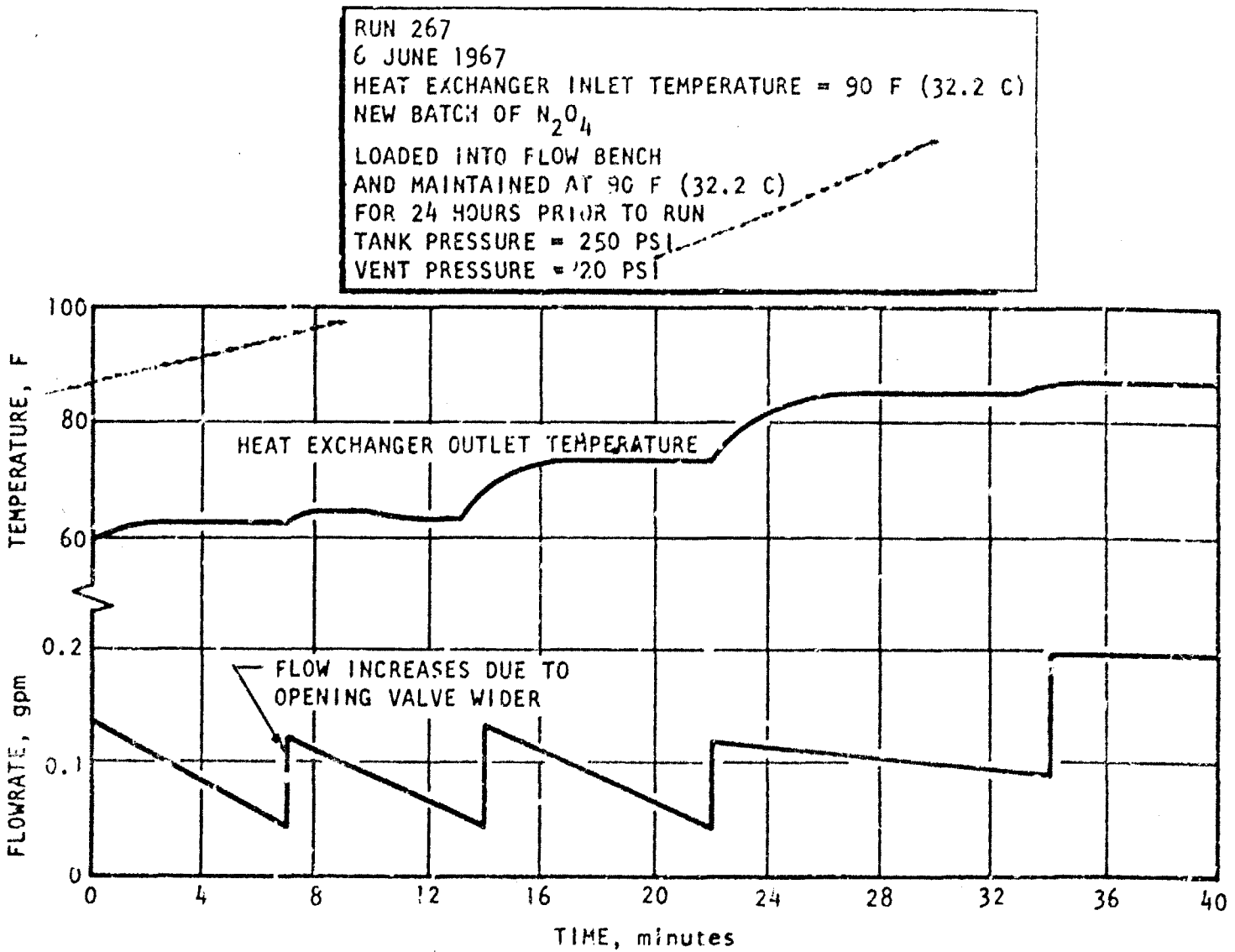

Figure 33. Flow Decay With 90 F Maximum Soak Temperature

system with the main tank at 90 F (32.22 C). At no time after loading into the flow bench was the N_2O_4 subjected to a temperature in excess of 90 F. Approximately 24 hours after loading, the experimental run was conducted. Strong flow decay was produced by cooling to temperatures below 75 F (23.89 C) in the heat exchanger. Coolant flow through the heat exchanger was reduced in several steps. Flow decay at a reduced rate was still occurring when the temperature drop through the heat exchanger was only 5 F. At a 3 F temperature drop, the flow decay disappeared.

Flow decay was also demonstrated at 80 F (26.67 C) soak temperature. However, this was accomplished with a batch of N_2O_4 which had previously been run at higher soak temperatures. It was uncertain whether the same result would be obtained with a new batch which had never been heated above 80 F (26.67 C). The only attempt to demonstrate flow decay with a new load of N_2O_4 at 80 F (26.67 C) was made during the Gemini flow tests. This attempt failed for several reasons (refer to Section VI). Following these tests, an improved heat exchanger system (used for the run in Fig. 33) was constructed but insufficient time was available for further runs to locate a minimum temperature. However, the existence of a temperature limit . some lower temperature would probably be of little value. It would be difficult to limit the maximum temperature of a practical system to le than 80 F (26.67 C).

Effect of Heat Exchanger ΔT. Because of run-to-run variations in flow-decay rate, it was possible to determine the effect of heat exchanger ΔT only with the variable temperature heat exchanger. This heat exchanger was specifically constructed with as low a surface area as possible, and therefore was limited as to cooling capacity. By reducing the N_2O_4 flowrate as much as possible, sufficient heat exchanger ΔT was available to demonstrate some of its effect on the rate of flow decay. One such run is illustrated in Fig. 33. A similar run in Fig. 34, again at a 90 F (32.22 C) soak temperature, was conducted with decreasing instead of increasing temperature drop through the run. Because of the low flowrates used during these runs, several minutes were required to attain temperature

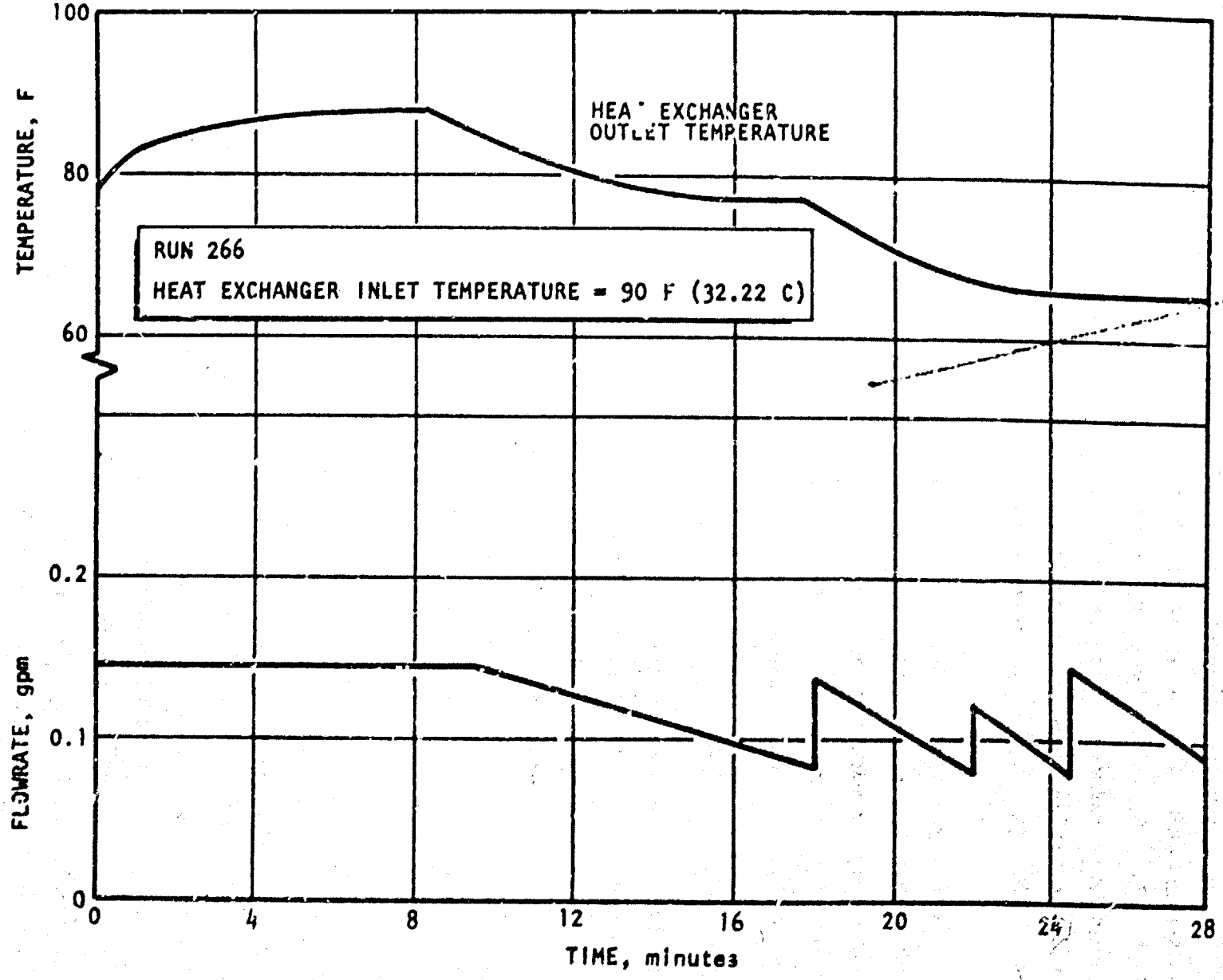

Figure 34. Flow Decay With Increasing Exchanger ΔT

equilibrium in the line when a change in the heat exchanger coolant flow was made. The linearity of flowrate vs time was extremely clear during most runs conducted with this heat exchanger system. A run in which the heat exchanger outlet temperature was first decreased and then increased is illustrated in Fig. 35.

Data from runs such as those in Fig. 33 through 35 provide an important clue as to the actual mechanism by which flow decay occurs. If, for instance, the formation of the solid deposits is accomplished through an equilibrium phase change, then a plot of flow-decay rate against heat exchanger outlet temperature should reveal a maximum outlet temperature above which flow decay does not occur. If a lower temperature limit to the solubility of flow decay material exists, then flow-decay rate should be a maximum at this heat exchanger outlet temperature, regardless of the initial soak temperature. If flow decay is simply a solubility phenomenon, and if the solubility increases linearly with temperature at all temperatures of interest, then a plot of flow-decay rate against heat exchanger ΔT should be similar for all runs. Because the variable temperature heat exchanger was installed late in the program, only approximately 10 runs with this type of heat exchanger were conducted during which the exchanger ΔT was deliberately varied during the run. The data from half of these runs yielded only widely scattered points with no apparent correlation when decay was plotted against either heat exchanger outlet temperature or ΔT. Data from the remaining five runs are presented in Fig. 36 and 37. Initial soak temperatures varied from 90 to 120 F (32.22 to 48.89 C) for these runs. When plotted as a function of ΔT (Fig. 36), the maximum decay rate for all runs can be included within a temperature span of approximately 15 F. When plotted vs heat exchanger outlet temperature (Fig. 37), a 30 F span is required to encompass all the points of maximum decay rate. Thirty degrees is exactly the range of initial soak temperature involved. Also, the horizontal displacement of the curves in Fig. 37 is exactly ordered with respect to initial temperature but those in Fig. 36 are not.

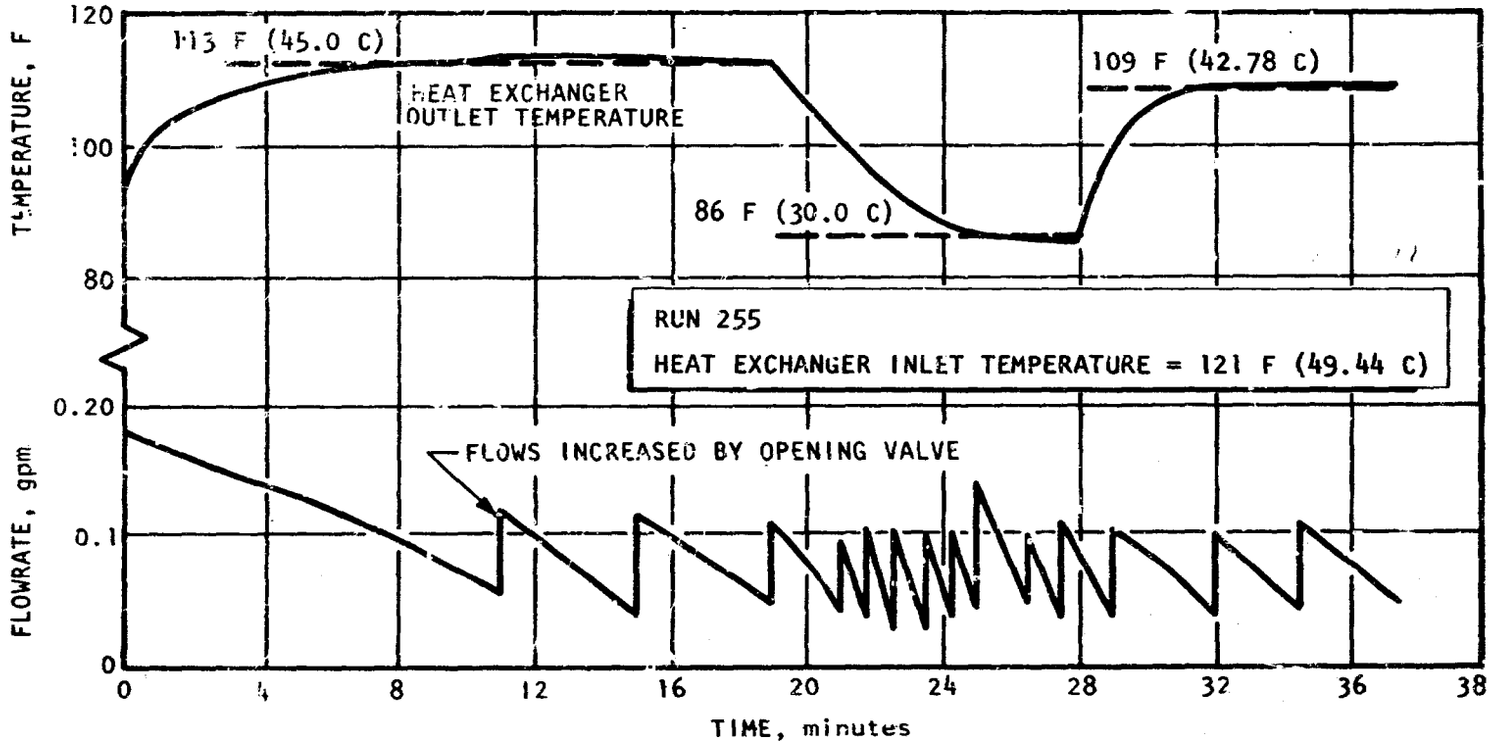

Figure 35. Flow Decay With Varying Heat Exchanger ΔT

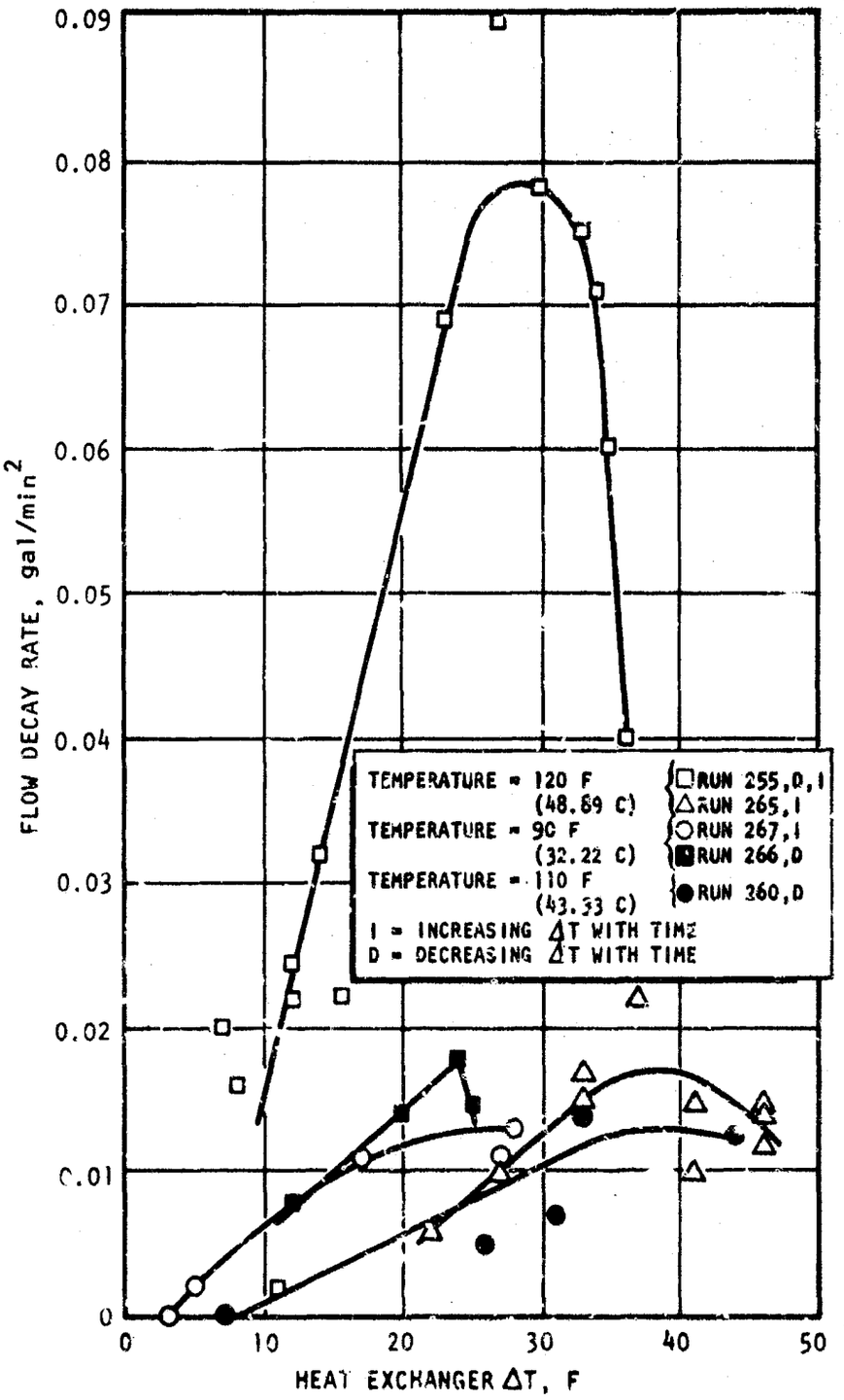

Figure 36. Effect of Heat Exchanger ΔT

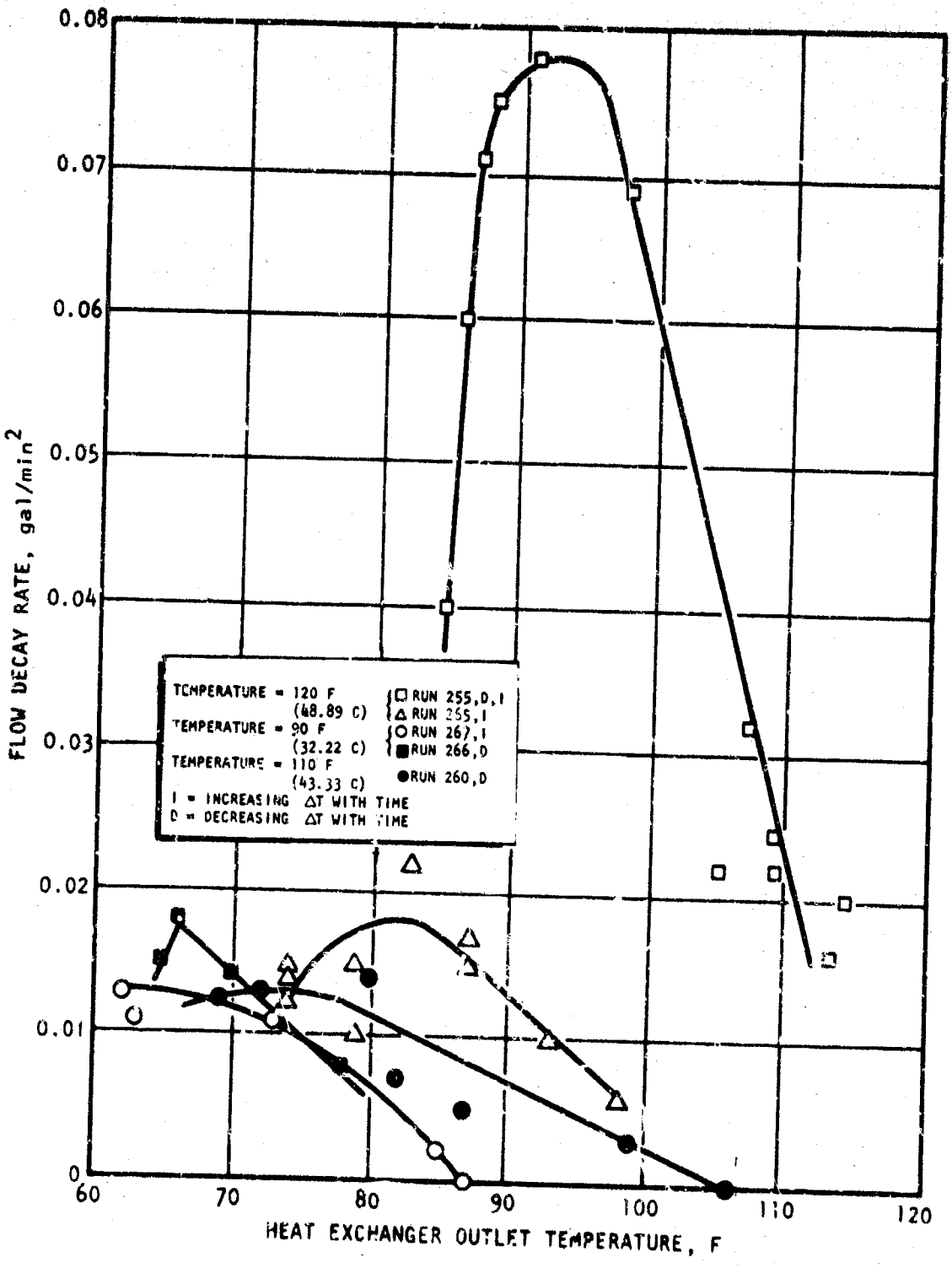

Figure 37. Effect of Heat Exchanger Outlet Temperature

These data are obviously too scattered to enable drawing precise conclusions, but they reveal no evidence of either upper or lower absolute temperature limits to flow decay. This would appear to rule out the presence of any process involving an equilibrium phase change (i.e., a freezing or melting point, etc.). The data tend to support the hypothesis of a solubility phenomenon, with solubility increasing as a function of temperature. However, if changes in solubility with temperature are the underlying cause, a constantly increasing rate of flow decay with increasing heat exchanger ΔT would be expected. The appearance of an apparent optimum in the curves is difficult to rationalize. It is possible that once a given temperature drop occurs in the exchanger, nucleation on the heat exchanger surface occurs and sufficient material begins to deposit at that point to reduce the deposition rate in the valve downstream. Additional data over a wider range of temperatures must be obtained before the existence of an optimum point can be verified.

Effect of Additives.

Acetonitrile. The first additive tested in the flow bench system was acetonitrile. During all additive tests, the procedure was to establish reproducible flow decay during a series of runs at constant conditions before injecting the additive. After injection of the additive, additional runs were conducted under the same conditions.

Two batches of N_2O_4 were tested with acetonitrile, as shown in Fig. 38. First, a series of runs (123 through 125) was conducted to demonstrate that the N_2O_4 and system were subject to flow decay, at the run conditions chosen (N_2O_4 soak temperature of 118 F (47.78 C), heat exchanger outlet temperature of 60 F (15.56 C), 250-psig tank pressure, and 0-psig vent pressure). These runs utilized the sight-glass needle valve with steel stem and seat. The flow-decay rate obtained was approximately 0.005 gpm/min (Fig. 38). During run 125, acetonitrile was injected into the flow line downstream of the needle valve (Fig. 21). Sufficient acetonitrile was added slowly, over a period of approximately 5 minutes, to yield a final

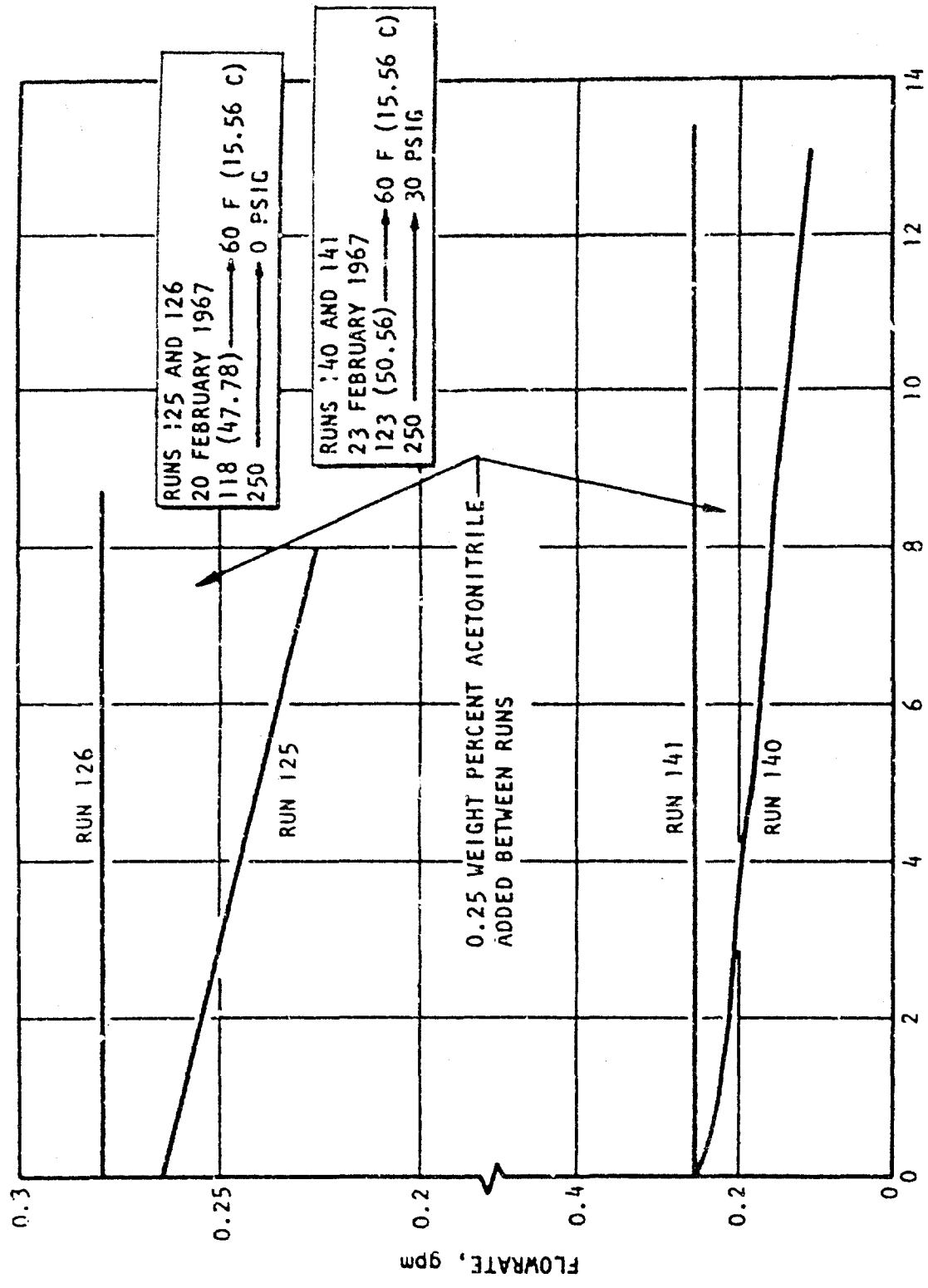

Figure 38. Effect of Acetonitrile

concentration of approximately 0.25 w/o. The N_2O_4 was then recycled to the main tank and allowed to reheat for 1 hour before the next run. During the first run (126) after introducing the additive, the initial flowrate was identical to the flow before any of the flow-decay runs, and it remained perfectly steady throughout the duration of the run. Five more runs conducted at the same conditions over a 2-day period revealed no evidence of flow decay.

The flow system was then emptied and reloaded with a new batch of N_2O_4. The first run with this new N_2O_4 supply was conducted less than 1 hour after loading and immediately exhibited flow decay. This was the first time that flow decay had been observed this brief a period after loading. Thus, it appears possible that although the acetonitrile effectively inhibited flow decay while present in the system, it may have affected the wall in such a way as to make the system more susceptible to flow decay. Acetonitrile was again added to the system between Runs 140 and 141 (Fig. 38). As before, the flowrate immediately recovered to its initial value and then remained constant. Continued flow tests were conducted over a period of 1 week with no evidence of flow decay.

Benzonitrile. The effect of benzonitrile was determined during a seri of experiments similar to that used with acetonitrile. Six runs, at 1-hour intervals, were conducted during a single day with the results shown in Fig. 39. A flow-decay rate of approximately 0.0023 gpm/min was observed during the first run (159). The rate of flow decay decreased slightly during the following three runs, in accordance with the normally observed pattern of behavior. One hour of reheating the N_2O_4 between runs is probably not quite sufficient to restore the equilibrium concentration of flow-decay material. During all these runs, the position of the flow-controlling needle valve, in which the deposits were being formed, was left unchanged. Because the pressures in the main tank and the catch tank were maintained constant for every run (250 and 30 psig), the initial flowrate was lower for each succeeding flow-decay run, because of the accumulation of deposits in the valve. Part of the

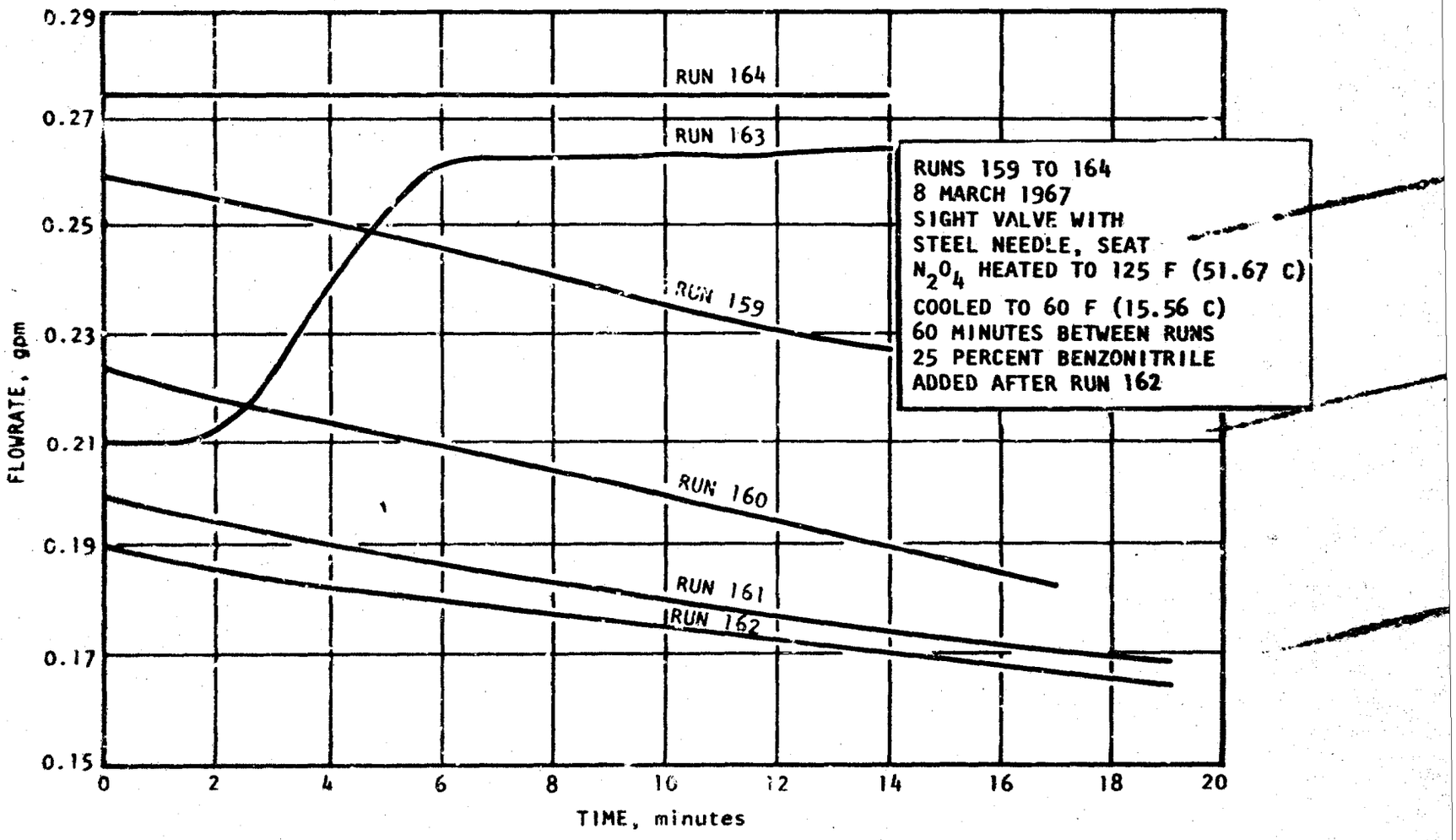

Figure 39. Effect of Benzonitrile

buildup of flow-decay deposit in the valve ordinarily redissolves during the 1-hour interval between runs; therefore, the initial flowrate may be higher than the flowrate at the end of the preceding run. Most runs were allowed to proceed until the entire contents of the main tank had been transferred. Thus, the decreasing flowrate level for runs 159 through 162 is also reflected in the increasing run time seen in Fig. 39.

During Run 162, 0.25 percent benzonitrile was added downstream of the flow-controlling valve. The subsequent run (163) exhibited a gradual recovery of flowrate throughout the run. During Run 164, flowrate had recovered completely and was constant throughout this and all succeeding runs. Benzonitrile clearly caused a re-solution of the flow-decay deposits present in the valve and the elimination of flow-decay behavior from the system. However, the efficiency of this process appears to be markedly different than with acetonitrile. In both trials with acetonitrile, flowrate recovered completely and almost instantaneously at the beginning of the first run with additive in the system. In the case of benzonitrile flowrate recovery was slow and gradual, and was still not complete at the end of 14 minutes of flow during Run 163. Acetonitrile is evidently much more efficient in dissolving the flow-decay deposits. Continued tests over a 10-day period with the benzonitrile-added system revealed no evidence of flow decay under any conditions.

Ethyl Acetate. Using the same test procedures as with acetonitrile and benzonitrile, the effect of 0.25 percent ethyl acetate was observed. Recovery of flowrate was immediate, as in the case of acetonitrile. This batch was then maintained in the system for 4 days with no flow decay during succeeding tests.

Pentafluorobenzonitrile (PFBN). The final additive to be tested in the flow bench system was PFBN at a 0.25 percent concentration. The previously established test procedure was again utilized. A series of three runs (220 through 222) was conducted to demonstrate the flow-decay

characteristics of the particular lead of N_2O_4 and test conditions used (Fig. 40). After adding the PFBN, the flowrate recovered slowly during the following run (223). The rate of recovery was at least as gradual as that observed with benzonitrile. Runs 220 through 223 were completed on April 7. The N_2O_4, with PFBN added, was maintained at a constant temperature of 130 F over the weekend. During the next run (224), April 10, rapid flow decay occurred, resulting in complete plugging of the valve after 6 minutes of run time. The valve opening was increased to restore flow, and rapid, somewhat erratic, flow decay continued at approximately the same rate for the duration of the run (Fig. 40). Succeeding runs all resulted in approximately the same flow-decay rate.

Although PFBN was temporarily effective in dissolving the flow-decay deposits, its effective lifetime at 130 F (54.44 C) is apparently very short for the additive concentration used. This contrasts to the unfluorinated benzonitrile, which remained effective for at least 10 days at approximately the same conditions and concentration. The rate of flow decay was much worse after the additive had deteriorated than it was before the addition of PFBN. This difference in decay rate may be due only to the longer soaking time at constant temperature. However, during the acetonitrile tests, the use of an additive appeared to make the system more susceptible to flow decay, once the additive had been removed.

Flow Tests With INTO

Because of the interest in developing inhibited nitrogen tetroxide (INTO) as a standard propellant, it was highly desirable to determine what effect the INTO additive (FNO_2) would have on the flow-decay phenomenon. Approximately 12 gallons of INTO containing 2.6 percent FNO_2 were obtained from the storage program under a current Air Force contractual effort. This propellant was contained in a 347 stainless steel tank which had been stored at ambient temperatures for approximately 1 month. The FNO_2 had been produced in situ by bubbling gaseous fluorine through the liquid N_2O_4.

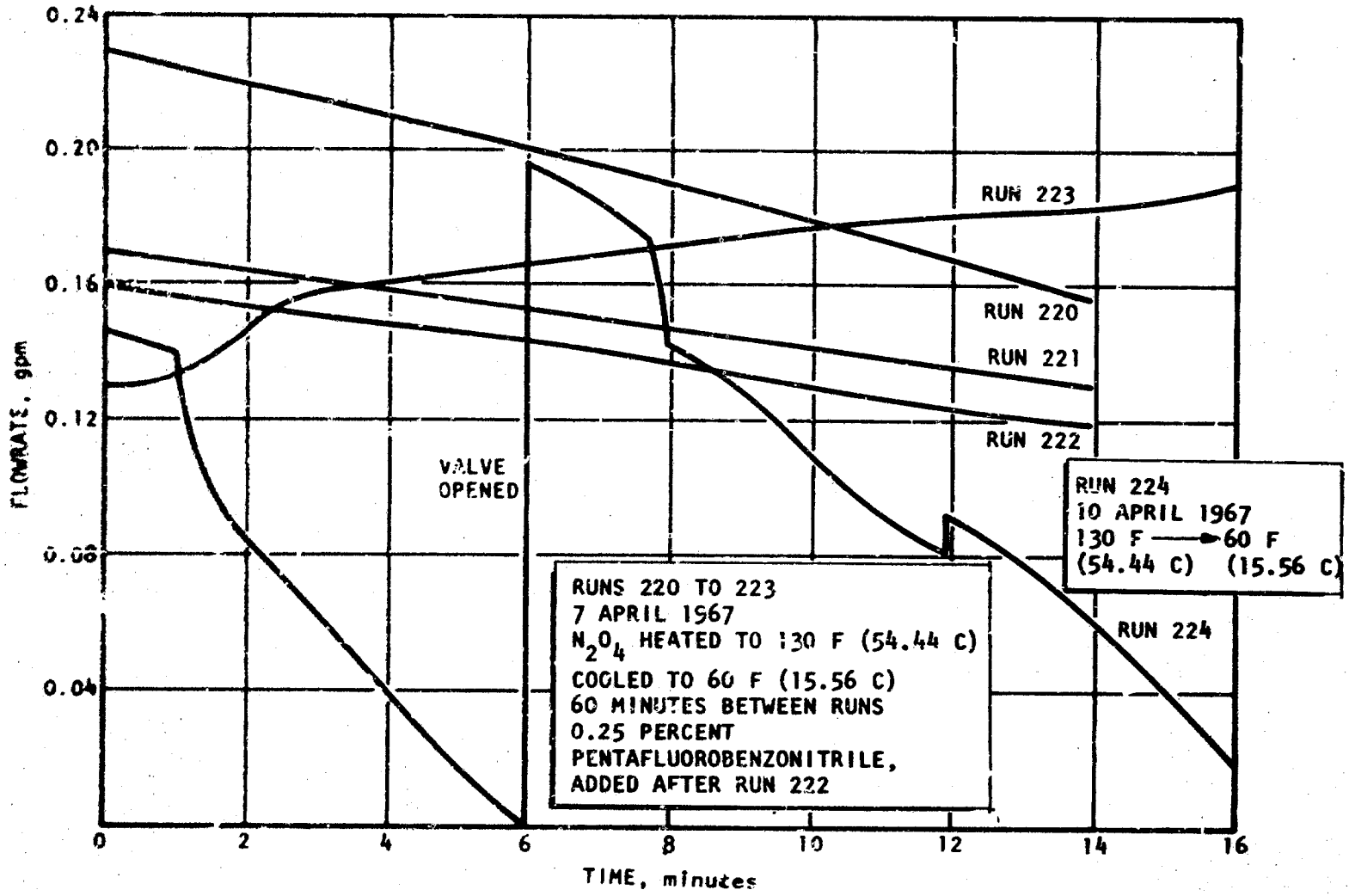

Figure 40. Effect of Pentafluorobenzonitrile

The first batch of INTO loaded into the flow bench was maintained there for 2 weeks at 120 F (48.89 C). Several flow runs were conducted during this time interval with no evidence of flow decay. At the end of the 2-week period, a sample was extracted from the system and analyzed for FNO_2. It was found that no FNO_2 remained, it having been converted to HF. The system was then dumped.

A second batch of INTO was loaded and maintained at 125 F (51.67 C) overnight. During the first run with this batch, a very slight decrease in flowrate was evident, dropping from 0.100 to 0.085 gpm over 22 minutes of run time. A second run on the following day yielded approximately the same results, decreasing from 0.108 to 0.090 gpm in 29 minutes.

Batch No. 3 was loaded into the flow bench, allowed to soak for 1 hour at 125 F (51.67 C) and then run immediately. No measurable decrease in flowrate occurred. After being maintained overnight at the same temperature, an extremely small rate of flow decay appeared (0.120 to 0.113 gpm in 25 minutes). This rate of change in flowrate was about the smallest change detectable with the instrumentation used.

The fourth and final batch of INTO was loaded into the flow bench and maintained overnight at 125 F (51.67 C) before running. All previous runs with INTO were conducted using the normal procedure of cooling through the heat exchanger to approximately 75 F (23.89 C). For the last run, the INTO was batch cooled in the main tank to 40 F (4.44 C) before flowing through the system. The flowrate decayed from 0.103 to 0.090 gpm in 19 minutes. After this run, the INTO in the system was analyzed and found to contain 1.5 percent FNO_2. Because of its greater volatility, FNO_2 is rapidly lost from the system during transfer and venting operations.

Because the first batch of INTO, which was found to contain only HF and no FNO_2, did not reveal any evidence of flow decay over an extended period of time, HF may be an effective decay-inhibiting additive. Although the later runs with fresh batches of INTO did reveal some

decrease in flowrate, the magnitude of the effect (less than 0.001 gpm per minute) was so small as to be negligible for practical systems.

Special Tests With Gemini Engine

At the request of NASA-Houston, a series of runs was conducted with a 25-pound-thrust SE-7 Gemini engine in the flow loop. The objective of these tests was to determine whether flow decay could occur in the Gemini feed system and whether conditions in the Gemini capsule during orbital missions could result in flow decay. To install the engine oxidizer feed system in the flow bench, the chamber was cut off and a stainless-steel fitting was welded to the front of the injector. The resulting configuration is shown in Fig. 41, with all ports capped off. When placed in the test section of the flow bench, the oxidizer inlet and injector fittings were connected to the N_2O_4 flow line. The chamber pressure tap was capped off and the back side of the fuel valve was connected to a 150-psi nitrogen line to prevent any N_2O_4 from leaking past the poppet into the fuel valve. To simulate spacecraft temperature conditions during orbit, a new batch of N_2O_4 was loaded into the system and heated to only 80 F (26.67 C). The N_2O_4 was cooled to approximately 60 F (15.56 C) in the heat exchanger before flowing into the Gemini oxidizer feed system. The production of flow decay with this low an initial soak temperature had not been attempted before; therefore, it was not too surprising when the phenomenon failed to appear. A repeat run, in which the heat exchanger temperature was reduced to approximately 40 F (4.44 C) by adding ice, was also unsuccessful in producing flow decay.

It was then decided to determine whether the absence of flow decay was simply due to the low soak temperature or to some special feature of the Gemini feed system, which included an orifice, filter, valve, and injector. The N_2O_4 was heated to 100 F (37.78 C) and allowed to soak overnight. On the first run of the next day, with cooling to 60 F (15.56 C), a small, barely detectable decrease in flowrate occurred. Succeeding runs revealed no evidence

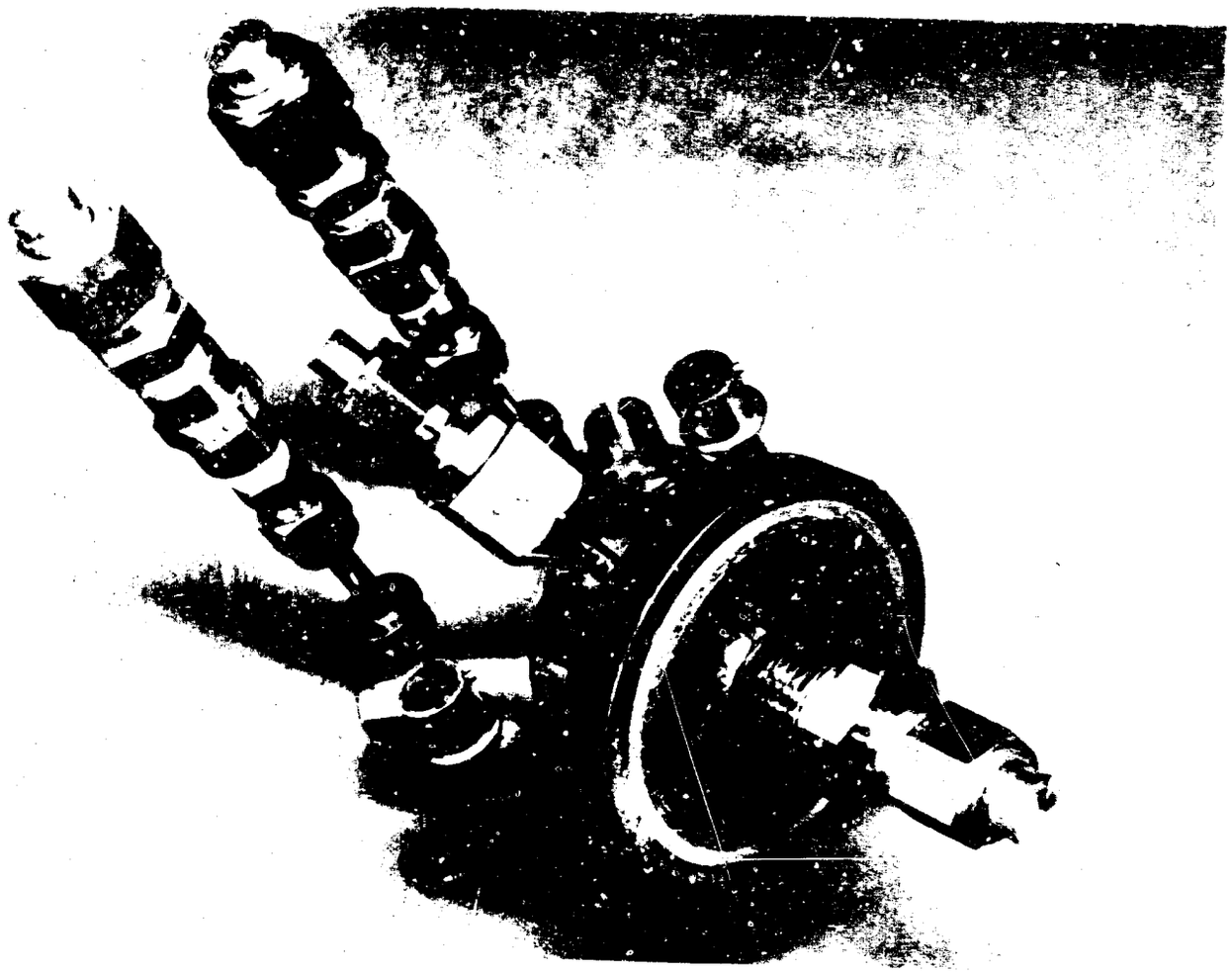

5AL44-4/14/67-S1A

Figure 41. Gemini SE-7 Engine

of flow decay. Then, the N_2O_4 in the flow bench was dumped and a new batch was loaded. The soak temperature was increased to 120 F. After an overnight soak, a run with cooling to 60 F in the heat exchanger resulted in only slight flow decay, but switching the flow to bypassing the heat exchanger resulted in steady flow decay. On succeeding runs with the same conditions, the flowrate recovered to its initial value. The last day of testing occurred after the N_2O_4 was allowed to soak over a weekend at 120 F. Again, flow decay was apparent only on bypassing the heat exchanger. While these experiments demonstrated that flow decay can occur in a Gemini feed system, (with proper N_2O_4 conditioning), they failed to produce any evidence that normal spacecraft conditions (80 F maximum temperature) would result in flow decay.

The results of the flow tests with the Gemini valve were confusing at the time for several reasons. Although flow decay had been obtained on several previous occasions with flow bypassing the heat exchanger, these cases were the exception, and flow decay always resulted also when passing through the heat exchanger. During the Gemini tests, flow decay occurred only when bypassing the exchanger. An explanation for this behavior was sought. It was noted that the Gemini flowrate (0.15-gpm flow at 300-psi tank pressure, 135-psi vent pressure) was slightly lower than that normally used in the flow bench during previous runs (usually 0.2 to 0.25 gpm). Therefore, after removing the Gemini engine from the system, a check run was conducted with the same batch of N_2O_4, a steel needle valve, and 0.25-gpm flowrate. No flow decay occurred when bypassing the heat exchanger. Flowrate and N_2O_4 temperature at the valve inlet are plotted in Fig. 42. The line temperature rose quickly to within approximately 3 F of the N_2O_4 bulk temperature. The run was terminated after 6 minutes and the line was allowed to reapproach ambient temperature. When the run was restarted at a lower flowrate (flowrate was decreased by partially closing the needle valve), steady flow decay initiated. The line temperature in this case began to rise much more slowly at first and then ceased rising altogether as the flow decayed to zero. When the needle valve was opened wider to restore flow, the line temperature

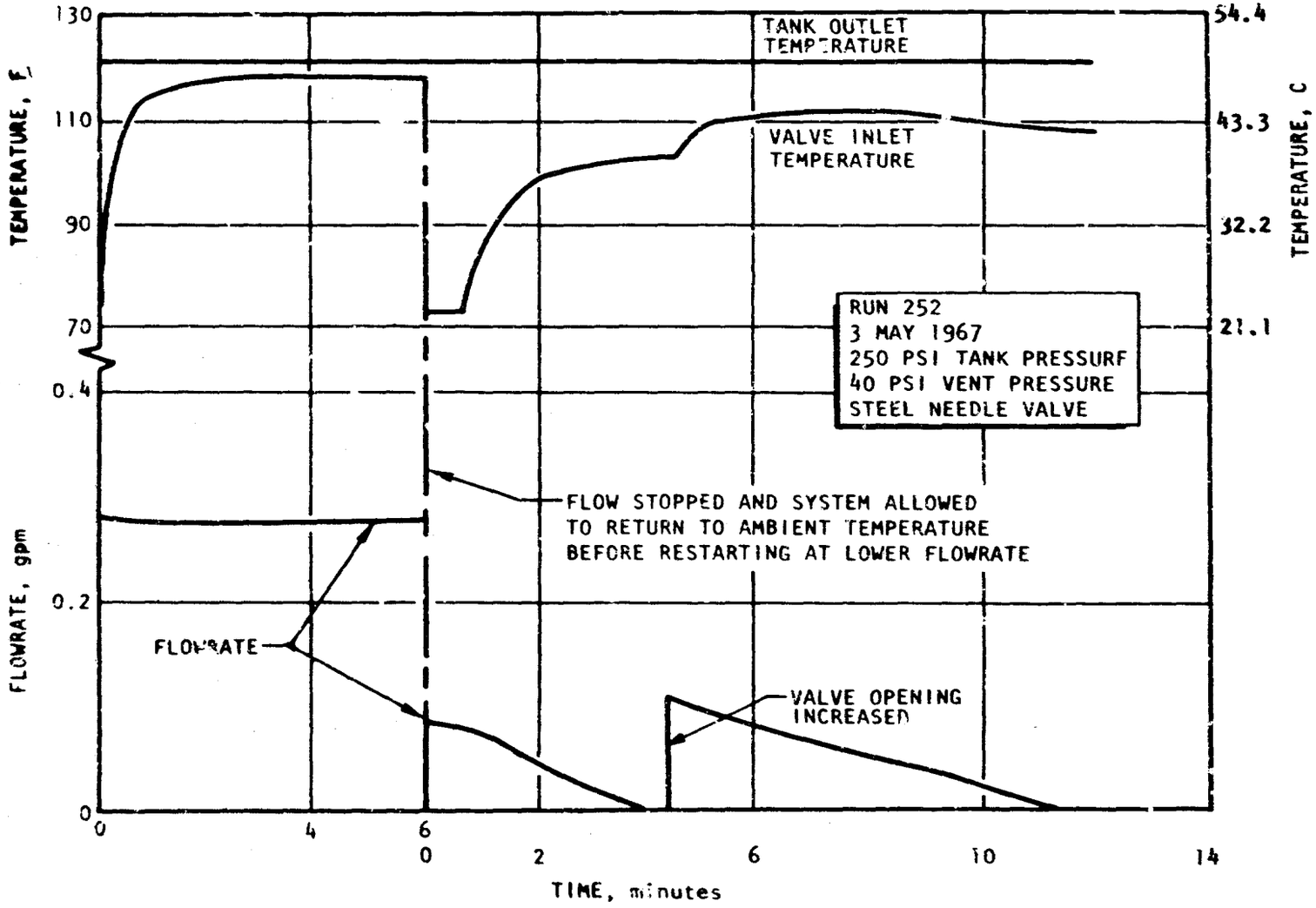

Figure 42. Effect of Initial Flowrate in Bypass Mode

again began to rise but soon reached a maximum approximately 9 F below the bulk temperature and then declined as flowrate again approached zero. Many previous runs, in which flow through the heat exchanger resulted in a constant line temperature regardless of flowrate, had demonstrated that the rate of flow decay was always essentially linear with time, regardless of the magnitude of the initial flowrate. Therefore, it was obvious that the behavior shown in Fig. 42 was caused by the increased temperature drop in the line at lower flowrates when bypassing the heat exchanger. At 0.25 gpm, the temperature drop of 3 F in the line from the tank to the valve was not sufficient to induce flow decay. However, at lower flowrates, a longer time is required to heat initially cold line components and a greater temperature drop will remain at steady state. This additional temperature drop was sufficient to induce flow decay with the particular batch of N_2O_4 being tested. Further runs verified that, when bypassing the heat exchanger, initial flowrate alone (with a corresponding temperature drop in the line) would determine the appearance or absence of flow decay when varied between 0.15 and 0.25 gpm. This provided an explanation for the Gemini tests in which flow decay occurred when bypassing the heat exchanger, in contrast to normal experience.

The most puzzling aspect of the Gemini tests was that no significant f decay occurred when the N_2O_4 was cooled from 120 to 60 F (48.89 to 15.56 C) by flowing through the heat exchanger. Although no quantitative evidence was available, it had been believed for some time prior to the Gemini tests that the heat exchanger surface was becoming more activated and perhaps causing much of the flow decay material to precipitate out in the exchanger. For instance, runs had been observed in which a higher rate of flow decay resulted when bypassing the heat exchanger than when flowing through the exchanger. Earlier cold-finger experiments had clearly established that the material could be precipitated out on a cold surface and the large (100 feet of 1 4-inch tubing) heat exchanger surface area was obviously a likely area for precipitation to occur. During the period prior to the Gemini tests, while the SE-7 engine was being modified and installed in the flow loop, the system remained idle for approximately 2 weeks. Considering all factors, it was thought that perhaps a combination of

such variables as the increased aging of the surface, unknown chemical differences in the new supply of N_2O_4, greater precipitation at lower flowrates, etc. had resulted in most of the flow-decay material being trapped out in the heat exchanger. To verify this hypothesis, the heat exchanger was removed from the system and a temporary low-surface-area heat exchanger was installed. Again utilizing the same load of N_2O_4 and same run conditions, strong steady flow decay resulted on cooling from 120 to 80 F (48.89 to 26.67 C) in the exchanger. This completed the explanation of the anomalous behavior observed during the Gemini tests. Flow decay was obtained when bypassing the heat exchanger because of the lower flowrate and increased temperature drop in the line. Flow decay did not result with flow through the heat exchanger because of precipitation on the heat exchanger surface.

Based on the previously discussed results, the low-surface-area variable-temperature heat exchanger for the flow bench was then built. With this improved system, flow decay was demonstrated in a standard valve with 80 F (26.67 C) initial N_2O_4 temperature. It was originally planned to return to testing with the Gemini engine in the new system after completion of the rest of the program. Further testing is obviously required to delineate exact conditions for which flow decay may occur in the Gemini system. However, insufficient time and funds prevented Gemini tests in the new flow bench system.

CONCLUSIONS

Mechanisms of Flow Decay

The experimental behavior observed during this phase of the program suggests that flow decay occurs as a four-step process. An initial long-term step is required for reaction with the tank wall before flow-decay material is produced in sufficient quantities to present problems.

A second step, which reaches equilibrium in a matter of hours, may be a further reaction or simply a solution process. This is the step which causes gradually decreasing rates of flow decay on succeeding flow bench runs spaced at 1-hour intervals.

The third, or precipitating step, is the creation of a saturated or supersaturated solution by a sudden decrease in temperature or pressure.

The fourth and final step of the process is the initiation of precipitation on suitable nucleation sites at the point of temperature and/or pressure change.

Susceptibility to Flow Decay

The buildup of flow-decay deposits is linear with time, regardless of flow-rate. Because the total amount of material present is extremely small, only flow systems with a very small cross section to flow will be appreciably affected. Relative susceptibility of valves to flow decay can be estimated from the ratio of length of wetted perimeter to cross-sectional flow area at the point of minimum area. A plain orifice is the least susceptible shape for introducing pressure drop.

Flow-decay material can be deposited on a wide variety of materials, but material and design influence the ability of the deposit to adhere.

Effect of Additive

Acetonitrile, benzonitrile, ethyl acetate, and pentafluorobenzonitrile were all effective in dissolving flow-decay deposits in the system when used at 0.25 percent concentration. There were marked differences in the speed with which the different additives dissolved the deposits. Pentafluorobenzonitrile lost its effectiveness in preventing flow decay after a relatively short period of time.

Flow Dec · With INTO

The addition of HF to N_2O_4 may effectively inhibit flow decay. Extremely small decreases in flowrate were observed with new batches of INTO. This suggests that, although INTO is not completely immune to flow decay, it may never be subject to disastrous flow-decay occurrences.

CONCLUSIONS

The anhydrous iron nitrate $NOFe(NO_3)_4$ has been successfully prepared and purified in sufficient quantities to meet the needs of the entire program. Evidence has been obtained to establish unequivocally the identity of this material with the actual flow-decay (N_2O_4 corrosion product) deposit.

The amount of iron that can be dissolved in anhydrous N_2O_4 from iron powder, iron oxide powder, or steel alloys is only 0.5 to 1.5 ppm. The iron concentration is apparently limited by the solubility of the iron compound(s) which forms in N_2O_4; a completely insoluble passive film does not form on the iron surface. The addition of 0.9 w/o water to the N_2O_4 increases the iron solubility limit somewhat and a second liquid phase is formed after prolonged contact of the "wet" N_2O_4 with iron powder.

A sample of propellant-grade N_2O_4 which had been stored in a small steel laboratory container for more than 1 year was repeatedly found to contain about 1.5 ppm soluble iron. Filtering and heating of this propellant-grade N_2O_4, under the limited conditions employed during this study, did not affect the concentration of soluble iron.

The solubility of the flow-decay compound in freshly distilled N_2O_4 over the temperature range 32 to 100 F, and in the presence of small concentrations of nitric oxide and water has been found to be quite low, on the order of 1 to 4 ppm in terms of iron concentration.

The feasibility of the principle of elimination of flow-decay deposit by the additive approach has been demonstrated.

Reagents with different functional groups have been discovered as effective complexing agents in N_2O_4 and therefore are prime candidates in the elimination of flow-decay deposits.

A convenient tool for the study of the flow-decay phenomenon on a laboratory scale has been developed.

The experimental behavior observed during this phase of the program suggests that flow decay occurs as a four-step process. An initial long-term step is required for reaction with the tank wall before flow-decay material is produced in sufficient quantities to present difficulties.

A second step, which reaches equilibrium in a matter of hours, may be a further reaction or simply a solution process. This is the step which causes gradually decreasing rates of flow decay during succeeding flow bench runs at 1-hour intervals.

The third, or precipitating step, is the creation of a saturated or supersaturated solution by a sudden decrease in temperature or pressure.

The fourth and final step of the process is the initiation of precipitation on suitable nucleation sites at the point of temperature and/or pressure change.

The buildup of flow-decay deposits is linear with time, regardless of flow-rate. Because the total amount of material present is extremely small, only flow systems with a very small cross-section to flow will be affected appreciably. Relative susceptibility of valves to flow decay can be estimated from the ratio of length of wetted perimeter to cross-sectional flow area at the point of minimum area. A plain orifice is the least susceptible shape for inducing pressure drop.

Flow-decay material can be deposited on a wide variety of materials. Material and design influence the ability of the deposit to adhere.

Acetonitrile, benzonitrile, ethyl acetate, and pentafluorobenzonitrile were all effective in dissolving flow-decay deposits in the system when used at 0.25 percent concentrations. There were marked differences in the speed with which the different additives dissolved the deposits. Pentafluorobenzonitrile lost its effectiveness in preventing flow decay after a relatively short period of time.

The addition of HF to N_2O_4 may effectively inhibit flow decay. Extremely small decreases in flowrate were observed with new batches of INTO. This suggests that, although INTO is not completely immune to flow decay, it may never be subject to disastrous flow-decay occurrences.

The N^{14} n.m.r. spectrum of solid iron nitrate is too broad to be useful, unless a single crystal of the material is available. The N^{15} n.m.r. spectrum may yield useful information on the structure of the flow-decay solid material. Techniques have been partially developed which will likely permit the sensitivity of the N^{15} n.m.r. technique to be increased to the point where the natural abundance of N^{15} in the solid becomes observable. The n.q.r. spectrum of N^{14} may permit the various kinds of nitrogen-containing groups to be identified in solids. Considerable additional effort would be required to increase the signal-to-noise ratio of the broad-line H^1 n.m.r. spectrum of iron nitrates to a useful level for detailed structural studies of water-containing iron nitrates. The technique of e.p.r. spectroscopy is apparently sufficiently sensitive for structural studies of iron nitrate species even in dilute solution. Unfortunately, the iron resonance is masked by the NO_2 resonance in N_2O_4 precluding the use of e.p.r. in these studies. Mossbauer spectrometry has shown that the iron site(s) in synthetic anhydrous iron nitrate has rather undistorted octahedral or tetrahedral symmetry, and that all of the iron sites are quite similar. This technique is capable of determining if the iron atoms in the actual flow-decay material exist in environments similar to those in the synthetic flow-decay material.

REFERENCES

1. R-6385, The Nitrogen Tetroxide Flow Decay Final Report, Rocketdyne, a Division of North American Aviation, Inc., Canoga Park, California, June 1966.
2. Challice, J. S. and G. M. Clarke, Spectrochim. Acta, 22, 63 (1966).
3. Cameron, F. K. and W. O. Robinson, J. Phys. Chem., 13, 251 (1909).
4. Hathaway, F. J. and A. E. Underhill, J. Chem. Soc., 648 (1960).
5. Addison, C. C. and D. J. Chapman, J. Chem. Soc., 819 (1965).
6. Starke, K., J. Inorg. Nucl. Chem., 11, 77 (1959).
7. Erley, D. S., Analyt. Chem., 29, 1564 (1957).
8. Addison, C. C., P. M. Boorman, and N. Logan, J. Chem. Soc., 4978 (1965).
9. Holm, Thurston, McConnell, and Davidson, Bull. Am. Phys. Soc., Ser. II, 397 (1956).
10. Beringer, R. and J. G. Castle, Jr., Phys. Rev., 78, 581 (1950).
11. Instructions for Operation of Large and Small Powder Camera, Types No. 52056-B and 52057-B, Philips Electronics, Inc., Mount Vernon, New York.
12. 8651-6042-SU000, Advanced Valve Technology for Spacecraft Engines, Final Report, Space Technology Laboratories, TRW Systems, TRW, Inc., August 1965
13. Recent Aspects of the Inorganic Chemistry of Nitrogen, Special Publication No. 10, The Chemical Society, Burlington House, London, 1957.

APPENDIX A

ANALYSIS OF IRON IN N_2O_4 BY 4,7 DIPHENYL 1,10-PHENANTHROLINE (BATHOPHENANTHROLINE)

SPECTROPHOTOMETER

A Cary Model-14 Spectrophotometer was employed for this study.

GLASSWARE

50-milliliter beakers, one for each sample

125-milliliter extraction funnels, one for each sample

25-milliliter volumetric flasks, one for each sample

pipettes, funnels, etc.

1-centimeter or 10-centimeter Pyrex absorption cells

> NOTE: All glassware should be cleaned thoroughly and soaked several hours in 1:1 HCl prior to use. The glassware employed in this analysis should be employed only for this analysis

REAGENTS

Iso-amyl alcohol, C.P.; absolute Ethyl Alcohol

Concentrated H_2SO_4, C.P.

Concentrated HCl, C.P.

Concentrated HNO_3, C.P.

Concentrated NH_4OH, C.P.

Deionized H_2O

10 Percent $NH_2OH \cdot HCl$

Dissolve 10 grams of $NH_2OH \cdot HCl$ in 50 milliliters H_2O (deionized) and dilute to 100 milliliters volumetrically.

2 M Sodium Acetate

Place 272.18 grams of $NaC_2H_3O_2 \cdot 3H_2O$ in a 1-liter volumetric flask, dissolve, and dilute to the mark with deionized H_2O.

0.8 Percent Bathophenanthroline

Dissolve 80 milligrams of 4,7 diphenyl 1,10-phenanthroline in ethyl alcohol and dilute volumetrically to 100 milliliters with ethyl alcohol.

10,000 ppm Fe Stock Solution

Harleco atomic absorption standard solution was used.

PROCEDURE

Hydrolyze 10 milliliters of N_2O_4 (15 grams) in 50 milliliters of frozen deionized water. When the hydrolysis is complete, fill a 50-milliliter beaker approximately half full with the sample and place the beaker on a hot plate set at approximately 350 to 400 C. Add 2 milliliters of concentrated H_2SO_4 and 2 drops of concentrated HCl to the sample. Evaporate slowly, adding more sample and finally washings, until the sample has boiled down to ~5 milliliters. Raise the temperature of the hot plate and evaporate to SO_3 fumes. Cool the sample and add 10 milliliters of H_2O and 2 milliliters of 10 percent NH_2OH HCl (during some of the early work $Sn Cl_2$ was used). Place the sample on the hot plate and bring to a boil. Cool to room temperature and adjust the pH to 4 to 5 with 1:1 NH_4OH

and 2 M NaAc. Transfer the sample to a 125-milliliter extraction funnel and add 5 milliliters of 0.08 percent Bathophenanthroline and 10 milliliters of iso-amyl alcohol. Extract for 10 minutes and transfer through filter paper to a 25-milliliter volumetric flask. Fill to the mark with iso-amyl alcohol, mix and age 15 minutes, and read the absorbance at 533 millimicrons against a reagent blank.

STANDARDS AND BLANK

Standards are prepared by micro pipetting Fe^{+++} from the 10,000 ppm Fe^{+++} standard solution into 1:1 HNO_3 (20 milliliters) in a 50-milliliter beaker and proceeding as with the samples.

SENSITIVITY

Using the method as described and a 1-centimeter cell, a total of 6.25 micrograms of Fe yields an absorbance of 0.1. This corresponds to 0.42 ppm Fe in a 15-gram N_2O_4 sample. Using 50-milliliter final volumes and a 10-centimeter cell, 0.08 ppm Fe in a 15-gram N_2O_4 sample should give an absorbance of approximately 0.1.

APPENDIX B

ANALYSIS OF IRON IN N_2O_4 BY 1,10-PHENANTHROLINE

SPECTROPHOTOMETER

A Cary Model 14 Spectrophotometer was used for this study.

GLASSWARE

50-milliliter beakers, one for each sample and standard

50-milliliter volumetric flasks, one for each sample and standard

100-milliliter volumetric flask, one for blank

1-centimeter or 10-centimeter Pyrex absorption cells

NOTE: Refer to note on treatment of glassware in Appendix A.

REAGENTS

Absolute Ethyl Alcohol

Concentrated NH_4OH

Concentrated H_2SO_4

Concentrated HNO_3

Deionized H_2O

0.5 Percent 1,10-phenanthroline

Dissolve 0.125 grams of 1,10-phenantholine in 2.5 milliliters of absolute ethyl alcohol and dilute to 25 milliliters volumetrically with deionized H_2O.

10 Percent $NH_2OH \cdot HCl$

Dissolve 10 grams of C.P. $NH_2OH \cdot HCl$ in deionized H_2O and dilute to 100 milliliters.

2 M Sodium Acetate

Dissolve 272.18 grams of $NaC_2H_3O_2 \cdot 3H_2O$ and dilute to 1 liter volumetrically with deionized H_2O.

10,000 ppm Fe Stock Solution

The Harleco atomic absorption standard solution was used.

PROCEDURE

Hydrolyze 10 milliliters (15 grams) of N_2O_4 in 50 milliliters of frozen deionized H_2O. After hydrolysis is complete, place ~ 20 milliliters of the hydrolyzed solution in a 50-milliliter beaker and add 2 milliliters of concentrated H_2SO_4. Place on a hot plate set at ~ 400 C. Evaporate the samples adding more sample and finally washings as the volume decreases. When the sample has evaporated to ~ 5 to 10 milliliters, raise the temperature of the hot plate and evaporate to SO_3 fumes. Transfer the sample to a 50-milliliter volumetric flask and add 1 milliliter of 10 percent $NH_2OH \cdot HCl$. Heat the sample in a water bath at ~ 60 C for 10 minutes. Cool the sample and adjust the pH to 3 to 6 with 1:1 NH_4OH and 2 M NaAc. Add 1 milliliter of 0.5 percent 1,10-phenanthroline and dilute to volume with deionized water. Mix and age for 30 minutes. Read the absorbance at 510 millimicrons against a reagent blank. Compare the absorbance with that of standard solutions.

STANDARD SOLUTIONS AND REAGENT BLANK

Standard solutions are made by adding Fe from the 10,000 ppm Fe solution to 20 milliliters of 1:1 HNO_3 in a 50-milliliter beaker and proceeding as with the hydrolyzed N_2O_4 samples.

The reagent blank is 40 milliliters of 1:1 HNO_3 treated as the hydrolyzed N_2O_4 samples except that twice as much of each reagent is added and the blank is diluted to 100 milliliters in the final step.

SENSITIVITY

An absorbance of ~ 0.1 can be obtained with the procedure described previously with a 15-gram N_2O_4 sample that is 0.15 ppm in Fe if 10-centimeter absorption cells are used

APPENDIX C

ANALYSIS OF IRON IN N_2O_4 BY ATOMIC ABSORPTION

ATOMIC ABSORPTION SPECTROPHOTOMETER

A Perkin-Elmer Model 303 Atomic Absorption Spectrophotometer was used for this study.

GLASSWARE

100-milliliter volumetric flasks, one for each standard and one for the reagent blank

~ 100-milliliter-capacity cylindrical Pyrex glass hydrolysis vessels with ball and socket cap

NOTE: Refer to note on treatment of glassware in Appendix A.

REAGENTS

Concentrated HNO_3

10,000 ppm Fe Stock Solution

The Harleco atomic absorption standard was used.

PROCEDURE

Freeze 50 milliliters of deionized H_2O in hydrolysis vessel. Add 10 milliliters (15 grams) of N_2O_4 and allow it to slowly hydrolyze. When hydrolysis has been completed, place the hydrolysis vessels in a hot water bath (~90 C)

until the color changes to a light blue and the vigorous bubbling has ceased. Cool the sample and mark the liquid level on the outside of the hydrolysis vessel. Aspirate the samples into a C_2H_2-air flame on the atomic absorption spectrophotometer and read the percent absorption at 248.3 millimicrons using a Boling burner. Standards and blanks are made up in 10 percent (v/v) HNO_3 by micropipetting stock Fe solution into 100-milliliter volumetric flasks containing 10 milliliters of concentrated HNO_3 and diluting to the mark with deionized H_2O.

SENSITIVITY

For a final hydrolyzed volume of 70 milliliters, 10X scale expansion and manual operation of the spectrophotometer, the limit of detection in a 15-gram N_2O_4 sample is ~ 0.14 ppm Fe.

UNCLASSIFIED

Security Classification

DOCUMENT CONTROL DATA - R&D

(Security classification of title, body of abstract and indexing annotation must be entered when the overall report is classified)

1. ORIGINATING ACTIVITY (Corporate author)

Rocketdyne, a Division of North American Aviation, Inc., 6633 Canoga Avenue, Canoga Park, California

2a. REPORT SECURITY CLASSIFICATION

UNCLASSIFIED

2b. GROUP

3. REPORT TITLE

METHODS FOR ELIMINATION OF CORROSION PRODUCTS OF NITROGEN TETROXIDE

4. DESCRIPTIVE NOTES (Type of report and inclusive dates)

Final Report (1 May 1966 through 30 June 1967)

5. AUTHOR(S) (Last name, first name, initial)

Cain, E.F.C.; Axworthy, A. E.; Gerbauser, J.; Fujikawa, C.; Rodriguez, S.; Sinor, J.

6. REPORT DATE	7a. TOTAL NO. OF PAGES	7b. NO. OF REFS
31 July 1967	156	13

8a. CONTRACT OR GRANT NO	9a. ORIGINATOR'S REPORT NUMBER(S)
b. PROJECT NO.	R-7136
c.	9b. OTHER REPORT NO(S) (Any other numbers that may be assigned this report)
d.	AFRPL-TR-67-277

10. AVAILABILITY/LIMITATION NOTICES This document is subject to special export controls and each transmittal to foreign governments or foreign nationals may be made only with prior approval of AFRPL (RPPR/STINFO), Edwards, California 93523.

11. SUPPLEMENTARY NOTES	12. SPONSORING MILITARY ACTIVITY
	Air Force Rocket Propulsion Laboratory Research and Technology Division Edwards, California

13. ABSTRACT

The deposition of a solid material from N_2O_4 in a propellant feed system has been studied in the laboratory and with an experimental flow bench. The solid material has been identified as $NO^+ [Fe(NO_3)_4]^-$. The conditions which cause the deposition were studied and the feasibility of the principle of elimination of flow-decay deposit by the additive approach has been demonstrated. The solubility of $NO^+ [Fe(NO_3)_4]^-$ in anhydrous iron-free nitrogen tetroxide was determined.

DD FORM 1 JAN 64 1473

UNCLASSIFIED

Security Classification

14 KEY WORDS	LINK A		LINK B		LINK C	
	ROLE	WT	ROLE	WT	ROLE	WT
Corrosion Products						
Nitrogen Tetroxide						
Flow Decay						

INSTRUCTIONS

1. ORIGINATING ACTIVITY: Enter the name and address of the contractor, subcontractor, grantee, Department of Defense activity or other organization *(corporate author)* issuing the report.

2a. REPORT SECURITY CLASSIFICATION: Enter the overall security classification of the report. Indicate whether "Restricted Data" is included. Marking is to be in accordance with appropriate security regulations.

2b. GROUP: Automatic downgrading is specified in DoD Directive 5200.10 and Armed Forces Industrial Manual. Enter the group number. Also, when applicable, show that optional markings have been used for Group 3 and Group 4 as authorized.

3. REPORT TITLE: Enter the complete report title in all capital letters. Titles in all cases should be unclassified. If a meaningful title cannot be selected without classification, show title classification in all capitals in parenthesis immediately following the title.

4. DESCRIPTIVE NOTES: If appropriate, enter the type of report, e.g., interim, progress, summary, annual, or final. Give the inclusive dates when a specific reporting period is covered.

5. AUTHOR(S): Enter the name(s) of author(s) as shown on or in the report. Enter last name, first name, middle initial. If military, show rank and branch of service. The name of the principal author is an absolute minimum requirement.

6. REPORT DATE: Enter the date of the report as day, month, year, or month, year. If more than one date appears on the report, use date of publication.

7a. TOTAL NUMBER OF PAGES: The total page count should follow normal pagination procedures, i.e., enter the number of pages containing information.

7b. NUMBER OF REFERENCES: Enter the total number of references cited in the report.

8a. CONTRACT OR GRANT NUMBER: If appropriate, enter the applicable number of the contract or grant under which the report was written.

8b, 8c, & 8d. PROJECT NUMBER: Enter the appropriate military department identification, such as project number, subproject number, system numbers, task number, etc.

9a. ORIGINATOR'S REPORT NUMBER(S): Enter the official report number by which the document will be identified and controlled by the originating activity. This number must be unique to this report.

9b. OTHER REPORT NUMBER(S): If the report has been assigned any other report numbers *(either by the originator or by the sponsor)*, also enter this number(s).

10. AVAILABILITY/LIMITATION NOTICES: Enter any limitations on further dissemination of the report, other than those imposed by security classification, using standard statements such as:

(1) "Qualified requesters may obtain copies of this report from DDC."

(2) "Foreign announcement and dissemination of this report by DDC is not authorized."

(3) "U. S. Government agencies may obtain copies of this report directly from DDC. Other qualified DDC users shall request through

_____."

(4) "U. S. military agencies may obtain copies of this report directly from DDC. Other qualified users shall request through

_____."

(5) "All distribution of this report is controlled. Qualified DDC users shall request through

_____."

If the report has been furnished to the Office of Technical Services, Department of Commerce, for sale to the public, indicate this fact and enter the price, if known.

11. SUPPLEMENTARY NOTES: Use for additional explanatory notes.

12. SPONSORING MILITARY ACTIVITY: Enter the name of the departmental project office or laboratory sponsoring *(paying for)* the research and development. Include address.

13. ABSTRACT: Enter an abstract giving a brief and factual summary of the document indicative of the report, even though it may also appear elsewhere in the body of the technical report. If additional space is required, a continuation sheet shall be attached.

It is highly desirable that the abstract of classified reports be unclassified. Each paragraph of the abstract shall end with an indication of the military security classification of the information in the paragraph, represented as *(TS), (S), (C), or (U)*

There is no limitation on the length of the abstract. However, the suggested length is from 150 to 225 words.

14. KEY WORDS: Key words are technically meaningful terms or short phrases that characterize a report and may be used as index entries for cataloging the report. Key words must be selected so that no security classification is required. Identifiers, such as equipment model designation, trade name, military project code name, geographic location, may be used as key words but will be followed by an indication of technical context. The assignment of links, rules, and weights is optional.